Advancements in Metered-Dose Inhaler Technology: Feasibility of Excipients and Particle Size Prediction

by

Zahra Minootan

A thesis submitted in partial fulfillment of the requirements for the degree of

Master of Science

Department of Mechanical Engineering
University of Alberta

© Zahra Minootan, 2024

`

Abstract

Chronic respiratory diseases such as chronic obstructive pulmonary disease (COPD) are one of the leading causes of death in the world. According to the World Health Organization (WHO), 262 million people were diagnosed with Asthma in 2019 alone. Among current drug delivery systems for the treatment of such conditions, pulmonary drug delivery is known as the most efficient route for delivery of drugs to the lungs. This thesis focuses on pressurized metered dose inhalers (pMDIs) as one of the most widely used devices in pulmonary drug delivery.

Chapter 1 gives an introduction to current inhaler devices and their advantages and disadvantages before providing further detail about pMDI formulations and designs. Additionally, particle engineering for manufacturing powders used in inhalers is discussed. Finally, methodologies to enhance the performance of pMDIs are reviewed and discussed.

Chapter 2 presents the details of an investigation into different suspension formulations and the feasibility of their use in pMDIs. A short-term accelerated stability study was conducted to investigate the physical stability of spray dried powders in pMDIs. Formulations were compared in terms of their suspension stability and particle morphology. Results of the study showed that factors such as the propellants used and the spray drying manufacturing conditions could affect the physical stability of particles emitted from pMDIs.

Chapter 3 provides a literature review of current models and simulation for predicting the aerosol performance of pMDIs. It then goes further in development of a Monte Carlo simulation to predict aerodynamic particle distribution of residual particles emitted from pMDIs. Using the simulation, various factors influencing APSD of emitted aerosols are discussed, and the potential of the simulation to account for different variables is explored.

In summary, this thesis aims to give a better understanding of pMDIs as established devices for pulmonary drug delivery, explore methods for evaluating their performance, and delve into the development of environmentally friendly inhalers with innovative formulations.

`

Preface

Chapter 2 of this thesis consists of one journal paper and two conference posters. Section 2.2 has been submitted as a research article,

> "Minootan Z, Wang H, Connaughton P., Lachacz K, Carrigy N, Ordoubadi M, Lechuga-Ballesteros D, Martin AR, Vehring R. On the feasibility of rugose lipid microparticles in pMDIs with established and new propellants. *AAPS PharmSciTech.* Submitted October 10, 2023"

I planned the study and carried out the literature review, spray drying, scanning electron microscopy, energy-dispersive X-ray spectroscopy, shadowgraphic imaging, filling and crimping of the metered dose inhalers, water content measurement using Karl Fischer coulometer and data interpretation. HW helped in designing the study and trained me on spray drying, water content measurement and shadowgraphic imaging and contributed to manuscript edits. PC, LK, DLB contributed to manuscript edits and provided feedback. MO proofread the paper and assisted in interpretation of results on leucine-trehalose particles. My co-supervisor, ARM, contributed to manuscript edits, helped in interpretation of the results and provided feedback. My supervisor, RV, was involved in conceptualization, discussion of results, and manuscript composition. Part of Section 2.2 was also presented as a poster,

> "Minootan Z, Wang H, Carrigy N, Lachacz K, Lechuga-Ballesteros D, Martin AR, Vehring R. Excellent Colloidal Stability of Rugose Lipid Particles in Established and New Propellants. *24th Congress of the International Society for Aerosols in Medicine*. Saarbrücken, Germany, August 26-30, 2023.

Section 2.3 was presented as a poster,

> Minootan Z, Wang H, Carrigy N, Lachacz K, Lechuga-Ballesteros D, Martin AR, Vehring R. The stability of novel rugose particles in pressurized metered dose inhalers. *AAPS PharmSci 360*, Orlando, FL, October 22-25, 2023.

This poster showcases additional findings derived from a 12-month extension of the stability study mentioned in section 2.3. Additionally, it presents results obtained from using an Aerodynamic Particle Sizer.

`

Chapter 3 will be submitted as a journal paper with some possible modifications. I conducted the literature review, defined the problem and developed the numerical simulation in Python. NC assisted in conceptualizing and defining the problem. RV and ARM provided feedback and helped in study design.

`

To my beloved husband Shayan—your love and support have lifted me up every step of this journey. Your humor and laughter have kept my spirit light even during the most difficult times. I could not have done this without you by my side.

To my parents, Hassan and Leila—you instilled in me from a young age the belief that I could achieve anything I set my mind to. Your pride in my accomplishments has motivated me to keep reaching higher, even when the path grew steep.

`

Acknowledgements

The completion of this work would not have been possible without the support and mentorship of many exceptional people.

I would like to express my deepest gratitude to my supervisor, Professor Reinhard Vehring, for his unwavering encouragement and guidance throughout this journey. His invaluable insights into both science and life have shaped me profoundly. I could not have wished for a better mentor.

I am also greatly thankful to my co-supervisor, Professor Andrew Martin, for sharing with me his expertise in aerosol science and guiding me through the ups and downs of research.

My sincere thanks to my colleague and mentor, Dr. Hui Wang, for patiently introducing me to the laboratory environment and challenging me to grow at every step. I have learned so much from him.

I wish to acknowledge my wonderful research teammates - Mani, Max, Isobel and David for making this group a truly special community in which to work and grow together. A special thanks to Luba Slabyj for her dedicated efforts in editing my writings and providing invaluable guidance through the complexities of paper-writing.

Finally, I would like to thank our industry partners at AstraZeneca – Dr. David Lachuga, Kellisa Lachacz, and Dr. Nicholas Carrigy – for their support and guidance throughout this collaborative journey.

`

Table of Content

`

`

List of Tables

`

List of Figures

`

`

List of Symbols

C_d	Drug concentration
C_{EtOH}	Ethanol concentration
C_f	Formulation density
C_{NV}	Concentration of nonvolatile components
d_r	Diameter of a residual particle
d_i	Diameter of an initial droplet
$d_{c,\,50}$	Content equivalent diameter
GSD_d	Geometric standard deviation of a drug
GSD_i	Geometric standard deviation of initial droplets
I	Possible number of drug particles in a droplet
M	Average number of drug particles in a droplet
MMD_d	Mass median diameter of a drug
MMD_i	Mass median diameter of initial droplets
m_r	Mass of a residual particle
M_t	Total mass of drug particles in #10000 droplets
N	Number of droplets
OD	Orifice diameter
P_A	Ambient pressure
P_e	Expansion chamber pressure
P_{mc}	Metering chamber pressure
$PPUV$	Number of particles per unit volume
q_e	Vapor quality in the expansion chamber
V_d	Total volume of drug particles within a droplet
V_i	Volume of an initial droplet
VS	Valve size
V_{ti}	Total volume of initial droplets
ρ^*	Reference density
ρ_d	Drug density
ρ_p	Propellant density
σ_p	Propellant surface tension
α	Thermal diffusivity

Chapter 1 Introduction

1.1. **Respiratory drug delivery and its advantages**

Respiratory diseases are a major global health challenge and contribute greatly to both morbidity and mortality worldwide. Examples of such conditions include tuberculosis, pneumonia, chronic obstructive pulmonary disease (COPD), asthma, lung cancer, and, more recently, COVID-19. COPD in particular claims the lives of 3.2 million individuals annually, ranking as the world's third-leading cause of death [1–4]. The COVID-19 pandemic has further emphasized the critical nature of respiratory health, with 5.7 million lives lost within a period of two years [2]. Moreover, cases of tuberculosis, which is known for its concealed yet highly infectious nature, were reported to be 10.4 million in 2017 [5]. These statistics highlight the widespread and complex nature of respiratory diseases on a global scale and the need for comprehensive strategies to address and improve respiratory health.

In the context of treating pulmonary conditions, inhalation therapy is one of the oldest and most widely used approaches for delivery of drug to the lungs. In ancient days, people used to inhale opium for both medicinal and recreational purposes by using tools like incense burners and pipes [6]. In modern medicine, inhalation drug delivery has gained a lot of attention, particularly in the treatment of respiratory conditions. Unlike other routes, the pharmacokinetics of inhaled pharmaceutical ingredients (APIs) are unique in offering a rapid onset through direct absorption in the lungs, localized effects, and limited systemic distribution. Factors such as particle size, formulation, pulmonary blood flow, and individual patient characteristics can greatly impact drug absorption [3]. Inhaled therapeutics may be eliminated through coughing, mucociliary clearance, alveolar macrophages or by metabolism in the lung tissue [7]. A good understanding of these complexities is very important to optimizing efficacy and lessening potential side effects in the treatment of respiratory conditions.

Respiratory medications for treating asthma and COPD are generally categorized into two main classes: bronchodilators and glucocorticoids. Bronchodilators can be further subcategorized into β-agonists and antimuscarinics. These two classes of bronchodilators differ mainly in the receptors they target and their mechanisms of action. Short-acting β-agonists (SABA) are effective for the rapid relief of bronchospasm, typically providing therapeutic effects for up to 4 hours. In contrast, Long-acting β-agonists (LABA) are recommended for the management of COPD and asthma,

`

offering a longer duration of action, usually around 12 hours. Antimuscarinics are mainly long-acting bronchodilators (LAMA) that are usually effective for COPD patients. Glucocorticoids (ICS) are commonly used to manage lung inflammation and have shown improvement in pulmonary function for asthmatic patients [8, 9]. Examples of these medication classes are outlined in Table 1.1.

Table 1.1. Selected active pharmaceutical ingredients (APIs) in the treatment of asthma and COPD [8]

Medication class	**API**	**Indication**	**Inhaler**
SABA	Epinephrine	Acute relief of symptoms associated with asthma only	pMDI
	Albuterol	Bronchospasm of any cause	pMDI, DPI, Nebulizer
LABA	Formoterol	Chronic treatment of asthma and COPD	DPI, Nebulizer
	Salmeterol	Chronic treatment of asthma and COPD	DPI, pMDI
SAMA	Ipratropium	Maintenance treatment of COPD	pMDI
LAMA	Tiotropium	Maintenance treatment of COPD	Single dose DPI, multidose SMI
	Glycopyrrolate	Maintenance treatment of COPD	Dingle dose DPI
ICS	Beclomethasone dipropionate (BD)	Asthma and COPD chronic use	pMDI
	Budesonide	Asthma and COPD chronic use	DPI

There are two main routes for aerosol drug delivery: intranasal delivery and oral inhalation. Intranasal delivery involves administering an aerosolized liquid formulation through the nostrils so that the drug is deposited in the nasal cavity. This route offers benefits like ease of use for patients but is limited by high mucociliary clearance, leading to poorer bioavailability than deposition in the lungs [3]. Oral inhalation delivers the drug formulation as an aerosol through the mouth directly to the lungs. This route provides more efficient drug delivery and higher bioavailability as the large surface area of the lungs allows rapid drug absorption into the circulatory system [3, 10]. Ultimately, the choice between intranasal and inhalation delivery depends on the specific drug and desired therapeutic effect. Factors like the drug's site of action, required dosage, and device design compatibility with patient factors (e.g. age, health condition) need to be considered [3, 11].

`

In the scope of improving drug delivery methods, researchers are focusing on the potential of inhaled vaccines. This method is gaining attention for its needle-free application, which provides a safer alternative for individuals suffering from needle phobia and minimizes the risk of needle-stick injuries. Inhaled vaccines are also capable of inducing both systemic and mucosal immune responses. However, they pose certain challenges with respect to cost, the selection of suitable inhaler devices, and the use of effective drug carriers and adjuvants [12]. These challenges further highlight the need for research and development in inhaler devices and formulations.

1.2. **Respiratory drug delivery devices**

Currently inhalers can be categorized into four main devices [13]:

a) Nebulizers
b) Dry powder inhalers (DPIs)
c) Soft mist inhalers (SMIs)
d) Pressurized metered dose inhalers (pMDIs)

Nebulizers are inhaler devices usually formulated with an aqueous suspension or solution that can deliver drug to a patient through tidal breathing. The process in which a nebulizer generates aerosol can generally be categorized into three techniques: jet nebulization, high frequency atomization and colliding jets. Each method has a different mechanical strategy to generate droplets, but detailed discussion of these is beyond the scope of this thesis. Traditional nebulizers were not portable and required patients to be in a hospital or at home with special facilities such as compressed gas. Despite their ability to deliver high dosages, these traditional nebulizers were time-consuming, often requiring several minutes to deliver their dose over multiple breaths [14]. Modern nebulizers, however, have evolved to be more portable and user-friendly, enabling more flexible use. These devices can deliver medication over several minutes, allowing patients to breathe normally during the process. This multi-breath, extended delivery time is a key characteristic of nebulizer use, and it is particularly beneficial for patients who may struggle with single-breath inhalers [15].

Dry Powder Inhalers (DPIs) are affordable devices with the capacity to deliver varied drug doses to patients. Unlike nebulizers, DPIs often operate passively, meaning that they rely on the patient's deep inhalation for drug intake. However, this reliance on inhalation poses challenges for very

`

young children or infants [16]. This dependence on the patient's breathing pattern also impacts dose content uniformity of the delivered drug. The dry nature of DPIs adds to their complexity, making them sensitive to environmental conditions such as humidity. Hence, under specific conditions DPIs can be susceptible to particle growth or crystallization [17]. Moreover, in contrast to pMDIs, whose standardized design across different brands simplifies their use, DPI devices exhibit diverse designs, and transitioning to a new class of DPIs may therefore require patient retraining. Despite such challenges, the pharmaceutical industry has shown an increasing interest in DPIs as potential replacement for pMDIs. This shift is driven largely by the lower global warming potential associated with DPIs, aligning them with the increasing emphasis on environmentally friendly healthcare practices [18].

pMDIs are the most widely used devices for treating pulmonary diseases. They were first introduced in 1956 by Riker Laboratories for the management of asthma and COPD, with their basic design resembling that of current pMDIs [19]. Early pMDIs used chlorofluorocarbons (CFCs) as propellants because of their non-toxic and compatible properties. However, after the signing of the Montreal Protocol in 1987 for the elimination of CFC propellants due to their contribution to ozone depletion, pharmaceutical companies began to develop alternative inhalers [20]. Through an extensive search for a replacement for CFCs, pharmaceutical companies identified HFA-134a and HFA-227ea as top choices. The first HFA pMDI was released to the market by 3M in 1995 [19]. This replacement was not only about changing the propellant. Many investigations were conducted to adjust the pMDI hardware (e.g., elastomers) and formulation (e.g., excipients) for greater compatibility with the new propellants [21].

In the formulation of pMDIs, the choice between suspending or solubilizing the drug in the propellant depends on the physicochemical properties of the components. The introduction of the first solution pMDI, QVAR, in 1995 marked a great advancement. In this formulation, ethanol was used as a co-solvent to solubilize BDP in the HFA-134a propellant, resulting in finer aerosol generation and enhanced peripheral lung deposition compared to traditional pMDIs [22]. Also, solution pMDIs exhibit greater homogeneity, eliminating the need for patients to shake the device before use. However, a challenge arises as most drugs are insoluble in HFA propellants, necessitating the use of co-solvents in the formulation. This addition can impact the delivery process. For instance, the addition of ethanol reduces the vapor pressure of the formulation,

`

directly influencing the atomization process and leading to the generation of coarser aerosols. Moreover, increasing the concentration of ethanol decreases the evaporation rate of droplets, leading to increased mouth-throat deposition and lower dose delivered to the lungs [23].

In suspension pMDIs the addition of suspending agents is often crucial to ensure proper dose content uniformity [24] and is not without its own challenges. For instance, the partial solubilization of the suspended drug can lead to particle growth through a phenomenon known as Ostwald ripening, in which smaller particles solubilize and larger particles grow to reduce the overall free energy of the system [25]. Despite such challenges, the formulation of pMDIs in a suspension format continues to be prevalent in commercial products. Several factors account for this choice, including the development of promising suspending agents, less drug degradation compared to solution pMDIs, and simplified manufacturing processes [23]. One approach to improving suspension stability in pMDIs is the use of cosuspensions, whose drug microcrystals irreversibly associate with porous particles, resulting in enhanced suspension stability and uniform delivery of respiratory drugs [26]. Thus, understanding the stability of suspension pMDIs formulations is quite essential, and exploring it involves investigating effective excipients and ensuring the physical stability of the inhaler, both of which subjects will be discussed more thoroughly in the next section.

1.3. **pMDIs and their contribution to global warming**

1.3.1. Propellants in pMDIs

As discussed in the last section, chlorofluorocarbon (CFC) propellants were phased out because of their ozone-depleting properties and replaced with hydrofluoroalkanes (HFAs). The transition to HFAs posed a challenge because of their solvation properties in pMDIs. Following European Union regulations set forth in 2011, which mandated the use of fluorinated gases with a global warming potential (GWP) below 150, various industries, including pharmaceutical companies, searched for alternatives to HFAs due to their high GWP (1530 for HFA-134a and 3600 for HFA-227ea) [27]. The GWP is a measure of a gas's 100-year warming potential relative to carbon dioxide (CO2), whose GWP is 1 [28]. In 2016, HFAs began to phase down under the Kigali Amendment to the Montreal Protocol despite the fact that HFA propellants in pMDIs contribute only around 0.05% to total greenhouse gas emissions [29–31]. Three potential replacements for

`

HFA propellants were introduced due to their low GWP: HFC-152a with a GWP of 138, and HFO-1234ze and HFO-1234yf, both with a GWP of less than 5 [32].

Several considerations must be taken into account when replacing HFAs with new propellants. The new propellants should be toxicologically safe, exhibit little to no flammability, and be compatible with pMDI components [33]. Studies on HFC-152a have not identified serious safety concerns for human inhalation, but its flammability can pose issues in pMDI production. HFO-1234yf, while showing lower inertness than HFAs, has shown potential health risks at high exposure levels (>75000 ppm) according to toxicology studies [34]. HFO-1234ze has been the focus of many recent medical propellant studies due to its low GWP and similarity to the established HFA-134a, but further investigations are required to ensure its safety for human inhalation use [35].

The challenge of using a new propellant such as HFO-1234ze in pMDIs requires a thorough assessment of its physicochemical stability when combined with established excipients and micronized drugs. Key factors influencing the performance of pMDIs include drug solubility, suspension stability, aerosol characteristics, and electrostatic charge [36]. Similar solubility patterns are observed in HFO-1234ze and HFA-134a, but with the former exhibiting lower water solubility. For hydrophilic drugs, reformulation to a suspension is suggested because of their insolubility in the established and new propellants. Because the majority of pMDIs are in suspension form, the density difference between the propellant and suspended particles significantly influences formulation stability, with HFC-152a potentially causing sedimentation that can be resolved using suitable excipients [27]. Electrostatic properties vary among propellants, with HFO-1234ze having a near-zero net charge, while HFAs and HFC-152a have a positive net charge, with HFC-152a exhibiting the highest. These arguments highlight the need for exploring the properties of new propellants and the selection of appropriate excipients to ensure optimal performance and stability in pMDI formulations [37].

1.3.2. Excipients in pMDIs

In the field of inhalation drug delivery, various excipients serve specific functions. Commonly used excipients such as sugars, phospholipids, amino acids, and oligopeptides play a pivotal role in stabilizing biologics that lack inherent stability. These excipients may function as glass stabilizers, suspension stabilizers, dispersibility enhancers, bulking agents, controlled release

`

agents, and more [38]. Glass stabilizers are typically inert sugar molecules in amorphous form that can elevate the glass transition temperature and protect biotherapeutics from desiccation. While suitable for spray-dried powders, cohesive sugars like trehalose may require the addition of a surface-active excipient. Examples of sugar molecules for glass stabilization include trehalose, glucose, and sucrose. Amino acids such as leucine and oligopeptides like trileucine are often combined with glass stabilizers to enhance the dispersibility of the formulation [34, 35]. These dispersibility enhancers are hydrophobic and can alleviate moisture-induced issues associated with amorphous sugars like trehalose, which tend to recrystallize upon exposure to moisture and can adversely affect aerosol performance [40]. Studies have shown that using sufficient amounts of leucine or trileucine along with trehalose enhances the dispersibility of dry powder formulations. It should be noted that, compared to leucine, a much smaller amount of trileucine is capable of increasing the stability of DPIs [41].

Phospholipids are endogenous materials that can be found in the lung surfactant. They consist of a hydrophilic phosphate head group and hydrophobic tail(s). Because of their unique amphiphilic structure, phospholipids aggregate in water and form various configurations like micelles, lamellae, and liposomes [42]. Also, phospholipids can be formed as microparticles, which, unlike the other configurations, do not have to be in a liquid formulation. DSPC (Distearoylphosphatidylcholine) and DPPC (Dipalmitoylphosphatidylcholine) are examples of lipid microparticles that have been extensively studied for their viability in drug delivery either independently or in combination with other components [43]. In particular, microparticles consisting of DSPC and $CaCl_2$ have undergone comprehensive research in the literature to produce new technologies such as the Pulmosphere^{TM} porous particle [44–46], cosuspension [26, 47, 48], and rugose lipid particles [49]. All of these microparticles are engineered using spray drying, a technology that will be discussed in the next section.

1.4. **Particle engineering using spray drying**

Spray drying is a well-established technique for designing and manufacturing particles with customized characteristics. The preparation of feedstock is a critical step prior to spray drying. Feedstock can range from a simple solution to a complex multiple emulsion or suspension. The design and preparation of the feedstock can add extra sophistication to the properties of final particles [50]. The spray drying process starts by pumping a well-mixed liquid feed to a rotary

`

atomizer or to twin-fluid atomizers placed inside industrial spray dryers. In rotary atomizers, the liquid feed breaks down into droplets by hitting a rotational disk with an adjustable rotation rate. In twin-fluid atomizers, atomizing gas with high pressure is used to create droplets, the size of which depends on the mass flow rates of the feed and atomizing gas. Subsequently, the droplets undergo a drying process, evaporate, and form residual particles that can be collected in the cyclone [51]. The process of particle formation in a spray dryer is well-understood and can be explained by particle engineering.

The control of particle morphology, including density, surface roughness, composition, radial distribution of components throughout the particle, etc., can be managed through the drying process for a given feed composition and droplet size. The drying process is a heat and mass transfer problem that can be analyzed by examining the radial dimension of a droplet [50–52]. This problem is governed by two key transport phenomena: evaporation and diffusion. The balance between these two effects is characterized by the Peclet number,

$$P_e = \frac{k}{8\,D}\,, \tag{1.1}$$

where k in the equation represents the evaporation rate and D is the diffusion coefficient. While finding the evaporation rate (k) for a single solvent system is straightforward, solving for co-solvent systems with different evaporation rates requires numerical modeling, which is beyond the scope of this discussion and has been thoroughly discussed in the literature [53].

The Peclet number describes the balance between the velocity of surface recession and diffusion. In high Peclet numbers, the evaporation rate at the droplet's surface is very fast compared to the diffusion rate of solute molecules within the droplet. As solvent evaporates rapidly from the surface, solute accumulates there because diffusion cannot keep pace to spread it evenly back into the interior. By contrast, in small Peclet numbers diffusion occurs, resulting in an even distribution of material throughout the droplets. Another useful parameter is E_i, which indicates the surface enrichment and can be found using equation [52]:

$$E_i = 1 + \frac{P_e}{5} + \frac{{P_e}^2}{100} - \frac{P_e^3}{4000} \quad \text{when } P_e < 20. \tag{1.2}$$

`

In scenarios with high Peclet numbers, when the surface reaches critical saturation different morphologies may form, leading to varied particle structures such as hollow, dimpled, wrinkled, porous, etc [50]. In pulmonary drug delivery, particles with low density are often desired because they have good dispersibility and aerosol performance. Engineered Pulmospheres^{MT} are low density particles made by spray drying an emulsion that consists of perfluorooctylbromide (PFOB), DSPC, $CaCl_2$ and a continuous phase. The active is suspended or dissolved in the continuous phase. PFOB functions as a pore former in the particle formation process. Its evaporation rate is slower than in the continuous phase. Therefore, as the drying process progresses and the initial particle morphology is established, PFOB evaporates, creating small voids within the particle [34, 47, 51, 52]. Cosuspension technology takes a similar approach; however, the active crystals are not added to the emulsion feedstock. Instead, porous particles and active crystals are added to the propellant separately. This cosuspension technique preserves the drug-crystals from possible changes during the spray drying and enables the formulation of combination pMDIs [43, 44].

Rugose lipid particles, on the other hand, have a similar feedstock to porous particles but lack PFOB as placeholders. During spray drying, as the droplets pass through the spray dryer, the temperature drops below the lipid's main phase transition temperature. At this point, because of their high Peclet number, suspended lipid nanoparticles accumulate on the surface of the particles, forming a shell. This shell later folds in the outlet dryer and creates a rugose structure. The degree of rugosity is highly dependent on the processing temperatures, with the feedstock and drying temperature being either above or below the glass transition of the lipid and to what extent. The detailed particle formation process is still not completely understood and requires further investigation. However, these particles have demonstrated excellence in terms of dispersibility and suspension stability, making them a strong candidate in drug delivery applications [39, 46, 53]. Figure 1.1 shows a graphical summary of the manufacture of pMDIs containing rugose lipid particles.

`

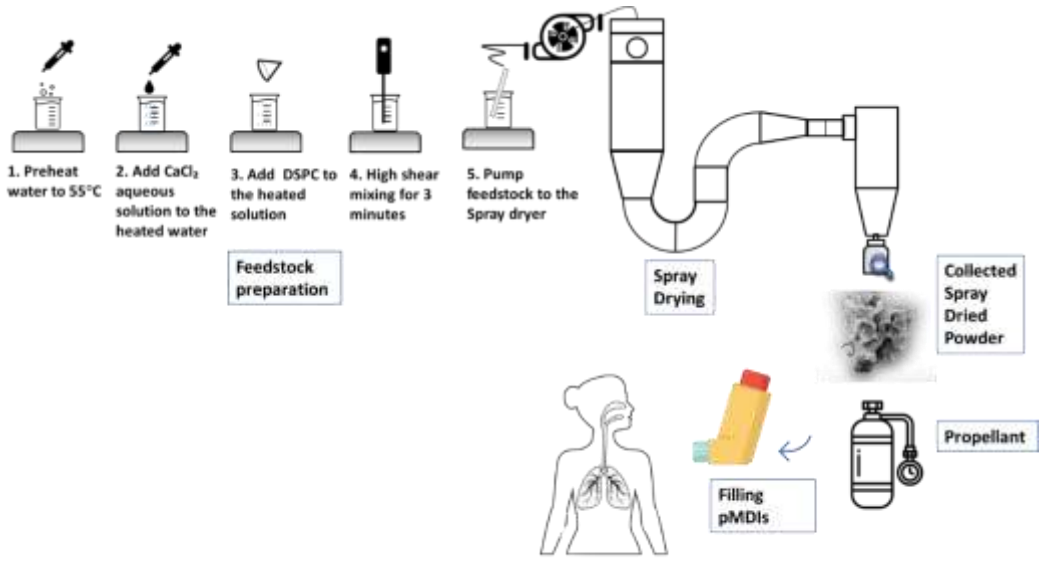

Figure 1.1. Feedstock preparation and spray drying process for making rugose lipid particles

1.5. **Introduction to Lung geometry and deposition mechanisms**

The human lung has a complicated branching structure and airflows that make it difficult to model the fate of particles throughout the respiratory tract. However, simplified lung models that capture basic airflow and transport phenomena can still provide useful insights into aerosol drug delivery [57]. Figure 1.2 shows a simplified schematic of the respiratory system. The lung is divided into three main regions: the extrathoracic region, the tracheobronchial region, and the alveolar region. The extrathoracic region includes structures like the mouth, nasal cavities, pharynx and larynx. The tracheobronchial region, often known as the conducting region, includes generations 0–16 of the branching airways, where little gas exchange occurs. The alveolar region consists of the most distal generations (17–23) and is the primary site of gas exchange via small air sacs called alveoli [54, 55].

For inhaled drugs to reach their targeted region, they must successfully navigate the conducting airways without any notable deposition until they reach that destination area. The site of deposition depends on factors like particle size and shape, and the inhalation manoeuvre being employed. For example, efficiently delivering anti-inflammatory agents requires depositing the drugs around

`

inflamed areas. By contrast, systemically acting drugs need to enter the bloodstream, a process that requires deposition in the alveolar region [59].

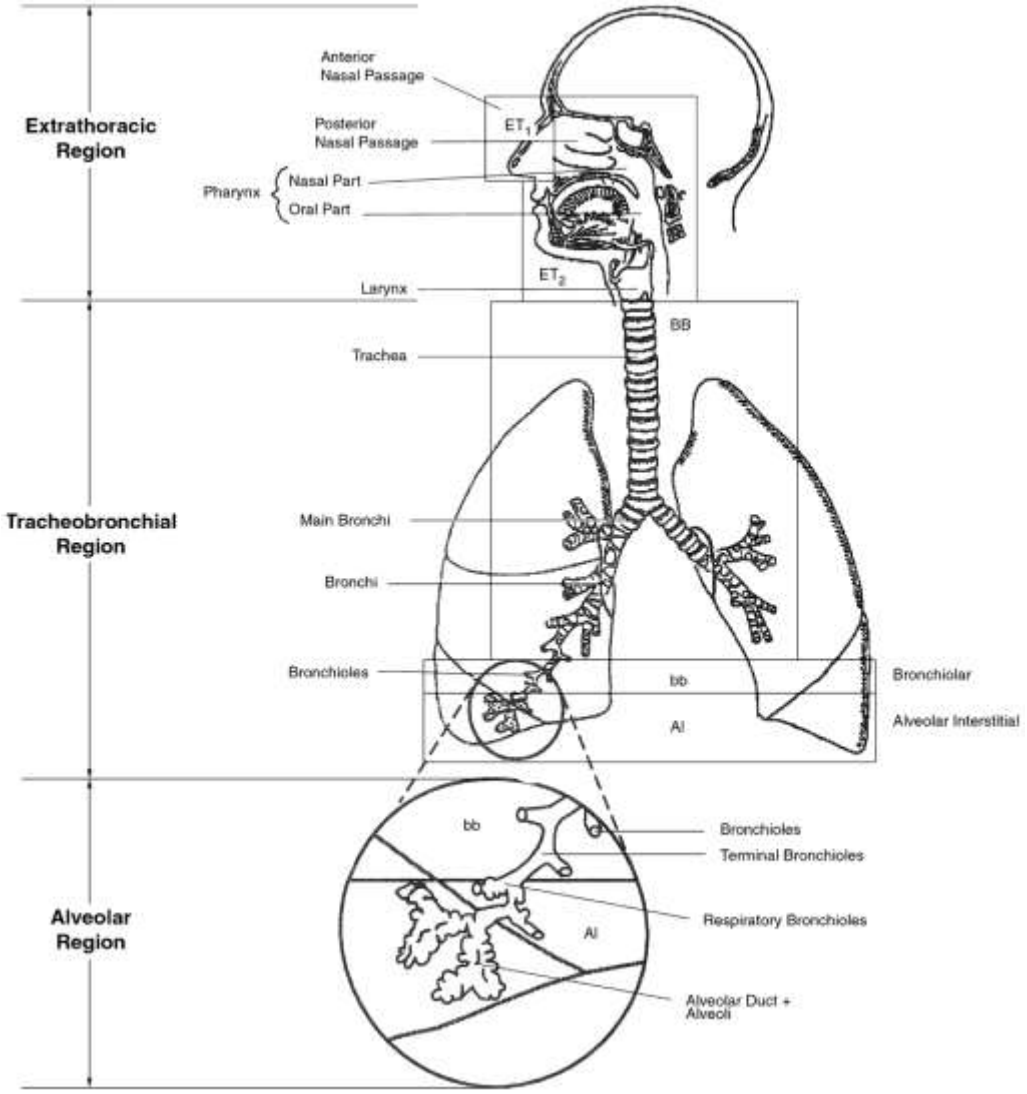

Figure 1.2. Human respiratory tract diagram (adapted from [60]*) .*

Deposition of particles in the respiratory system is governed mainly by three mechanisms: gravitational sedimentation, inertial impaction and Brownian diffusion. The contribution of each mechanism depends on the inhalation flow rate, size and density of the particles, as well as on the lung geometry. Deposition by inertial impaction occurs in bifurcations like the trachea-to-bronchus transition, where the larger momentum of particles fails to closely adhere to the rapidly shifting airstream. The probability of particle deposition due to inertial impaction rises with increases to the particle size, particle density and/or inhalation flow rate. Inertial impaction is most likely to

`

occur in the upper respiratory tract. Particles in the range of 1-8 μm that escape upper impaction deposit in the lower airways via gravitational sedimentation [59]. Smaller particles are most likely to deposit by Brownian diffusion, a mechanism in which small particles exhibit random motions due to their collision with gas molecules. This type of deposition occurs mainly in the alveolar region. Generally, in high flow rates particles deposit more readily through inertial impaction rather than diffusion or sedimentation [59, 60]. This high-level summary shows the significance of factors such as flow rate and particle size for efficient drug delivery to the lungs. In the next section, the process by which pMDIs perform is described, and the influence of different variables on the performance of these devices is discussed.

1.6. **How pMDIs work**

Figure 1.3 shows a schematic of a pMDI. A pMDI consists of three main components: a canister, an actuator, and a metering valve, with the drug formulation contained within the canister. The canister is securely sealed, and when a patient presses down on the canister to activate the pMDI, the valve stem moves through the metering valve, allowing a precise dose of the drug formulation to be released from the canister. The formulation then enters an expansion chamber within the device, where it undergoes atomization from a liquid to a spray plume as it rapidly mixes with air. The actuator features an orifice through which the spray plume passes on its way to potential deposition sites in the respiratory tract [58, 59].

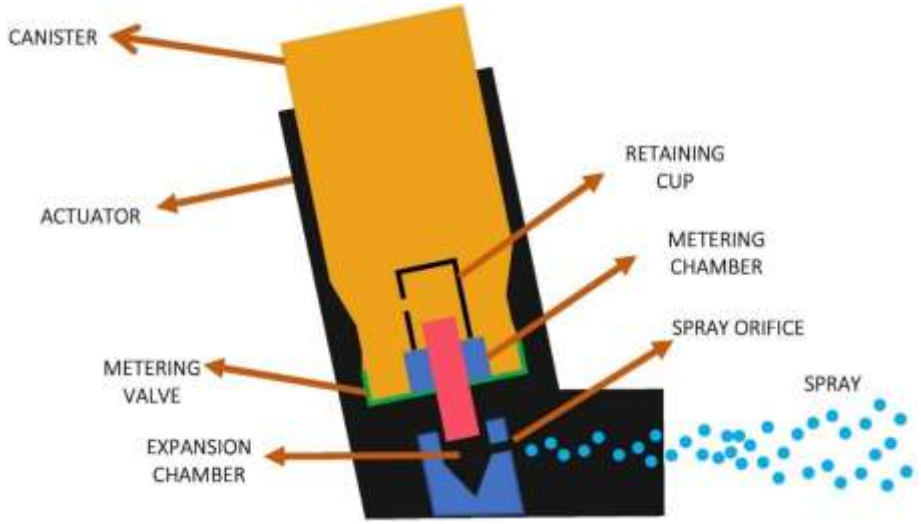

Figure 1.3. Schematic of a pressurized metered dose inhaler and its components (adapted from [63]*)*

`

1.6.1. pMDI plume

The characteristics of a pMDI plume, such as its velocity, duration and temperature, can significantly impact deposition in the respiratory tract. Obsolete CFC propellants often produced high velocity, cold plumes leading to greater impaction in the mouth-throat and lower lung dose than the more gentle HFA plumes [64]. Specifically, higher initial plume velocities upon actuation result in greater inertial impaction in the throat region, reducing the fraction of inhaled particles that can penetrate into the lungs [65]. However, the high initial velocity decays rapidly as the aerosol plume expands and slows down after leaving the actuator orifice [65]. In addition to plume velocity, some propellants, such as HFC-152a, cause significant evaporative cooling, producing plumes well below 0°C that are unpleasant for the patients and compromise coordination of actuation with inhalation [66]. The specific spray properties like velocity, duration, and temperature depend on multiple factors including pMDI geometry, propellant type, vapor pressure, and drug concentration [67]. Expansion chamber volume can also influence the properties of generated plume, albeit minimally [19]; that is, larger expansion chambers can provide adequate space and time to the bubbles to nucleate and produce fine aerosols [68]. Smaller actuator orifices can increase plume exit velocity but may not increase throat deposition if coupled with a slow-moving, wide angle “soft mist” plume [69, 70]. Spacers placed on the mouthpiece increase the travel distance of the plume, allowing more time for deceleration and expansion, which decrease oropharyngeal deposition [71]. Overall, optimizing characteristics like velocity, temperature, duration and geometry through the careful selection of propellants, co-solvents and device design is critical to improving the efficiency of pMDI delivery to the lungs. [19].

1.6.2. Effect of environmental conditions

Studies have suggested that elevated relative humidity can negatively impact inhaled aerosolized drugs. Hygroscopic growth in aerosolized droplets, a phenomenon in which evaporating cooled droplets reach the air’s dew point resulting in water condensation on the droplets, occurs more frequently under high humidity conditions. This happens because the dew point increases with the relative humidity [72]. As discussed earlier, larger aerosol droplet sizes contribute to greater mouth-throat deposition, subsequently reducing pulmonary drug delivery efficiency. Furthermore, studies have demonstrated that changes in ambient air temperature can impact the performance of pMDIs [73]. Shemirani et al. observed that suspension-based pMDI formulations exhibit minimal alterations in lung and throat deposition at higher temperatures; however, for solution-based

`

pMDIs, they noted that increasing the temperature results in a notable reduction in throat deposition and increase in lung dose [74]. They hypothesized that this reduction is linked to changes in spray plume velocity and evaporation rates. Furthermore, Morin et al. have shown that lower ambient temperatures (-10 – 0 °C) are associated with a noticeable decrease in respirable lung dose for both suspension and solution pMDIs, emphasizing the influence of temperature on aerosol characteristics [73].

Overall, environmental factors such as relative humidity and air temperature influence the efficacy of inhaled aerosolized drugs by impacting droplet size and deposition patterns in the respiratory tract. These in turn ultimately affect pulmonary drug delivery efficiency to targeted sites in the lungs. Careful control and monitoring of these parameters is critical when evaluating the performance of existing and novel inhalation products.

1.7. **Assessing the performance of pMDIs**

1.7.1. Experimental methods

One of the criteria against which the performance of pMDIs can be evaluated is the physical stability of the emitted particles, particularly their morphology and size. The United States Pharmacopeia (USP) has established a standard according to which the mass median aerodynamic diameter (MMAD) of these particles should be less than 5 micrometers for optimal delivery to the lungs [75]. This standard is part of compendial testing, a method used to assess and describe the performance of both the device and the formulation. Compendial testing adheres to the recommendations of organizations like the USP and the European Pharmacopoeia, or the guidance of regulatory bodies such as the United States Food and Drug Administration and the European Medicines Agency. The goal of these recommendations is to ensure that devices on the market meet quality control metrics like consistency and accuracy in delivered dose [76].

Given the inherent polydispersity of aerosolized drugs, it is crucial to assess the aerodynamic particle size distribution (APSD) [77]. This assessment provides reliable insights into *in vivo* deposition when conducted accurately. The Next Generation Impactor (NGI), introduced in 2003, is a seven-stage impactor with adaptable flow rates that has improved productivity over cascade impactors [78]. The NGI can be equipped with model throats capable of capturing particles depositing in the mouth-throat region [79]. The USP induction port is a simplified geometry

`

designed to capture large fast-moving particles that would most likely deposit in the mouth-throat region [80].

Alternative throat models, such as the Alberta Idealized Throat (AIT), may improve *in vitro-in vivo* correlations (IVIVCs) [81]. The AIT is an idealized model of the human throat used to study the deposition of inhaled pharmaceutical aerosols. It is designed to mimic the average human throat and is used to predict the deposition of aerosols in the human respiratory tract [81]. NGI measurements yield the mass of particles at different stages with specific cut-off diameters, enabling the calculation of the Fine Particle Fraction (FPF), which represents particles with aerodynamic diameters less than 5 μm [75]. The APSD can also be measured using the NGI and is required by the Food and Drug Administration (FDA) for pMDI and DPI development inasmuch as it provides information on lung dose distribution [82]. From the APSD measurement, the MMAD and geometric standard deviation (GSD) can be derived.

Another instrument, the Aerodynamic Particle Sizer (APS), can directly measure the APSD of aerosols by determining particle aerodynamic size through the measurement of particle velocity in an accelerating airflow. This technique allows for the calculation of the aerodynamic diameter of each particle [83]. Delivered Dose Uniformity (DDU) is also vital for pMDI assessment, as emphasized by the FDA [82]. DDU involves measuring the emitted drug mass at various time points to ensure consistent dosage throughout the product's lifespan [82].

Additionally, the morphology of residual particles significantly impacts drug delivery efficiency, with high-density particles more likely to deposit in the extrathoracic region [59]. In suspension pMDIs, particle fusion or crystal growth can lead to a drastic increase in the APSD of emitted particles, resulting in higher mouth-throat deposition [23]. The role of suspension stability in emitted dose properties is extensively discussed in Chapters 2 and 3, which highlight the need for valid methods, such as shadowgraphic imaging [56], to monitor suspension behavior over the product's shelf life.

1.7.2. Simulation methods

While *in vitro* measurements such as APSD, DDU, and suspension stability play a crucial role in pMDI and DPI development, pre-measurement simulations are also highly useful and desirable. These simulations can reduce the need for extensive trial and error, providing an understanding of

`

the proximity to ideal measurements and formulations where components do not interact. Over the past few decades, various models have been developed to predict the performance of pMDIs. One approach involves using computational fluid dynamics (CFD) to simulate pMDI plume characteristics and predict drug deposition in the human airway [84]. Another popular approach, introduced by Clark, involves using numerical models to assess the atomization process in pMDIs equipped with twin-orifice systems to predict the size of initial droplets emitted from pMDIs [85]. This method has more recently been modified by other researchers to enhance predictions of temporal droplet size and spray velocity, which significantly impacts drug deposition in the human airway system [75, 76]. Yet another approach uses dimensional analysis to create an empirical equation for estimating initial droplet size based on the propellant characteristics [88]. A straightforward yet effective method that is discussed extensively in Chapter 3 is the use of Monte Carlo simulation—a random-number-based technique to predict the APSD of residual particles. Initially introduced by Chan and Gonda [89], this model has been further developed by Stein et al. [90] and can provide valuable insights for predicting size distribution in various formulations with diverse propellant types, drug sizes, and concentrations.

1.8. **Summary of the thesis**

So far, an overview of respiratory drug delivery has been presented with a specific emphasis on understanding pMDIs. The thesis will concentrate on examining the physical stability of particles emitted from pMDIs containing various drug formulations and propellants. The research presented uses both experimental and modeling approaches to investigate parameters influencing the stability of suspended particles in pMDIs, such as the correlation between colloidal stability and overall pMDI performance. The objective is to enhance our understanding of pMDI aerosol properties, providing insights for enhanced formulation design and device engineering.

Chapter 2 investigates the feasibility and stability of novel rugose lipid particles (RLPs) as suspending excipients in pMDIs containing both established HFA propellants and the new low-GWP propellant HFO-1234ze. RLPs produced at two different spray drying temperatures will be compared to assess the impact of manufacturing conditions on particle morphology and performance over time. A quantitative analysis of the propellants' relative suspension stability will be presented with reference to measurement techniques such as shadowgraphic imaging and visual evidence from scanning electron microscopy. RLP suspensions will be benchmarked against a

`

trehalose-leucine formulation and engineered porous particles to provide perspective on their viability. This discussion will provide valuable insights into the compatibility of RLPs with current and future propellants for pMDIs.

Chapter 3 will focus on the use of modeling approaches to predict the aerodynamic particle size distribution (APSD) of aerosols emitted from pMDIs. In particular, it will discuss the use of a Monte Carlo simulation method implemented in Python to investigate how properties of a formulation, such as initial droplet size distribution, drug particle size distribution and concentration, impact the APSD of residual particles exiting the pMDI. The simulation outcomes will be compared to experimental APSD data to assess the accuracy of predictions. Additionally, this chapter will outline the use of the Monte Carlo simulation in a parametric study to demonstrate how effectively it can account for various parameters known to influence pMDI performance. The key goal is to evaluate the usefulness of simplified numerical models in providing initial guidance during pMDI formulation development when experimental data is not yet available.

`

Chapter 2 Novel rugose lipid particles for stabilizing biologics

2.1. Introduction

Pressurized metered dose inhalers (pMDIs) have long been recognized as one of the most popular and effective devices for delivering drugs to the lungs. Over the past few years, their role has gained even greater importance due to their potential for delivering vaccines. However, with the increasing focus on environmental sustainability and the need to reduce greenhouse gas emissions, there has been a pressing call to transition to low-global-warming-potential propellants in pMDIs. This transition was initiated following the Montreal Protocol, which outlined critical steps to phase out substances that contribute to ozone depletion and global warming.

Because of these environmental considerations, we need to conduct thorough studies to make sure these new, environmentally friendly propellants work well with the common excipients and active medicines in inhalers. This is crucial to ensure the safety and effectiveness of the medicines for patients.

The study I am discussing here is a detailed investigation of using a new propellant known as HFO-1234ze in pMDIs. In this study, we have used novel rugose particles (developed by Hui Wang in particle engineering research group at University of Alberta) as suspending agents. Our main goal was to assess how well pMDIs with HFO-1234ze perform in comparison to those with two others established propellants (HFA-134a and HFA-227ea). To reach better perspective about performance of these pMDIs, their physical stability was also compared to pMDIs with well-known excipients. Section 2.2 is presented without alteration but header numbers of the submitted manuscript[1]. Section 2.3 is presented in a conference proceeding[2] and is slightly modified to save the chronological order and coherence of the chapter.

[1] Minootan Z, Wang H, Connaughton P., Lachacz K, Carrigy N, Ordoubadi M, Lechuga-Ballesteros D, Martin AR, Vehring R. On the feasibility of rugose lipid microparticles in pMDIs with established and new propellants. *AAPS PharmSciTech.* Submitted Octobor 10, 2023

[2] Minootan Z, Wang H, Carrigy N, Lachacz K, Lechuga-Ballesteros D, Martin AR, Vehring R. The stability of novel rugose particles in pressurized metered dose inhalers. *AAPS PharmSci 360*, Orlando, FL, October 22-25, 2023

`

2.2. On the Feasibility of Rugose Lipid Microparticles in Pressurized Metered Dose Inhalers with Established and New Propellants

2.2.1. Introduction

Chronic respiratory diseases are a growing problem worldwide due to an aging population and greater exposure to risk factors such as airborne pollutants, tobacco use, and allergens [4]. Among the current therapeutic approaches used for delivering medications to the lung for managing such diseases, the pulmonary drug delivery route is considered advantageous because aerosolized drugs can target the lung directly [9, 47, 80]. Moreover, pulmonary drug delivery offers the potential for quick treatment at a low dosage with fewer systemic side effects, higher patient satisfaction, and simpler administration compared to other delivery routes [1, 5]. Depending on dosing requirements, formulation options, and the target patient population, different delivery devices can be used. Nebulizers, dry powder inhalers (DPIs), and pMDIs are well-developed devices for delivering inhalable therapeutics to the lung [13].

pMDIs have been widely used for drug delivery to the lungs since their invention in 1956. The enduring popularity of pMDIs stems largely from their portability and low manufacturing cost [6]. A pMDI formulation consists of a suspension, or solution, of drug in a volatile liquid propellant held under its own vapor pressure inside a canister. Propellants are a crucial component of pMDI formulations, providing the required pressure and energy to drive droplet atomization [22]. Prior to the 1990s, chlorofluorocarbons (CFCs) were used as the propellants in pMDIs, but CFCs were gradually phased out as ozone-depleting substances following the 1987 Montreal Protocol [31]. Since then, ozone-friendly hydrofluoroalkane (HFAs) have primarily been used by pharmaceutical companies in their pMDI products [31]. However, due to the high global-warming potential (GWP) of currently used HFA-134a and HFA-227ea propellants, a transition to low-GWP alternatives is now underway [30]. HFO-1234ze is a new propellant candidate currently under consideration for use in pharmaceutical applications. It has several advantages over other propellants, such as a near-zero GWP, low flammability, and low toxicity. Its physicochemical properties are fairly similar to those of HFAs [23, 25]. Nevertheless, it is important to conduct further research and development to investigate the compatibility of pMDI formulations with HFO-1234ze, owing to differences in properties such as water solubility and density when compared to conventional HFA propellants. The results of such studies are valuable in determining whether HFO-1234ze is a feasible propellant for future pMDI products [35].

`

Developing a new pMDI formulation is a complex process that requires various challenges to be addressed. The insolubility of most drugs in propellants has led to the prevalence of suspension formulations. A main challenge is to ensure the physicochemical stability of the formulation, which depends on the compatibility of drugs and excipients with the chosen propellant [23]. In the case of suspension pMDIs, the addition of stabilizing agents and excipients may be necessary to prevent issues such as aggregation and rapid flocculation and to maintain a particle size range of 1-5 μm [93–95]. One of the common types of excipient used in pMDI formulations is surfactants, which are usually used to increase drug solubility, prevent particles from sticking to container walls or valve components, and stabilize the drug dispersion by reducing particle agglomeration [96]. Also, for low-dose suspension pMDI formulations, bulking agents like lactose can help improve dosing reproducibility by minimizing the mobility of the drug particles and ensuring consistent sampling of the formulation by the valve [23]. However, selecting appropriate excipients such as surfactants can be challenging, as studies have demonstrated that no clear relationship can be found between the concentration of the surfactant used and the aerosol performance of the pMDI. Thus, the process of finding an optimal surfactant concentration can be a complicated task [85, 86]. Because of the aforementioned issues, assessing suspension performance during the pMDI development process becomes crucial, and usually a quantitative method is required to examine the suspension stability over time [56]. Many approaches such as dose content uniformity tests [72, 83], dynamic light scattering techniques [94], and visual observations [93] have been developed to determine the colloidal stability of pMDIs. Shadowgraphic imaging is a novel technique that can analyze the colloidal stability of pressurized suspensions quantitatively, and, unlike other methods, it is capable of measuring very unstable samples as well [56].

Unlike stabilizers such as surfactants [23], lipid-based excipients, such as phospholipids, do not need to be dissolved in the propellants, and their unique engineered structure often makes them an excellent suspending agent. They are biodegradable, usually nontoxic, biomaterials that can be spray dried at certain conditions to control their phase transition [99]. Phospholipids, due to their amphiphilic structure, have the capability to form various structures within different size ranges including unilamellar or multilamellar liposomes, micelles, solid lipid particles or porous particles, depending on factors such as their concentration in water and the chosen processing methodology [42]. Phospholipid microparticles with engineered porous structure have been widely used in

`

pMDI formulations and have demonstrated excellent colloidal stability. To manufacture these particles, perflubron oil droplets are used as pore formers, which evaporate at the end of the spray drying process, creating porous-structured microparticles [45]. Recently, rugose phospholipid particles were developed using a novel spray drying approach without the need for a pore former in their manufacturing process. These particles exhibited rough surfaces and good dispersibility in DPI formulations, but their performance in pMDIs has yet to be explored. The particle properties can be adjusted by changing the conditions of the spray drying process, such as the feedstock temperature and drying temperature. To obtain and maintain a rugose particle structure, spray drying conditions, particularly the outlet temperature of the spray dryer, should be kept below the main transition temperature in a way that nevertheless allows for complete drying [39, 46].

Although previous studies found that spray drying temperatures must be maintained within an optimal range to ensure sufficient drying and to maximize particle rugosity, the effect of temperature on the long-term stability of these lipid particles was not clear. Therefore, further research work is needed to evaluate the performance of the new RLPs in inhaler devices such as pMDIs. In this study, the colloidal and physical stability of RLPs manufactured at different temperatures was examined in HFA and HFO-1234ze propellants, and the results were compared with well performing phospholipid microparticles.

2.2.2. Materials and Methods

2.2.2.1. Materials

DSPC (1,2-distearoyl-sn-glycero-3-phosphocholine, 18:0 PC; #850365, Avanti Polar Lipid Inc., AL, USA) and calcium chloride dihydrate ($CaCl_2 \cdot 2H_2O$, Sigma Aldrich, ON, Canada) were used to prepare the spray drying feedstock for the model RLPs. Additionally, PFOB (perfluorooctyl bromide or perflubron) was used as a pore former to prepare engineered porous particles for performance comparison. Trehalose dihydrate (Cat. No. BP2687-1, Fischer Scientific, NJ, USA) and L-leucine (Cat. No. BP385-100, Acros Organics BVBA, Geel, Belgium) were dissolved in demineralized water to make the spray drying feed solution for a lipid-free comparator formulation. Test particles were filled in 10 mL aluminum canisters, capped with 50 µL metering valves (BK357, Bespak Ltd, Kings Lynn, UK), and pressure-filled with propellant to make custom pMDIs for stability tests. For each formulation, a separate pMDI was filled in a custom-designed transparent glass vial for shadowgraphic colloidal stability measurements. Propellants tested in

`

this study included HFA-134a (Part No. GD120-R134a, Gregg Distributors LP, AB, Canada), HFA-227ea (CAS. No. 431-89-0, Solkane® 227 Pharma, Germany), and HFO-1234ze(E) (Solstice® ze, Honeywell, NJ, US). A fresh cylinder of HFA-134a and an aged (> 2 year) cylinder of HFA-134a, presented as aged HFA-134a, were used in this study to examine the effect of propellant moisture content on formulation stability.

2.2.2.2. Spray drying

- *Rugose lipid particles*

Feedstock preparation and spray drying processes for the RLPs were conducted according to Wang et al. [49]. Briefly, DSPC and calcium chloride dihydrate were added to heated water (55 °C) at a molar ratio of 2 to 1, to reach a 20 mg/mL solids concentration in the feed. After being kept at 55 °C on a hotplate for 30 minutes, the liquid feed was subjected to high shear mixing (T-18 Ultra-Turrax, IKA, NC, USA) for 3 minutes at 25,000 rpm. Through the use of a peristaltic pump, the feedstock was fed to a twin-fluid atomizer while continuing to be heated and mixed, with the high-shear mixing probe running at 5,000 rpm to prevent lipid flocculation. The atomizer was operated at a fixed feed flow rate of 2.5 mL/min and a dispersing gas flow rate of approximately 20-25 L/min, resulting in an air-liquid ratio of about 10. Initial droplet diameters were approximately 9 μm for the preparation of all test particles [100]. All formulations were spray dried using a lab-scale spray drier [101] at a fixed drying gas flow rate of 600 SLPM. Previous studies found that the spray drying temperatures must be maintained within an optimal range to ensure sufficient drying and to maximize particle rugosity [49]. In this study, two batches of test particles prepared at different spray drying temperatures were used to investigate the effect of temperature on the stability of RLPs in propellants: one batch with a higher inlet temperature of 75 °C (RLP75) and an outlet temperature of 46.1 ± 0.5 °C, close to the main transition temperature of DSPC at 55 °C; and a second batch with a lower inlet temperature of 55 °C (RLP55) and a lower outlet temperature of 35.5 ± 0.5 °C. This information is summarized in Table 2.1, along with the yield and the results of the water content measurement, described below.

- *Trehalose-leucine particles*

In this study, a supplementary batch of powder containing 80% w/w trehalose and 20% w/w leucine (80T20L) was spray dried and compared to the lipid-based formulations. Its compatibility with different propellants was also tested. Trehalose and leucine were first dissolved in water at

`

room temperature at a mass ratio of 4:1 targeting a solids concentration of 20 mg/mL. The prepared feedstock solution was spray dried directly at an inlet temperature of 55 °C, which corresponded to an outlet temperature of 36.1 ± 0.2 °C.

- *Engineered porous particles*

The processes of feedstock preparation and spray drying for the manufacturing of engineered porous particles have been described elsewhere in detail [26]. Briefly, a mixture of DSPC and calcium chloride anhydrous at a molar ratio of 2:1 was prepared and then transferred into heated water while PFOB was slowly added. High shear mixing was used to ensure the emulsion was fully dispersed and was followed by high pressure homogenization. With an emulsion flow rate of 58 mL/min, the spray dryer was operated at an inlet temperature of 135 °C and an outlet temperature of 70 °C.

Table 2.1. Rugose lipid particle and leucine-trehalose formulations spray dried for stability study in propellants – composition and selected process parameters.

Powder	Composition	Inlet temperature	Outlet Temperature	Yield	Water Content
RLP55	DSPC + $CaCl_2$:2 H_2O	55 ˚C	39.1 ˚C	80%	1.00%
RLP75	DSPC + $CaCl_2$:2 H_2O	75 ˚C	49.5 ˚C	69%	0.90%
80T20L	80% w/w Trehalose, 20% w/w Leucine	55 ˚C	36.2 ˚C	83%	1.47%

Table 2.2. Measured water content and selected properties of propellants used in this study at 20 °C.

Properties	HFA-134a aged	HFA-134a	HFA-227ea	HFO-1234ze
Measured Water content (ppm)	95	11	13	15
Molar mass (g/mol) [102]	102	102	170	114
Liquid density (g/cm^3) [102]	1.22	1.22	1.41	1.18
Surface tension (mN/m) [90, 91]	8.69	8.69	6.96	8.55
Water solubility (ppm) [90, 91]	1300	1300	610	225
Dipole moment (Debye) [102]	2.06	2.06	0.94	1.44
Vapor pressure (kPa) [91, 92]	572	572	390	427
GWP [105]	1530	1530	3600	1.37

2.2.2.3. pMDI filling

A propellant filling and crimping station (Lab Plant, Pamasol AG, Switzerland) was used to crimp valves to the pMDI canisters and pressure fill the propellants. Either aluminum canisters or glass

`

canisters were used to make the pMDI samples. To ensure the complete drying of the pMDI components, all valves and canisters were preconditioned in a glove box with <1% RH for at least 24 hours before use. Five aluminum canisters of each propellant (Table 2.2) were filled to determine the moisture content of each pure propellant. Aluminum canisters were also used to prepare suspension pMDIs for physical stability measurements such as morphological and elemental analysis. Each canister was filled with 60 mg of powder and 10 mL of propellant to target a suspension concentration of 6 mg/mL. Glass canisters with a volume of 21 mL were used to prepare suspension pMDIs for colloidal stability measurement by shadowgraphic imaging. Each canister was filled with 96 mg of powder, crimped with a 50 µL metering valve, and pressure-filled with 16 mL of propellant to target the same suspension concentration. All fresh pMDI samples were subjected to an initial sonication for 10 seconds immediately after propellant filling to disperse aggregated particles.

Table 2.3. List of suspension pMDIs used for stability study under different storage conditions.

Batch	Powder	Propellant	Time points	Storage condition
#1	RLP55	HFA-134a	0d*, 2w, 1mo, 2mo, 3mo	40°C, 7%±5% RH
#2	RLP75	HFA-134a	0d, 2w, 1mo, 2mo, 3mo	40°C, 7%±5% RH
#3	RLP55	HFA-227ea	0d, 2w, 1mo, 2mo, 3mo	40°C, 7%±5% RH
#4	RLP75	HFA-227ea	0d, 2W, 1mo, 2mo, 3mo	40°C, 7%±5% RH
#5	RLP55	HFO-1234ze	0d, 2w, 1mo, 2mo, 3mo	40°C, 7%±5% RH
#6	RLP75	HFO-1234ze	0d, 2w, 1mo, 2mo, 3mo	40°C, 7%±5% RH
#7	RLP55	HFA-134a aged	0d, 1d, 2d, 3d, 4d, 6mo	Ambient
#8	RLP75	HFA-134a aged	0d, 2w, 1mo	Ambient
#9	80T20L	HFA-134a	0d, 2w, 1mo, 2mo, 3mo	40°C, 7%±5% RH
#10	80T20L	HFA-227ea	0d, 2w, 1mo, 2mo, 3mo	40°C, 7%±5% RH
#11	80T20L	HFO-1234ze	0d, 2w, 1mo, 2mo, 3mo	40°C, 7%±5% RH

*d – days; w – weeks; mo – months

2.2.2.4. Stability study

pMDI formulations containing the test particles (RLP55, RLP75, or 80T20LC) in one of the selected propellants (HFA-134a, HFA-227ea, or HFO-1234ze) were stored at 40 °C for a three-month stability study. Samples with aged HFA-134a were prepared separately for a longer stability study and were kept at room temperature for approximately two years. At each time point specified in Table 2.3, the glass suspensions were transferred to a shadowgraphic imaging setup, and colloidal stability was twice tested individually for 30 minutes. Particles were extracted from the pMDIs in aluminum canisters for morphological analysis by field emission

`

scanning electron microscopy (FESEM). In addition, the water content in each aluminum canister was measured at the end of the study. Samples were returned to the incubator immediately after each set of measurements. Ambient humidity and temperature were recorded hourly (VWR® TraceableLIVE® Wi-Fi Data Logging Hygrometer and Thermometer, VWR International) and reported as average values of 25% ± 16% RH and 21 °C ± 1 °C.

2.2.2.5. Water content measurement

- *Powder moisture content measurement*

The water content of powders has been reported to influence their physical stability in the propellant, making it a critical factor in the quality control of inhalation formulations [106]. The moisture content of the spray-dried powder was measured using a coulometric Karl Fischer titrator (C30, Mettler Toledo, ON, Canada) equipped with an oven autosampler. To prevent moisture uptake during sample preparation, all parts necessary for the measurement, including sample vials, drift vials, aluminum caps, and rubber seals, were kept in a glove box with less than 1% RH for about one hour. To verify the system's performance, a water standard was tested before the measurement. Roughly 60 ± 10 mg of powder was used for each measurement. The powder was placed in a sample vial, transferred to the oven autosampler, and heated to 130 °C to vaporize any moisture content. The water vapor was carried by dry and clean nitrogen gas at a flow rate of approximately 80 mL/min to the titration cell, where the reagent (HYDRANAL™, Coulomat AG, Honeywell, ON, Canada) reacted with the released water to produce coulometric signals. It should be noted that in this study, water content measurements were conducted only once for each sample. The uncertainty associated with these single-point measurements was estimated by calculating the average range based on past data[3]. The past data consisted of 12 replicates obtained from other samples tested with the same Karl Fischer Coulometer. This approach provided valuable insight about the uncertainty associated with the powder water content measurements, indicating an uncertainty of approximately ±0.1%.

[3] Water content of each replicate sample was measured three times and the standard deviation of the three measurements was calculated. The final uncertainty (±0.1%) is the approximate average of the standard deviations calculated for each replicate sample.

`

- *Propellant moisture content measurement*

A custom-designed cannula assembly was used to control release of propellant into the titration cell for moisture content measurement. The cannula, together with all parts involved in the measurement, was preconditioned in a less than 1% RH environment for at least one hour. In Karl Fischer coulometry settings, drift indicates the water entering the titration cell from the environment. A stable and low drift below 20 µL/min is required throughout the test to ensure the measured value remains stable and consistent over time, without any significant deviation from the initial reading. Each pMDI canister was shaken in a valve-down orientation for 5 seconds and actuated twice through the cannula into the Karl Fischer titration cell for priming purposes. After the drift stabilized below 10 µL/min, canisters were actuated ten times into the titration cell using the cannula assembly. For each actuation, the canisters were held in the actuated position for one second to allow complete emptying of the metering chamber. The canisters were weighed before and after measurement to determine the net mass of titrated propellant. For each propellant, five canisters were filled, and the water content for each canister was measured three times. Water content results are reported as average values with standard deviations.

2.2.2.6. Colloidal stability measurement

Colloidal stability is an important attribute of pMDIs that is directly related to product performance, e.g., delivered dose uniformity. A shadowgraphic imaging method [53, 95] was employed to measure the colloidal stability of suspensions at different time points of the stability study. Briefly, this instrument takes sequential shadowgraphic images of the sample at a given frequency for a certain period, and the acquired images are then transferred for post data processing. In this study, the colloidal stability tester was programmed to obtain shadowgraphic images with an exposure time of 0.14 ms and a frame rate of 0.5 Hz. A driving current of 1.0 A and a pulse width of 1.0 ms were used to drive the backlight LED. Each glass vial was manually shaken for 30 seconds and immediately placed in the sample holder of the instrument for 30 minutes' observation. Two suspension samples were prepared for each formulation, with two measurements being conducted for each sample.

An instability index function [56] was obtained by processing the transmission profiles derived from the obtained shadowgraphic images. The instability index is a dimensionless number ranging from 0 to 1, with 0 corresponding to an ideal suspension with no creaming or settling and 1

`

corresponding to a suspension that experiences extreme creaming or sedimentation resulting in a completely clear propellant with no suspended particles. The rate of destabilization is described by the slope of the instability index plot over time. In this study, formulations with final instability indices below 0.1 by the end of the 30-minute observation period were considered suspensions with excellent colloidal stability that experienced little or no creaming or sedimentation during this time frame.

2.2.2.7. Morphological and elemental analysis

A field emission scanning electron microscope equipped with an energy dispersive X-ray spectroscopy detector (EDX detector X-max 150, Oxford Instruments, England) was used for morphological and elemental analysis of the particles collected from spray drying and the particles extracted from the pMDI canisters. Spray dried particles were first dispersed on sample stubs covered with double-sided adhesive carbon tape. Particles from the pMDIs were extracted for morphological and elemental analysis at different time points as listed in Table 2.3. A single nozzle impactor [108] operated in a single-stage collection configuration was used for the non-destructive extraction of particles from the pMDI samples. Two doses of each pMDI were actuated into a US pharmacopeia (USP) induction port, and aerosolized particles were collected on standard SEM stubs for subsequent analysis.

For imaging, a sputter coater (Desk II, Denton Vacuum, NJ, USA) was used to coat the particles with gold nanoparticles to a thickness of 16 nm. To prevent sample surface charging or electron beam damage, a low acceleration voltage of 4-5 keV was used. A higher acceleration voltage at 20 KeV was used for EDX measurements. Energy-dispersive spectra of extracted lipid particles collected from selected regions of interest were analyzed for comparison.

2.2.3. Results and discussion

2.2.3.1. Morphology of Model Particles

Morphological transition of particles suspended in pMDI formulations undergoing storage can be used as a good indicator for compatibility with propellants. The morphology of the spray dried RLPs is shown in Figure 2.1 (a-b). RLP55 and RLP75 both showed a highly rugose structure, as expected. It was believed that the rugose structure was formed by spray drying the feedstock at a temperature close to the main transition temperature of the lipid, in which condition the lipids exist as the mixture of a mobile liquid crystalline phase and a less mobile subgel/gel phase. Lower

`

magnification micrographs (data not shown) indicated that the majority of the collected lipid particles were within the respirable range. The highly rugose surface structure of the particles is effective in improving the powder dispersibility and has been reported to create potential drug loading sites [97, 98]. The engineered porous particles are based on phospholipids and have a sponge-like structure as shown in Figure 2.1 (d). Although they have a composition similar to that of RLPs, their spray drying process differs by including PFOB as a pore-former and a multi-pass high pressure homogenization process. Drugs can be incorporated into these porous particles by spray drying suspension, solution, or co-suspension-based feedstocks [47]. The same methods can be used to incorporate therapeutic actives into the proposed RLPs [44]. The engineered porous particles have been demonstrated to be very stable in pMDI formulations [26]. Having the same composition and a similarly folded structure, the RLPs are expected to present good chemical and physical stability in pMDI formulations.

The morphology of particles containing 80T20L is presented in Figure 2.1(c). Trehalose is known as a glass stabilizer that can protect biologics by forming a rigid glassy matrix in pharmaceutical applications [111]. It has been recommended that a dispersibility enhancer such as leucine be added to spray dried trehalose particles, because pure trehalose particles have been found to be very cohesive [51]. As presented before by Wang et al. [43], the formation of a crystalline leucine shell near the surface of trehalose particles results in a core-shell structure with increased surface rugosity. The formation of these particles has been well-studied [35, 39, 100, 101], and it has been shown that introducing leucine to the dense spherical trehalose particles initiates early shell formation resulting in slightly larger, more corrugated particles. In comparison to the lipid particles with a highly rugose surface and low density, these trehalose-leucine particles present lower particle rugosity and high particle density [113].

`

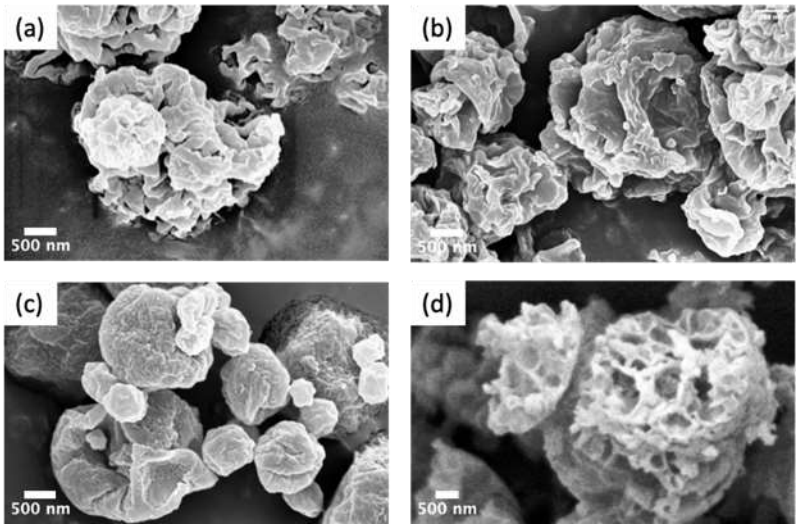

Figure 2.1. Particle morphology of spray dried particles: Rugose DSPC lipid particles produced with different dryer outlet temperatures of (a) 55 °C and (b) 75 °C; (c) particles composed of 80% trehalose- 20% leucine; (d) engineered phospholipid porous particles.

2.2.3.2. Colloidal stability

Delivered dose uniformity and aerodynamic particle size distribution are typically crucial factors that affect the performance of a pMDI product [82]. For suspension-based pMDIs, these properties are strongly affected by the colloidal stability of the suspension; for instance, rapid migration of suspended particles in the canister after agitation can lead to inconsistencies in the delivered dose. Thus, measuring suspension stability can be a useful tool in predicting final pMDI product performance [114].

Engineered phospholipid porous particles have been employed in commercial products as co-suspending agents to enhance the suspension stability of micronized drug crystals [115]. Having an amphiphilic corrugated structure, such particles exhibit excellent colloidal stability by decreasing cohesion between particles [44, 104, 105]. The suspension stability of the RLPs in pMDIs of different propellants was measured and compared with that of formulations containing the well-established engineered porous particles.

The colloidal stability of freshly made pMDI suspensions was first measured, with the results presented in Figure 2.2 (a). For the samples containing RLPs in HFA-134a, no creaming or sedimentation was observed throughout the 30-minute measurement period, and the instability indices of those samples remained below 0.01, indicating excellent colloidal stability. Minor creaming was observed at the top of the HFA-227ea and HFO-1234ze suspensions. The instability

`

index for HFA-227ea formulations increased by up to 50% of their maximum value within the first 3 minutes and then slowly further increased over the following 30 minutes. This initial destabilization process after initial agitation was even faster for the samples in HFO-1234ze propellant, being almost complete within one minute before plateauing for the rest of the observation period. In comparison, the suspension containing engineered porous particles experienced a steady and slow increase in the instability index over the 30 minutes, reaching ~0.02 at the end point. The suspensions containing 80T20L in HFA-134a and HFA-227ea followed a trend similar to that of other batches showing an excellent colloidal stability, but the batch with 80T20L in HFO-1234ze was destabilized within the first minute and maintained a consistent relatively high instability index of about 0.23. The RLP suspensions tested here exhibited maximum instability indices below 0.05 in all propellants, results that were comparable to those for the pMDI formulation consisting of engineered porous particles in HFA-134a. These values are indicative of excellent initial colloidal stability of the RLP-based pMDI formulations.

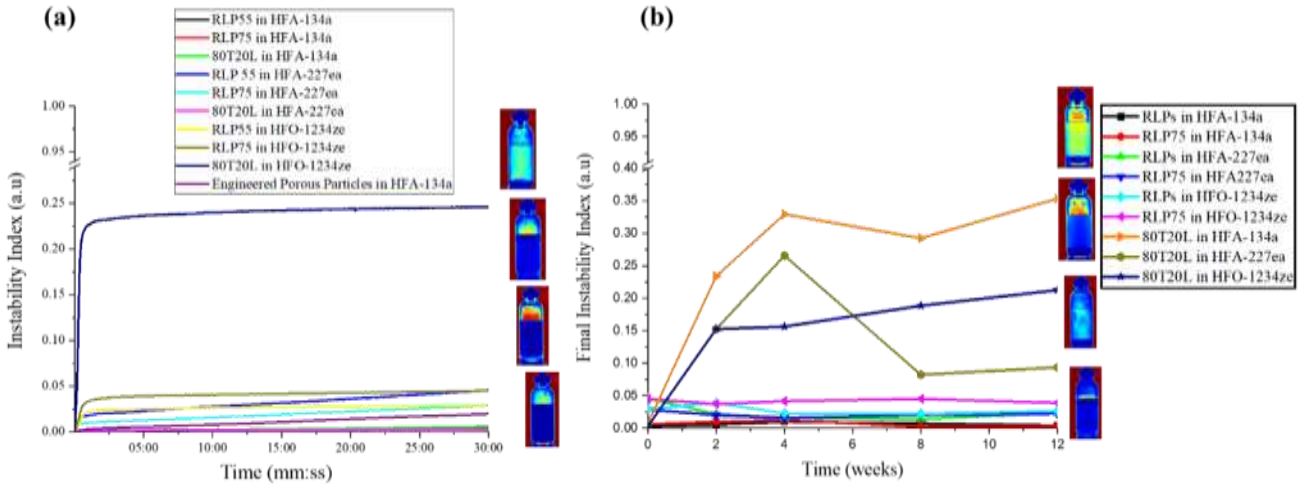

Figure 2.2. (a) The colloidal stability of rugose lipid particles (RLP) and comparators for fresh vials before storage. Each vial was examined for 30 minutes after 10 seconds of manual shaking. The shadowgraphic images displayed to the right of the plot represent the final suspension state after 30 minutes for, from top to bottom, 80T20L in HFO-1234ze, RLP75 in HFO-1234ze, engineered porous particles in HFA-134a, and RLP55 in HFA-134a. (b) The colloidal stability of MDIs containing RLPs and 80T20L after storage at 40°C for up to 12 weeks. The shadowgraphic images show the final suspension state after 30 minutes' measurement for 3-months old samples containing, from top to bottom, 80T20L in HFA-134a, 80T20L in HFA-227ea, 80T20L in HFO-1234ze and RLP75 in HFO-1234ze, the latter of which represents the least stable RLP suspension.

Following the day zero measurement, the suspension samples in different propellants were stored in an incubator set to 40 °C for up to 12 weeks and examined for their colloidal stability at different time points. Suspension stability was measured twice for each vial, and the average instability

`

index was calculated. The results from the two measurements were in good agreement, indicating a negligible difference between the two measurements, lower than 0.02. Colloidal stabilities of RLP suspensions in all tested propellants remained consistent, with instability indices maintained below 0.05 over time. In comparison, 80T20L suspensions in HFA propellants had excellent colloidal stability at day zero but deteriorated significantly after only two weeks, which is evidenced by the fact that the final instability indices at the end of the 30-minute measurement for these samples were in a relatively high range of 0.15 to 0.33. The deteriorated colloidal behavior is likely due to the fusion of trehalose-leucine particles in propellant upon storage as presented in the micrographs shown in Figure 2.3. After four weeks of storage, it was noticed that particles in pMDI samples consisting of 80T20L powder suspended in HFA-134a or HFA-227ea adhered to the glass pMDI canister following agitation. This result also suggested a modification in the particle characteristics due to storage. The adhesion of particles resulted in diminished light transmission and a reduction in the instability index, leading to fluctuations in the instability index plots for these samples, as depicted in Figure 2.2 (b).

2.2.3.3. Morphology and elemental composition of particles extracted from pMDIs

The presence of morphological transitions in microparticles is an important characteristic that can be used to indicate the compatibility between suspended particles and propellant in pMDI formulations. Figure 2.3 shows the particle morphology of 80T20L extracted from the HFA-134a canister. At time zero, particles were well dispersed and had a slightly rugose structure, but after two weeks they started to fuse and form fiber-like structures. Moreover, the morphology of 80T20L indicates a decrease in small-scale surface roughness of the particles in all the propellants, which could explain the significant increase in the instability index of these MDIs.

It has been shown that spray drying parameters can directly affect the morphology of the spray dried lipid particles [118]. In a previous study, Wang et al. demonstrated that the spray drying temperature influences the particle morphology of RLPs [49]. Particle morphology of RLPs spray dried with different dryer outlet temperatures of 55 °C and 75 °C is presented in Figure 2.1 (a-b). They were then transported to pMDI canisters, filled with propellants, and subjected to ultrasonication and manual shaking. Figure 2.4 display FESEM micrographs of RLPs extracted from the pMDIs at time zero, to ensure that the particle structure was not affected by the filling and sample preparation processes. Particle morphologies after three months of storage in

`

propellant at 40 °C were also collected and are included for comparison (Figure 2.5). Generally, all RLPs retained their morphology after 3 months, regardless of the type of propellant and the inlet temperature used during their manufacturing, proving good physical stability in pMDI formulations.

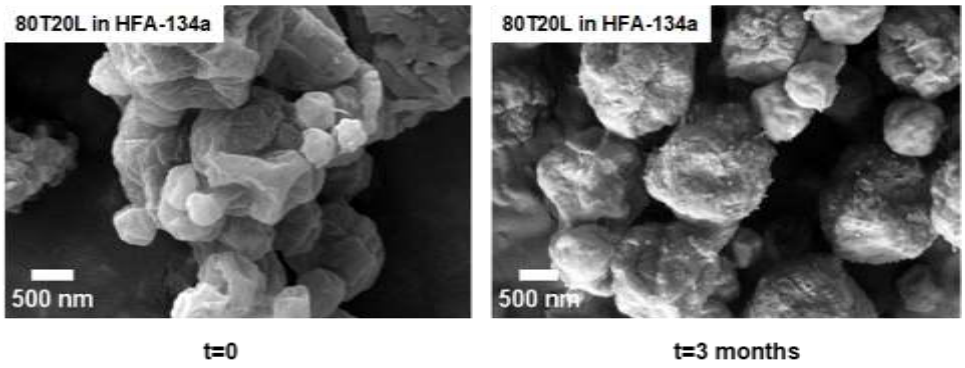

Figure 2.3. Micrographs of 80T20L in HFA-134a showing morphological change due to fusion among particles after 3 months of storage in HFA-134a at 40 °C. Arrows indicate locations of fibers and particle fusion.

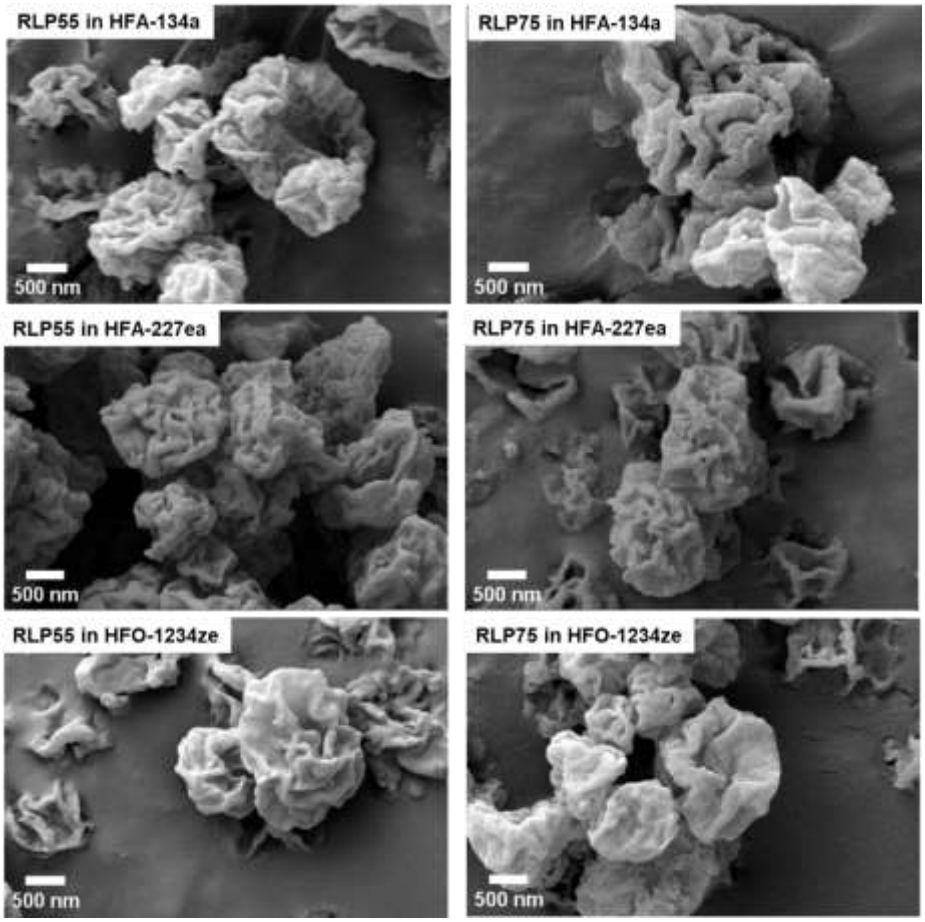

Figure 2.4. Micrographs showing the particle morphology of RLPs extracted from pMDIs at t0.

`

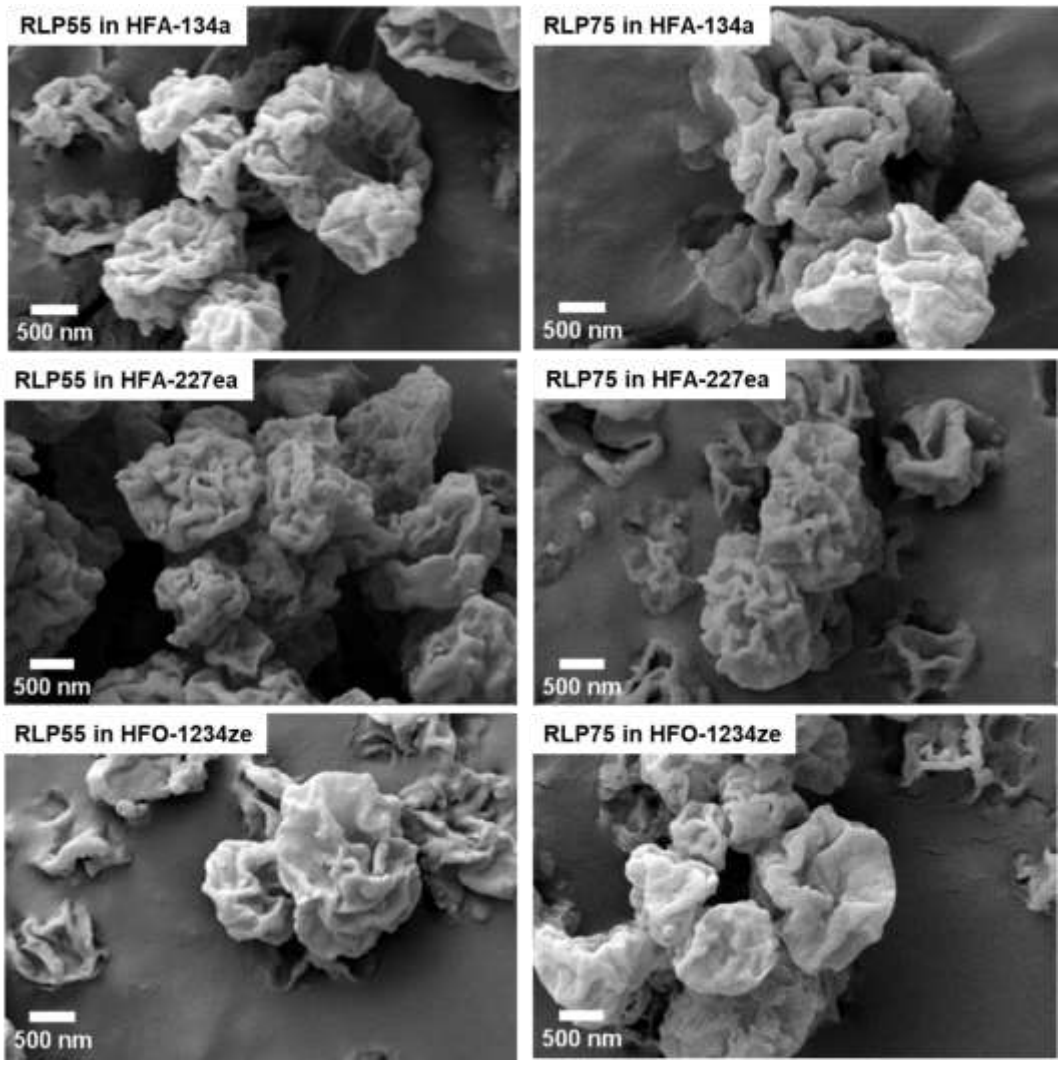

Figure 2.5. Micrographs showing the particle morphology of RLPs extracted from pMDIs after three months. Morphology remained unchanged after three months of storage at 40 °C.

Sheet-like structures were occasionally detected in particles extracted from the pMDIs containing RLP75 after two months of storage, as shown in Figure 2.6 , Figure 2.7 and Figure 2.8. To determine whether these sheets were composed of lipids or of foreign particulate matter, EDX analysis was conducted on several sheets and the results compared with spectra collected from regular RLPs. The respective areas of detection are indicated in the micrographs. Elemental spectra illustrated that the rugose particles and sheets had similar compositions in all cases. In particular, phosphorus and in some cases calcium, constituent elements of RLPs, were detected in both sheets and rugose particles, but the intensity of calcium and chlorine peaks was slightly lower in the reformed sheets, as indicated in Figure 2.6, Figure 2.7 and Figure 2.8, spectrum 7, 15 and 4. No such lipid sheets were detected in any of the pMDI samples containing RLP55.

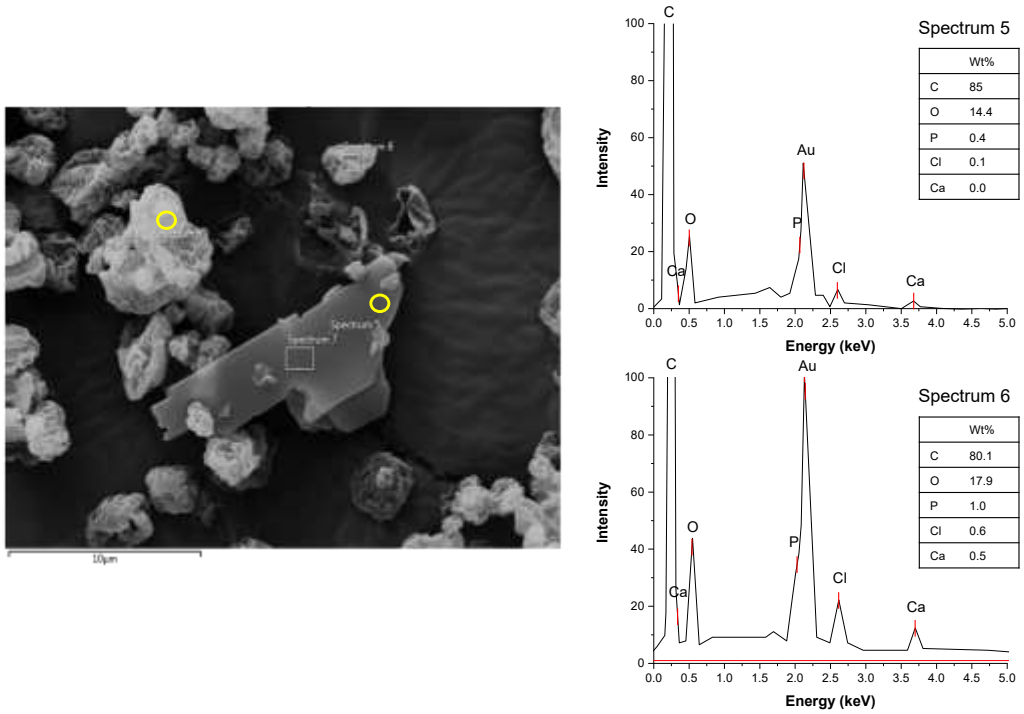

Figure 2.6. Micrograph and EDX spectra of RLP75 after 3 months' storage in HFA-134a at 40 °C. EDX spectra collected on newly formed sheets and regular rugose particles illustrate their similar elemental composition.

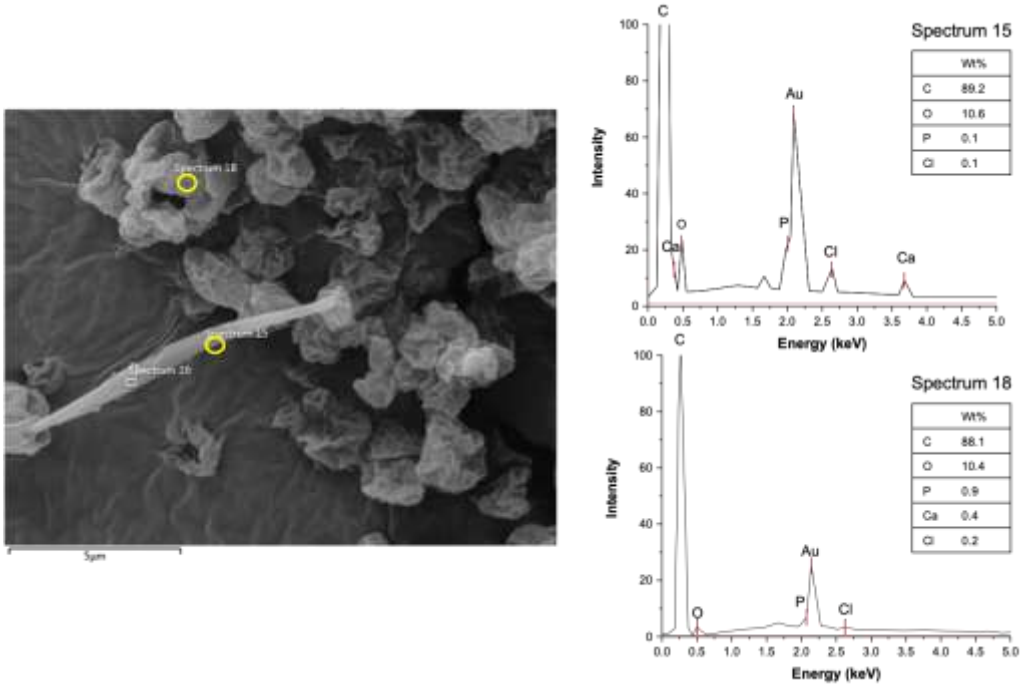

Figure 2.7. Micrograph and EDX spectra of RLP75 after 3 months' storage in HFA-227ea at 40 °C. EDX spectra collected on newly formed sheets and regular rugose particles illustrate their similar elemental composition.

`

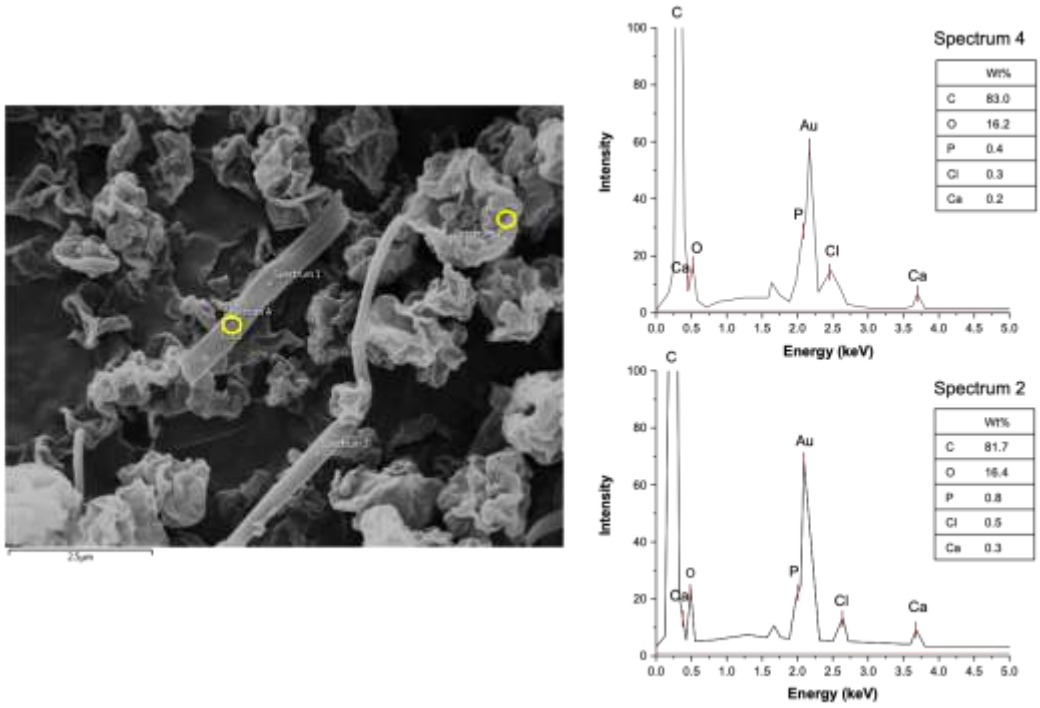

Figure 2.8. Micrograph and EDX spectra of RLP75 after 3 months' storage in HFO-1234ze at 40 °C. EDX spectra collected on newly formed sheets and regular rugose particles illustrate their similar elemental composition.

During the spray drying process, calcium chloride binds with the phospholipid headgroup, enhancing the stability of lipid particles in a humid environment [44]. Weers et al. [119] have shown that increasing the concentration of calcium ions can raise the transition temperature of DSPC, improving the long-term physicochemical stability of the phospholipid. By promoting dehydration of the lipid headgroup, calcium ions decrease the susceptibility of the pMDI formulation to humidity [119]. Therefore, any factor that causes Ca^{2+} to migrate out from the lipid particles may increase their susceptibility to destabilization from moisture ingress. RLP75 particles were manufactured at an outlet temperature closer to the transition temperature (T_m), which may cause differences in lipid structure such that the likelihood of Ca^{2+} ions separating from the particles is increased. However, despite the formation of the lipid sheets, all RLP-based pMDIs retained excellent colloidal stability. The quantity of the lipid sheets was insufficient to affect the flocculation behavior of the suspension. Nevertheless, both batches of the rugose lipid particles, especially RLP55, demonstrated excellent robustness in pMDI formulations undergoing storage at an elevated temperature.

`

2.2.3.4. Effect of water content on physical stability of RLPs

The fact that the water content of the propellant can affect the performance of pMDI products is often overlooked. Increased moisture content in pMDI formulations can influence the particle size distribution or lead to adhesion of drug particles to the canister walls [33, 108]. To investigate the effect of formulation water content on the physical stability of RLPs, crimped pMDI canisters loaded with RLP55 or RLP75 were filled either with HFA-134a propellant with a higher moisture content of 95 ppm, or fresh propellant with a lower water content of 11 ppm. The former represents aged propellant that was stored under room conditions for an extended period of time during which moisture had slowly diffused into the cylinder [120].

Since all pMDI hardware components were preconditioned to remove any residual water, this study considered three primary sources for the water content in pMDI formulations: water residue in the powder, water content in the propellant, and water that diffused into the pMDI canister over time. The initial water content of all MDI samples was calculated according to the following equation,

$$M_{\mathrm{t}} = \sum W * C \qquad (1),$$

where M_{t} is the average formulation moisture content assuming an equilibrium can be reached, W is the water content of propellant or powder, and C is their respective mass fraction.

Additional moisture ingress can occur over time by water diffusing through the valve components. The final moisture content of all pMDI samples (W_{MDIs}) was measured at the end of the three-month stability study, with the results listed in Table 2.4. The water content of suspensions increased over time as expected. All suspensions consisting of RLPs in HFA-134a had a moisture uptake of more than 110 ppm over the course of 3 months' storage at 40 °C and 7% ± 5% RH. In comparison, the moisture uptake for MDIs with RLPs in HFA-227ea and HFO-1234ze was in both cases below 60 ppm. The difference in moisture uptake was likely due to the different molecular polarities of the propellants, based on their respective dipole moments or water solubility values as shown in Table 2.2. Trehalose-leucine suspensions experienced significantly more moisture uptake than samples containing RLPs. Trehalose has a strong tendency to absorb water vapor because of its high hygroscopicity [121].

`

Overall, despite the increased water content due to moisture ingress, RLPs manufactured using an inlet temperature of 55 °C retained their morphology (Figure 2.9) and colloidal stability (Figure 2.10) in all the propellants after 6 months' storage in ambient conditions.

Table 2.4. Measured and calculated moisture content of pMDI formulations

Formulation	Powder Moisture content: measured	Propellant Moisture content: measured (ppm)	Initial formulation moisture content: predicted using Eq.1 (ppm)	Final Formulation moisture content: measured (ppm)	Moisture uptake: calculated (ppm)
RLP55 in HFA-134a	1.00%±0.10%	14±1	60±6	173±3	109±9
RLP75 in HFA-134a	0.99%±0.10%	14±1	60±6	184±3	122±9
80T20L in HFA-134a	1.47%±0.10%	14±1	75±5	264±8	186±13
RLP55 in HFA-227ea	1.00%±0.10%	13±2	55±6	102±6	47±11
RLP75 in HFA-227ea	0.99%±0.10%	13±2	56±7	82±5	25±12
80T20L in HFA-227ea	1.47%±0.10%	13±2	73±7	151±10	78±17
RLP55 in HFO-1234ze	1.00%±0.10%	15±1	67±6	96±1	29±7
RLP75 in HFO-1234ze	0.99%±0.10%	15±1	67±6	131±8	63±14
80T20L in HFO-1234ze	1.47%±0.10%	15±1	91±6	243±18	151±24
RLP55 in aged HFA-134a	1.51%±0.10%	95±3	168±11	227[1]±13	59±24
RLP75 in aged HFA-134a	1.65%±0.10%	95±3	175±11	244[1]±13	70±24

1. water content of aged MDIs measured after two-and-a-half years of storage in ambient conditions as explained in section 2.2.2.5.

As shown in Figure 2.9, there was no discernible change in particle morphology for RLP55 batches in aged propellant after six months of storage at ambient conditions (21 °C, 25%±16% RH). Moreover, the instability index of RLP55 in aged HFA-134a was maintained below 0.015 through 30 minutes of measurement after 6 months (Figure 2.10 a). However, despite no apparent change in particle morphology, a clear decrease in the colloidal stability of RLP75 was observed after one month of storage. In other words, the instability index of RLP75 in aged HFA-134a increased from below 0.01 on the first day of measurement to more than 0.15 after one month of storage in ambient conditions (Figure 2.10) .According to Murata et al. [122], for every pMDI formulation there is a critical moisture level above which fine particle dose drops and can critically affect the drug delivery. Thus, it is possible that RLP75 in aged HFA-134a with a moisture content of about 240 ppm had passed the critical moisture level and had led to a decrease in the colloidal stability.

`

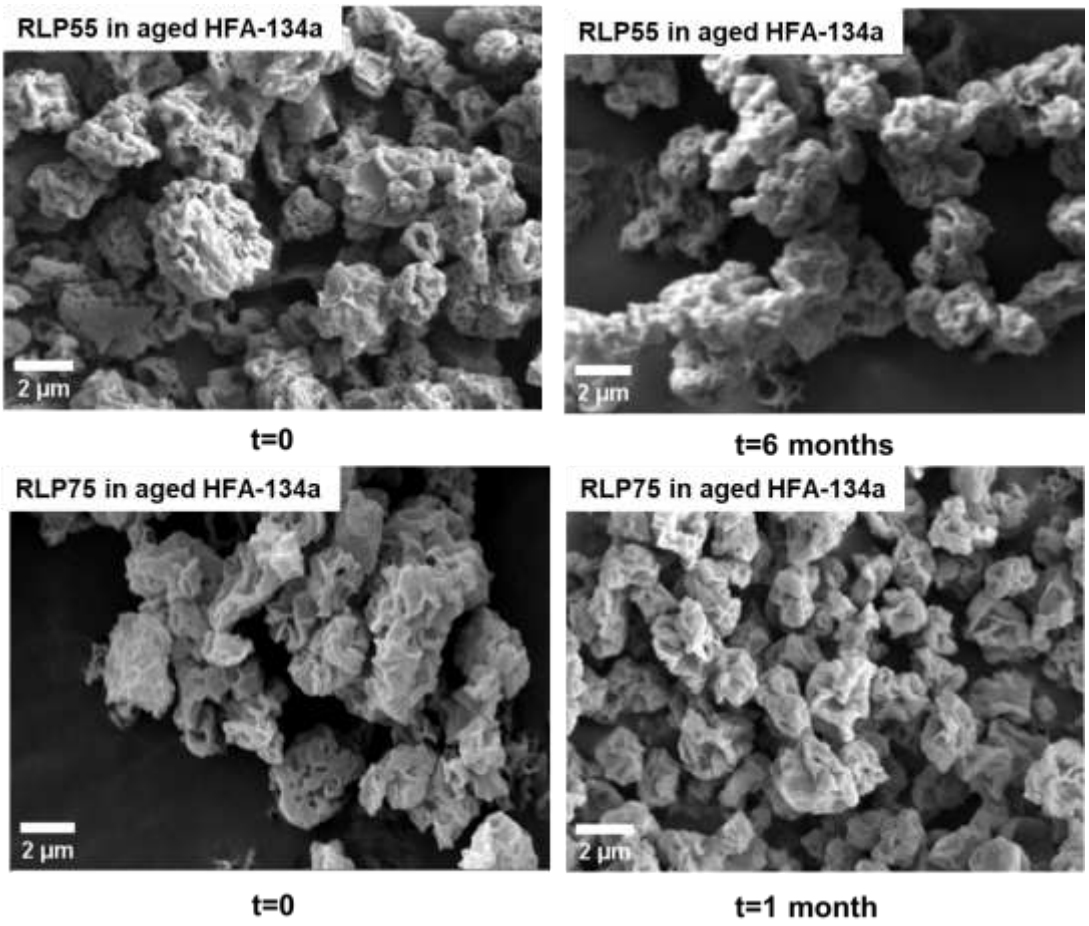

Figure 2.9. Particle morphology of RLP55 and RLP75 in aged HFA-134a with high water content. Morphology remained unchanged.

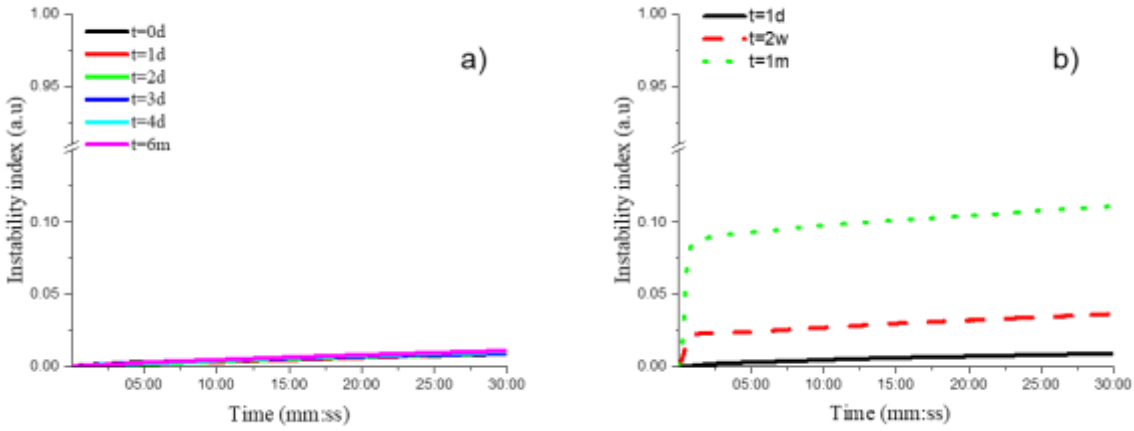

Figure 2.10. RLP75 in aged HFA-134a with high water content destabilized after two weeks' pMDI storage under ambient conditions, while a) RLP55 retained colloidal stability after six months' storage under ambient conditions.

`

2.2.4. Conclusions

This study investigated the compatibility of RLPs in pMDI propellants and found that these particles are feasible for use in both commonly used HFA propellants (HFA-134a, HFA227ea) and the new low-GWP propellant HFO-1234ze. The colloidal stability of RLPs suspended in pMDIs was found to be excellent and comparable to that of the engineered porous particles with known excellent performance, irrespective of the propellant used. This fact suggests a strong possibility of achieving good dose uniformity with these particles. The RLPs maintained their physical stability in pMDIs at a high storage temperature (40 °C) for up to 3 months, a trait essential for successful inhalation products, which require consistent product quality, including stable aerosol performance, uniform delivered dose, and durable shelf life at room temperature. To ensure good physical stability of pMDI products containing such rugose lipid particles, manufacturing parameters such as spray drying conditions, propellant quality, and in particular the moisture content of the powder, need to be well controlled. Further exploration is still needed to assess the behavior of RLPs in conjunction with APIs in pMDI formulations.

`

2.3. Excellent physical stability of rugose lipid particles in pMDIs with new low global warming potential propellant after one year of stability study

2.3.1. Purpose

The one-year stability study was conducted to evaluate the characteristics of rugose lipid particles (RLPs) emitted from pMDIs. The aerodynamic particle size distribution of RLPs was analyzed in pMDIs with established propellants (HFA-134a and HFA-227ea) and the new low global warming potential propellant (HFO-1234ze).

In addition to particle size distribution, the suspension stability of pMDIs was assessed and their water content was quantified. Furthermore, the study was carried out to investigate the phenomenon of particle reformation, which may affect the morphology of the emitted particles, and investigate any potential changes in the elemental composition of these particles.

2.3.2. Methods

The pMDIs used in this study were, indeed, those described in section 2.2.2.4, but they had been stored for over a year in an incubator [49]. However, only the RLP55 batches were used for this study because of their superior performance compared to RLP75. The morphology and elemental composition of RLPs were evaluated using field emission scanning electron microscopy equipped with an energy-dispersive X-ray spectroscopy detector. The aerodynamic particle size distribution of the RLPs after pMDI actuation and propellant evaporation was measured by actuating the MDIs through an 0.32 mm orifice size actuator to a glass buffer chamber connected to an Aerodynamic Particle Sizer via an aerosol diluter. The water content of the pMDIs was tracked using a Karl Fischer titrator. The colloidal stability of RLP suspensions was assessed using a shadowgraphic imaging method and compared to a control vial containing well-known engineered porous particles and HFA-134a propellant [56].

2.3.3. Results and Discussion

RLPs demonstrated excellent colloidal stability in pMDIs with either HFA propellants or HFO-1234ze, after a year of storage at 40°C and ambient humidity. The colloidal stability of the pMDIs was characterized by an instability index, a dimensionless number from 0 to 1 based on light transmission change (Figure 2.11). The instability indices for all RLP suspensions were maintained

`

below 0.05 after 30-minute measurements at different time points, which represents excellent colloidal stability. The colloidal stability of RLP formulations were also comparable to that of the formulation of engineered porous particles in HFA-134a, the latter of which are proven good co-suspending agents [26]. The water content measurement revealed that the HFA-134a formulation exhibited a moisture uptake of over 110 ppm after storage, while the moisture uptakes for the other samples were below 80 ppm. This difference in water uptake may be attributed to the different dipole moment of HFA-134a (2.06 Debye) compared to HFA-227ea (0.93 Debye) and HFO-1234ze (1.44 Debye). A small quantity of lipid sheets (Figure 2.12) was also detected in particles extracted from the HFA-134a formulation after one year storage. EDX analysis showed that those sheets exhibited lower intensity of Ca^{2+}-related peaks in its EDX spectrum when compared to regular rugose lipid particles, which could also be a result of the uptaken moisture interacting with the suspended particles. Despite the increased water content and formation of lipid sheets, rugose lipid particles retained overall physical stability in all propellants after one year of storage at 40 °C. The particle size distributions from actuated pMDIs containing RLPs are presented in Figure 2.13. All tested pMDIs maintained a mass median aerodynamic diameter (MMAD) of 2.6 to 3.1 µm in the respirable range and geometric standard deviation (GSD) in the range of 1.5-1.65.

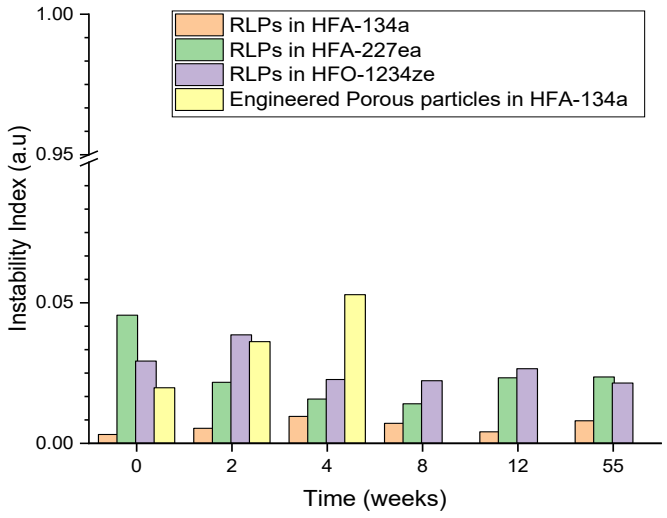

Figure 2.11. Instability indices stood below 0.1 from scale of 0 to 1 for all tested MDIs throughout different time points. Instability indices presented here were collected at the end of each 30-minute shadowgraphic imaging.

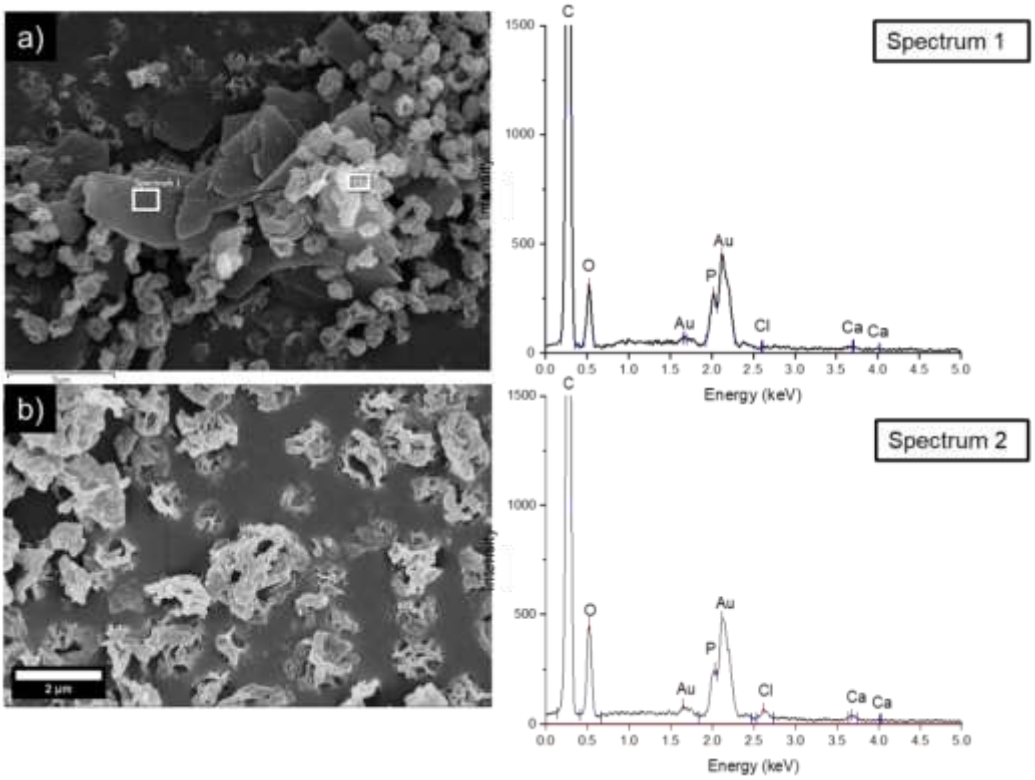

Figure 2.12. EDX Spectra of an RLP (Spectrum 1) and a lipid sheet (Spectrum2) visually observed after storage of RLPs in HFA-134a. RLP structure was retained after 1-year storage in HFA-134a at 40°C and ambient humidity. Lipid sheets were occasionally observed.

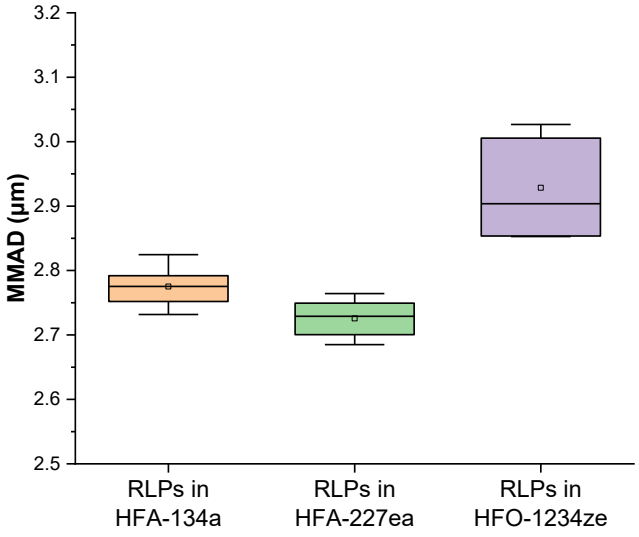

Figure 2.13. Mass median aerodynamic diameters (MMAD) of particles produced by pMDIs containing RLPs in different propellant. Five measurements were conducted for each sample.

`

2.3.4. Conclusions

The study demonstrates the potential of RLPs as drug carriers in pMDIs. These lipid particles exhibit both excellent colloidal stability and physical stability in conventional and low global warming potential propellants, making them a promising co-suspending excipient for pMDI formulations. After being stored at 40°C and ambient humidity for one year, RLPs remained within the respirable size range, suggesting that there was no enduring particle fusion or aggregation. This further demonstrates the robustness of RLPs suspended in propellants. Further research and development studies will explore the performance of pMDI formulations loaded with active pharmaceutical ingredients**.**

`

Chapter 3 A Model for predicting particle size distribution of residual particles emitted from pMDIs

3.1. Introduction

pMDIs stand as the foremost drug delivery devices used for the management and treatment of various lung diseases. These devices have been the focus of numerous studies over the past seven decades [123].

A typical pMDI is a compact and portable inhalation system consisting of three main components: a metal canister, a valve, and an actuator [124]. The metal canister holds a formulation consisting of a propellant, the active drug, and possible excipients. This formulation can take the form of a suspension or solution, designed to ensure stability and effectiveness of drug delivery to the lungs. The canister is securely sealed with a metered valve. When a patient activates the pMDI by pressing down the canister, placed within the actuator, a series of organized events occurs. The valve stem moves through the metering valve, allowing the formulation to exit the canister. The formulation then travels into an expansion chamber within the device. In this expansion chamber, the formulation undergoes atomization and is then released into the atmosphere as a fine spray [61]. The atomization process in pMDIs occurs in two stages: primary atomization and secondary atomization. Primary atomization refers to the initial breakup of the bulk liquid formulation into droplets upon discharge from the device nozzle. Secondary atomization includes processes like droplet evaporation, collision, and coalescence as the spray travels from the actuator to the patient's respiratory tract.

This atomized spray is suitable for inhalation and efficient drug delivery into the respiratory system where the drug can reach peripheral parts of the lungs. The pMDI's compact and user-friendly design makes it a popular choice for patients, but the complexities of its functioning, as well as the formulation within, have been the subject of in-depth research to optimize efficacy of drug delivery. One of the factors influencing the pMDIs performance is the aerodynamic particle size distribution of residual particles emitted from pMDIs [125]. Content equivalent diameter relates the size distribution of the initial droplets formed during primary atomization to the final particles deposited in the lungs after secondary atomization processes, as follows [88]:

$$d_{\mathrm{c.50}} \cong \sqrt[3]{\frac{\rho^*}{C_{\mathrm{NV}}}} \sqrt[6]{\frac{\rho^*}{\rho_{\mathrm{p}}}} MMAD_{\mathrm{r}} \tag{3.1}$$

`

Here $d_{c.50}$ is the mass median content equivalent diameter, $MMAD_r$ is the mass median diameter of residual particles, ρ^* is the reference density (equals to 1000 kg/m^3), ρ_p is the solid particle density and C_{NV} is the concentration of nonvolatile components.

The importance of aerodynamic particle size distribution (APSD) of residual particles to the efficacy of pulmonary treatment is well-established and has been the subject of numerous studies over the past four decades (Table 3.1). Despite this extensive research, a reliable simulation for predicting the aerosol performance and atomization process of various pMDIs is still needed. To address this gap, the present study focuses on the development of a Monte Carlo simulation capable of estimating the APSD of residual particles from various pMDIs irrespective of the type of propellant used. The impacts of different factors such as drug concentration and properties of the propellant used will also be discussed in detail.

Table 3.1. Review of some previous studies about aerosol performance and atomization process of pMDIs

Year	Research summary	Title and authors
1985	A cascade impactor was used to measure the size distribution of 10 different MDIs in both dry and humid air. The study focused on the effect of different aspects such as inhaler design and formulation on the residual particle size distribution. Experimental results showed a shift to higher MMADs in 90% RH.	Size Aspects of Metered-Dose Inhaler Aerosols. Kim CS. et al. [126].
1987	A statistical framework was used to investigate particle clusters generated in the drying process of aerosol droplets. The model was able to predict the aerodynamic size distribution of particles emitted from suspension pMDIs.	Development of a systematic theory of suspension inhalation aerosols. II. Aggregates of monodisperse particles nebulized in polydisperse droplets. Chan HK, Gonda I. [89].
1991	This thesis investigated the metered and continuous discharge of CFC and HFA propellants through twin-orifice valve assemblies. A computer model was created to predict propellant behavior, correlating droplet size with chamber conditions.	Metered atomization for respiratory drug delivery. Clark AR. [85].

`

2006	The process of aerosol generation was simplified into two main phases, droplet formation and aerosol maturation. An understanding of the MMD and GSD of the initial droplet was argued as being key to droplet formation. Aerosol maturation was also proposed as a factor in the volatility of propellants and excipients.	The relative influence of atomization and evaporation on metered dose inhaler drug delivery efficiency. Stein SW, Myrdal PB. [127].
2008	An empirical equation was used to predict the MMD of the initial droplet for HFA-134a. The investigator compared the number of particles emitted by different commercial pMDIs using the results of cascade impactor measurements.	Estimating the number of droplets and drug particles emitted from MDIs. Stein SW. [128].
2012	A model based on random sampling was used to predict the APSD of residual particles emitted from pMDIs containing suspended particles and HFA-134a.	A model for predicting size distributions delivered from pMDIs with suspended drug. Stein SW, Sheth P, Myrdal PB [90].
2013	The APSD of residual particles in suspension pMDIs was shown to be more susceptible to drug concentration and micronized drug size than to the MMD of initial droplets.	The influence of initial atomized droplet size on residual particle size from pressurized metered dose inhalers. Sheth P, Stein SW, Myrdal P. [129].
2014	The investigators found an empirical equation for calculating APSD of residual particles emitted from pMDIs with only one suspended drug using statistical simulation and occurrence of multiplets.	Factors Influencing Aerodynamic Particle Size Distribution of Suspension Pressurized Metered Dose Inhalers. Sheth P, Stein SW, Myrdal P. [125].
2014	The investigators found an empirical equation using several cascade impactions results to estimate content equivalent diameter in solution pMDIs irrespective of the propellant used.	A Correlation Equation for the Mass Median Aerodynamic Diameter of the Aerosol Emitted by Solution Metered Dose Inhalers. Ivey JW, Lewis D, et al. [88].

`

2015	A previously used model was further developed to estimate the APSD of pMDIs with complex formulations. The investigators used the GSD and MMD of initial droplets of a certain formulation and modified their simulation to be able to estimate the APSD of a pMDI containing propellant, a dissolved drug and a suspended drug.	Modeling and Understanding Combination pMDI Formulations with Both Dissolved and Suspended Drugs. Stein SW, Sheth P, et al. [130].
2020	The investigators developed a simulation similar to that of Stein et al. but they used a volume-based method instead of Poisson distribution to allocate drug particles to each droplet.	Predicting the composition and size distribution of dry particles for aerosols and sprays of suspension: A Monte Carlo approach. Chow M, Kwok P, et al. [131].
2023	The content equivalent diameters for pMDIs with established and new propellants were compared using a back calculation method. The effect of ambient humidity on aerosol performance of pMDIs was also investigated.	Understanding the performance of pressurized metered dose inhalers formulated with low global warming potential propellants. Wang, Leal J, et al. [132].

3.2. Materials and methods

3.2.1. Monte Carlo Simulation

The structure of this simulation was adapted from Stein et al.[90] and evaluates only the formation of initial droplets after atomization and their conversion to dried polydisperse particles. This model was developed in Visual Studio using Python and was designed to study mainly pMDIs with two components: 1) propellant and 2) suspended particles. The suspension was assumed to be ideal, with no interaction among the components. Certain inputs needed to be known before running the simulation; the following default values were derived from an experimental study conducted by the author on rugose lipid particles in suspension pMDIs:

1. Mass median diameter of the initial droplets (MMD_i). Various empirical equations have been introduced in the literature to estimate MMD_i. There are also studies suggesting a range for MMD_i. (Table 3.2)
2. Geometric standard deviation of the initial droplets (GSD_i). Different studies suggested various ranges for the GSD_i. (Table 3.2).

`

3. Numbers of droplets (N=10,000)
4. Density of formulation ($C_{f=}$1.226 g/cm^3)
5. True density of drug ($\rho_{d=}$1.1 g/cm^3)
6. Concentration of drug ($C_{d=}$0.005 g/g)
7. Mass median aerodynamic diameter of the micronized drug ($MMAD_{d=}$2 μm)
8. Geometric standard deviation of the micronized drug ($GSD_{i=}$1.6)

Table 3.2. Geometric standard deviation and mass median diameter of initial droplets presented from selected studies

#	**GSD_i**	**MMD_i**	**Study**
1	1.75 – 2.4	$MMD_{\mathrm{i}} = \frac{8.02}{q_{\mathrm{e}}^{046}(\frac{P_{\mathrm{e}} - P_{\mathrm{A}}}{P_{\mathrm{A}}})^{0.46}}$	Clark 1991 [85]
2	1.6 – 1.8	$MMD_i = 6.90 + 0.0441 \times VS + 23.6 \times C_{\mathrm{EtOH}} - 63.8 \times C^2_{\mathrm{EtOH}} + 24.7 \times C_{\mathrm{EtOH}} \times OD - 0.129 \times C_{\mathrm{EtOH}} \times VS$	Stein et al. 2012 [90]
3	1.8 – 3.1	$MMD_{\mathrm{i}} = \frac{416\,\sigma_{\mathrm{pa}}}{P_{\mathrm{mc}}}$	Ivey et al. 2014 [88]
4	Not given	$MMD_{\mathrm{i}} = 1274\,\frac{\sigma_{\mathrm{p}}}{P_{\mathrm{mc}}} - 139 * 10^3 \frac{\alpha^2 * \rho_{\mathrm{p}}}{\sigma_{\mathrm{p}}}$	Shemirani et al. [62]
5	Not given	MMD_{i} =10.5 –13.2	Wang et al. [132]

Before the simulation was started, the mass median diameters (MMD) were converted to count median diameters (CMD) using the Hatch-Choate equation for lognormal distributions:

$$CMD = MMD * \exp\left(-3 * (\mathrm{Ln}\, GSD)^2\right). \quad (3.2)$$

The simulation began by generating N=10,000 initial droplets of various sizes (d_i) by randomly selecting from the size distribution of the initial droplets. The volume of each droplet was calculated using this equation:

$$V_{\mathrm{i}} = \frac{\pi}{6} {d_{\mathrm{i}}}^3. \quad (3.3)$$

All the volumes were stored in an array. Then, the total volume of droplets was calculated using the following equation:

`

$$V_{ti} = \sum_{1}^{N} V_i \, . \tag{3.4}$$

Next, a loop was initiated to generate drug particles under the condition that the total mass of drug particles did not exceed the maximum amount capable of existing in the total volume of the droplets ($M_t \leq V_{ti}$ *C_f* C_d). In the process of generating the drug particles, the initial step involved determining the quantity of drug particles within a specific droplet (first volume in the droplets array). To achieve this aim, we calculated the approximate number of particles per unit volume (PPUV):

$$PPUV = \frac{\exp(4.5 * (\ln(GSD_D))^2) * C_D * \rho_I}{\frac{\pi}{6} * \rho_D * (MMD_D)^3} \tag{3.5}$$

Researchers have implemented various methods in different studies to determine the number of drug particles in each droplet (N_d). One approach involves randomly selecting drug particles from a list of generated drug particles [133]. In a recent study, a volume-based method was used to allocate drug particles to droplets, which is another technique to determine N_d [131]. Additionally, some researchers have utilized a Poisson distribution, a probability distribution commonly used for counting events when these events are discrete and do not interact [90]. In the current study, the researchers also used the Poisson distribution as a method to calculate N_d:

$$P(I) = \frac{e^{-M} * M^I}{I!} \text{, where } M = PPUV * V_i \tag{3.6}$$

'M' in the equation refers to expected number of drug particles in a given droplet and 'I' is the possible number of suspended particles in the droplet (0, 1, 2, …).

Subsequently, #N_d particles were generated and allocated to the droplet, ensuring that the total volume of particles (V_d) within the droplet was equal to or less than the droplet volume (V_i). The corresponding diameter (d_r) and mass (m_r) of each residual particle were then determined using the following equations, enabling the plotting of the APSD of residual particles:

$$d_r = \sqrt[3]{\frac{6 * V_d}{\pi}} \tag{3.7}$$

$$m_r = \rho_d * V_d \tag{3.8}$$

`

3.3. Results and discussions

3.3.1. Effect of size distribution of initial droplets

Many studies have indicated that the size distribution of the initial droplets has a direct influence on the size distribution of particles emitted from pMDIs. In an early investigation conducted by Kim et al., the impact of formulation variables and hardware characteristics on the size distribution of pMDI aerosols was examined [126]. Later, Clark investigated the atomization process of pMDIs and established that the size of the initial droplets is influenced by expansion chamber conditions. Clark introduced an empirical equation to estimate the MMD of the initial droplets, which is a function of ambient and expansion chamber pressure, as well as the vapor fraction of vapor-liquid mixture in the expansion chamber (Table 3.2 row #1) [85]. Subsequently, Stein et al. conducted an experimental study to evaluate the effects of volatile components like propellants and excipients such as ethanol, in addition to device variables like valve size and orifice diameter, on the size of initial droplets [134]. Their research resulted in the development of an empirical equation, shown in Table 3.2 row #2, to describe this relationship between solution pMDIs and HFA-134a propellant. Following these earlier studies, Ivey et al. employed dimensional analysis to find an empirical equation for estimating the MMD of initial droplets. Their equation is designed specifically for solution-based pMDIs and is applicable to a wide range of propellants and propellant co-solvent mixtures [101]. Subsequently, Shemirani et al. expanded on this research by incorporating the thermal properties of the propellant and investigating how these properties influence the size of the initial droplets. This additional dimensional analysis added depth to our understanding of the factors influencing the formation of initial droplets in pMDIs [62]. A recent study conducted by Wang et al. investigated the impact of factors such as ethanol concentration, the type of propellant used, and the orifice diameter on the content equivalent diameter. Additionally, they explored the effects of water condensation under different humidity conditions on the aerosol performance of pMDIs [135].

In this study, the mass median diameter of the initial droplets (MMD_i) was calculated using approaches #2, #3 and #5 in Table 3.2. Approach #4 was not used as it was only applicable to a narrow range of data. These calculations were carried out under the assumption of a constant temperature of 20°C, and the results obtained from these different calculation methods were then compared and analyzed. Additionally, the mass median aerodynamic diameter of residual particles ($MMAD_r$) was computed, and the occurrence of droplets with no particles (empty), only one

`

particle (singlets), and more than one particle (multiplets) was assessed. These computations were carried out using the Monte Carlo simulation method, which was detailed in the materials and methods section. Importantly, these calculations were performed for different propellants. This part of the study aimed to understand how the choice of propellant and its corresponding MMD_i influences the aerodynamic size of residual particles and the occurrence of multiplets.

Initially, the MMD_i for pMDIs containing HFA-134a propellant was calculated using methods #2, #3, and #5 in Table 3.2; afterwards, the $MMAD_r$ was computed using the simulation. The GSD_i was assumed to be 1.8 across all cases to maintain consistency and facilitate comparison. The results, shown in Table 3.3, revealed that experimental $MMAD_r$s were in close agreement for all propellants. Notably, with HFA-134a propellant, there was stronger alignment with the Stein (#2) and Wang (#5) studies than with the Ivey study (#5). Overall, the Ivey correlation yielded initial droplet diameters (MMD_i) nearly 3 µm smaller than the other two correlations. However, the final $MMAD_r$ did not exhibit significant differences from the other studies, with variations ranging from about 0.7 to 0.4 microns.

Regarding the occurrence of multiplets and singlets, the Ivey correlation resulted in a higher number of empty droplets, and many of the occupied droplets were singlets. By comparison, in the Stein study and even more so in the Wang study, due to the larger initial droplets there were more droplets occupied by one or more suspended particles (Figure 2.1).

Table 3.3. Comparison of results obtained from different correlations used in this study

Propellant	Study	MMD_i (μm)	computed $MMAD_r$ (μm)	Experimental $MMAD_r$ (μm)
HFA-134a	Stein et al. (2012)	9.1	2.5	2.8
	Ivey et al. (2014)	6.4	2.1	2.8
	Wang et al. (2023)	10.5	2.7	2.8
HFA-227ea	Ivey et al. (2014)	7.4	2.3	2.7
	Wang et al. (2023)	10.8	2.7	2.7
HFO-1234ze	Ivey et al. (2014)	8.3	2.4	2.9
	Wang et al. (2023)	11.5	2.8	2.9

`

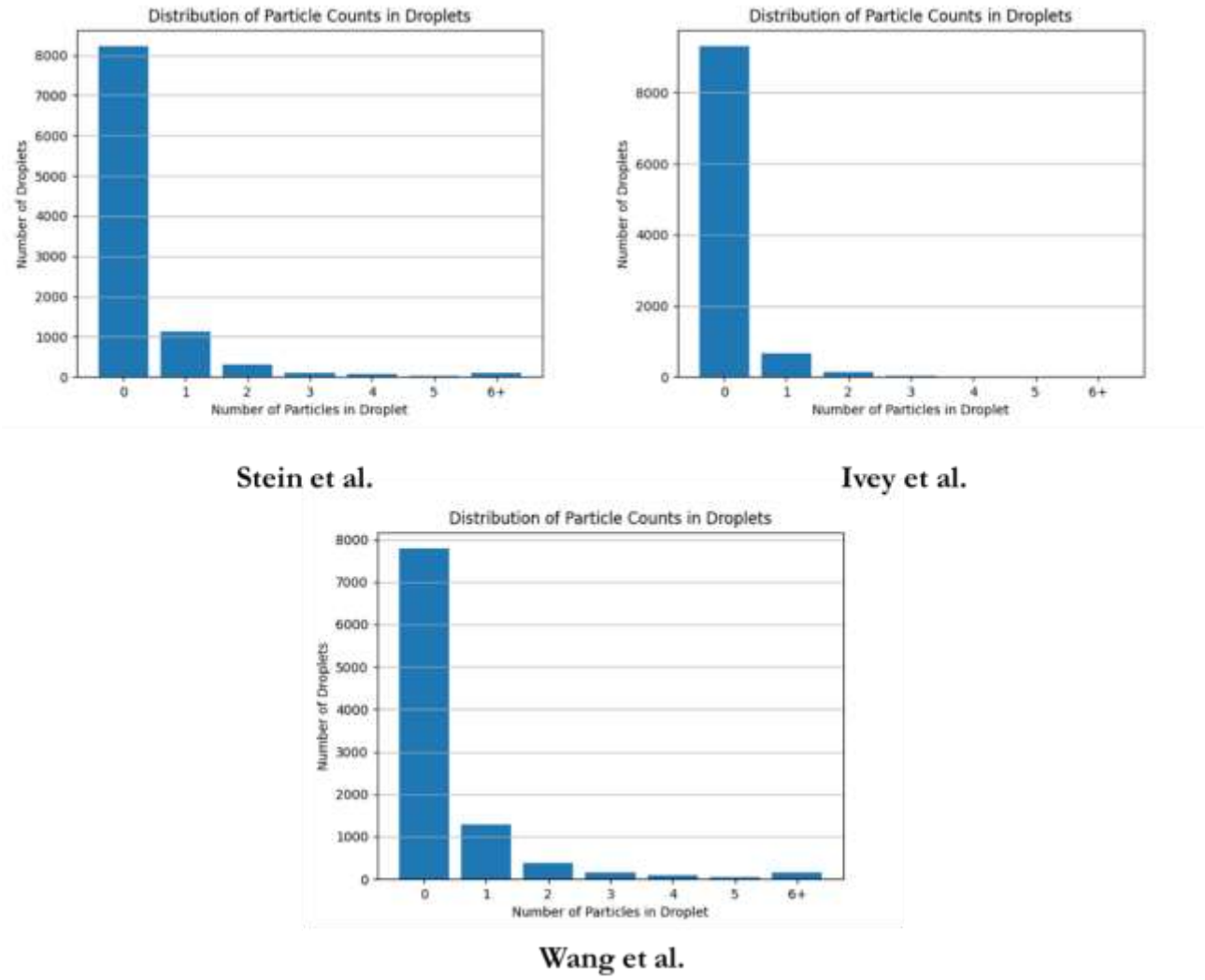

Figure 3.1. Distribution of particle counts in droplets representing occurrence of multiplets and singlets in different correlations. The majority of droplets ended up being empty

3.3.2. Effect of size distribution of micronized drug

Berry et al. [136] conducted an extensive study on the impact of micronized drug size on the APSD of emitted aerosol and the stability of HFA pMDIs. They studied particles with median sizes ranging from 1.14 to 1.77, as measured by laser diffraction. Their results showed that larger micronized drugs exhibit a broader distribution or higher GSD, resulting in an increase in $MMAD_r$ and a decrease in the fine particle fraction.

`

In another study, Sheth et al. [137] investigated the influence of parameters such as drug concentration and size distribution on the final $MMAD_r$ and the occurrence of multiplets. According to their findings, an increase in micronized drug size leads to a decrease in the percentage of multiplets and the corresponding $MMAD_r$.

Stein et al. [90] compared experimental $MMAD_r$ with simulated MMADr in micronized drugs with three different mass median aerodynamic diameters ($MMAD_d$): 1.22, 1.77, and 2.62. Their results demonstrated a good agreement between experimental and simulation results, indicating that increasing the $MMAD_d$ led to an increase in the $MMAD_r$.

In our current investigation, the $MMAD_r$ was computed for pMDIs filled with HFO-1234ze propellant using the MMD_i obtained from the Wang study (#5), and $MMAD_d$ values of 100 nm, 500 nm, 1µm, 3µm, and 6µm (Figure 3.2). The remaining variables remained at default values, as explained in section 3.2. For 100nm particles, no empty droplets were observed; all droplets formed multiplets, resulting in an $MMAD_r$ identical to that of a solution pMDI. This result aligns with expectations, as a well-suspended nanoparticle pMDI behaves similarly to a solution where:

$$d_{\mathrm{r}} = \sqrt[3]{\frac{6*\nu_{\mathrm{i}}*C_{\mathrm{f}}*C_{\mathrm{d}}}{\pi*\rho_{\mathrm{d}}}} \tag{3.9}$$

For 500 nm particles, approximately 80 percent of droplets formed multiplets, and the resulting $MMAD_r$ was almost identical to that of 100nm particles, indicating that these particles also behaved similarly to a solution. 1µm particles exhibited a slightly larger $MMAD_r$ with about 40% empty droplets. For 3µm and 6µm particles, most of the droplets were empty, resulting in $MMAD_r$ values of approximately 4µm and 6µm, respectively. No multiplets were found for 6µm particles (Figure 3.3).

In the real world, poorly micronized drug particles may accumulate in the canister, leading to poor dose content uniformity. In the simulation, however, if the volume of particles exceeds the droplet size, the droplet grows to the size of the drug particle. Furthermore, a very large $MMAD_r$ leads to a very small PPUV, drastically decreasing the likelihood of droplets being occupied by one or more particles. Thus, iterations repeat until the desired mass of drug particles is achieved.

`

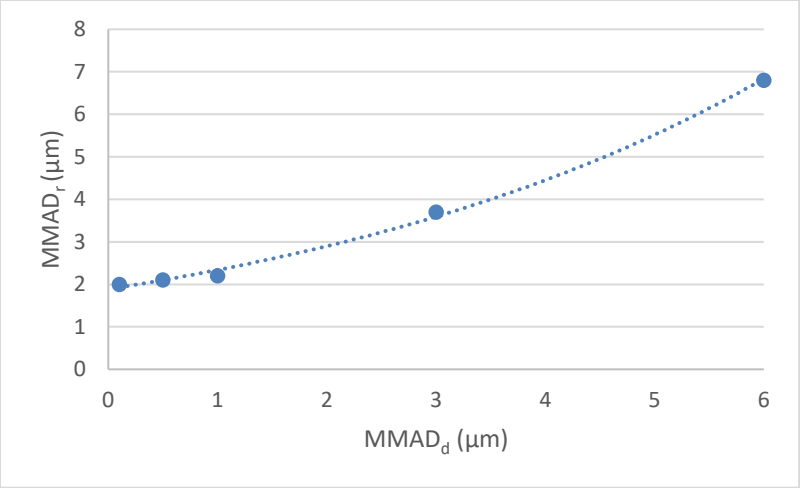

Figure 3.2. Simulated results for mass median aerodynamic diameter of residual particles ($APSD_r$) for different micronized drug diameters ($MMAD_d$). Increasing the $MMAD_d$ caused a gradual increase in the $MMAD_r$.

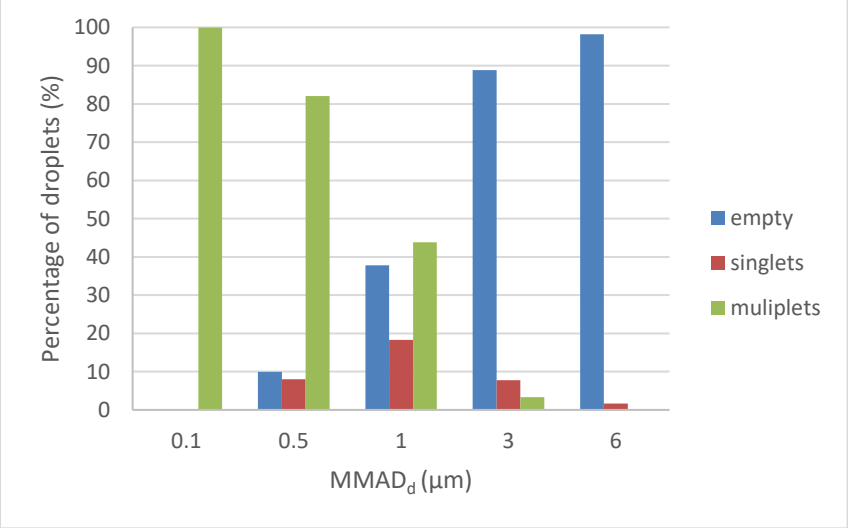

Figure 3.3. Percentage of empty droplets, singlets and multiplets for different micronized drug diameters ($MMAD_d$). Increasing the $MMAD_d$ resulted in a considerable decrease in the percentage of multiplets.

3.3.3. Effect of drug concentration

To ensure that a pMDI delivers the nominal dose to the patient, maintaining a minimum drug concentration is crucial. Higher drug concentrations require fewer actuations for the patient. However, beyond a certain threshold, high drug concentration can negatively impact suspension stability and uniformity of emitted dose, and may therefore lead to valve clogging.

`

An early study by Polli et al. [138] highlighted this impact, showing that an increase in drug concentration from 1.43 mg/g to 2.86 mg/g dramatically altered the MMD of the aerosol particles, which shifted from 3.2 µm to 18 µm.

In a 2015 study, Stein et al [130] used a cascade impactor to measure the Aerodynamic Particle Size Distribution of residual particles ($APSD_r$) in pMDIs containing varying concentrations of suspended and/or solubilized drug particles along with approximately 8% ethanol. Their observations indicated that an increase in concentrations of dissolved and/or suspended drug led to a rise in $MMAD_r$. In addition, their results showed that the impact of dissolved drug concentration became more pronounced at higher suspension concentrations. Running a simulation on their data similar to this study, and comparing simulated and experimental $APSD_r$, they found good agreement, confirming the simulation's potential for expediting the performance of single or combination pMDIs.

In our investigation using HFO-1234ze propellant entries and default drug data, a variety of concentrations from 0.001 to 0.1 was used to evaluate particle count distribution and $MMAD_r$. Simulated results demonstrated a gradual increase in the $MMAD_r$ from 2.3 µm to about 5.5 µm. This increase in the $MMAD_r$ could potentially compromise pMDI performance, as previously explained, since it resembles a power function with increasing drug concentration (Figure 3.4). Furthermore, as the drug concentration increased from 0.001 g/g to 0.1 g/g, a gradual decrease in the number of empty droplets and a simultaneous increase in the number of multiplets were observed. The number of singlets remained within a consistent range of 15-18%, indicating that drug concentration minimally affects the number of singlets (Figure 3.5).

`

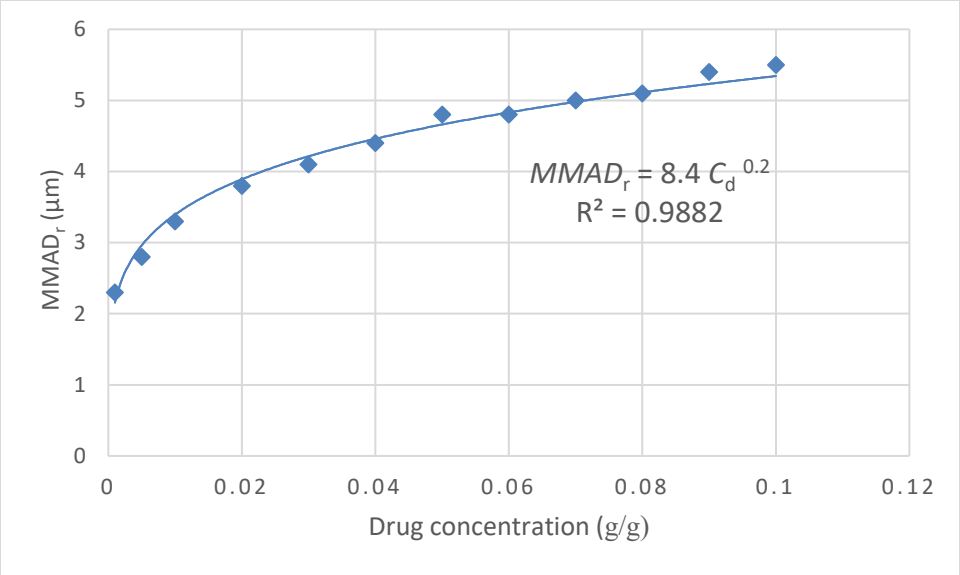

Figure 3.4. Increasing the drug concentration gradually increased the $MMAD_{r,,}$ resembling a power function.

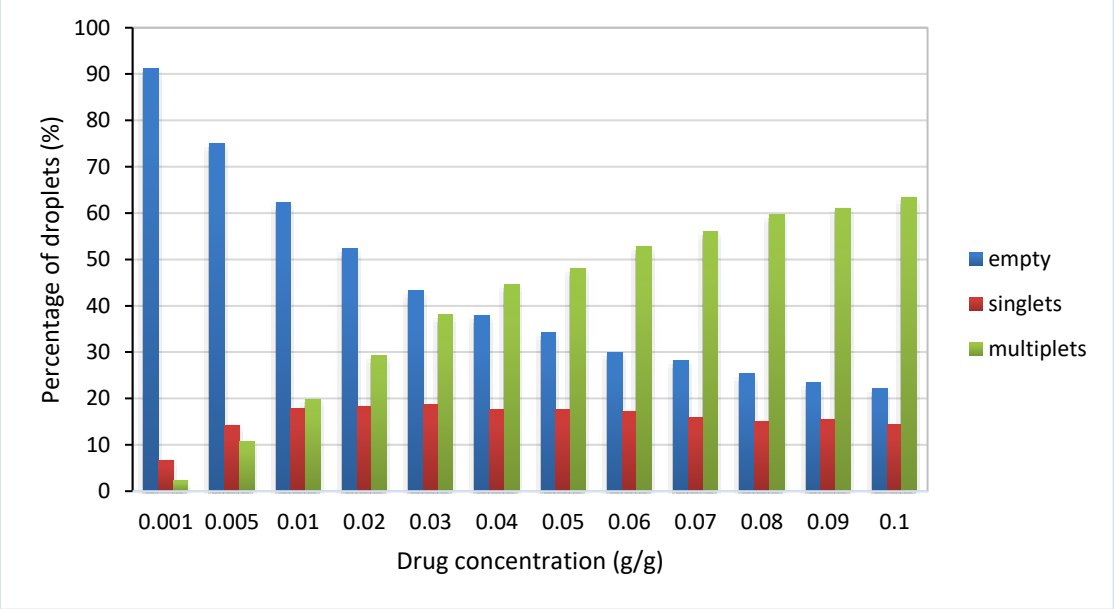

Figure 3.5. The percentage of empty droplets decreased with an increase in the drug concentration, simultaneously increasing the percentage of multiplets, with no notable impact on the percentage of singlets.

3.3.4. Effect of suspension stability

Suspension stability directly affects the dose content uniformity and $APSD_r$ of pMDIs. Various factors can influence suspension stability, including but not limited to the level of agitation or shaking [139–141], physical properties of the propellant used such as density [21], suspension concentration [142], and the use of stabilizers [25]. In a study conducted by Chierici et al. [141],

`

the emitted dose of various commercial pMDIs without shaking or with delayed firing after shaking was investigated. The results demonstrated that using a pMDI without shaking led to a decrease or increase in the delivered dose, resulting in inconsistently delivered doses throughout the product's shelf life. Similarly, delays in firing after shaking affected the delivered dose, although not as significantly as not shaking it at all. Although no-shaking compromised the consistency of delivered dose in all suspensions, different pMDI formulations exhibited varying trends, with some formulations showing minimal changes in emitted dose. This variation was explained by the gravitational stability of the formulation, which is influenced by the different density of each component. As explained in depth by Wang et al. [56], the governing equation for suspension stability that results in creaming or sedimentation is Stoke's law:

$$v_{\mathrm{s}} = \frac{(\rho_{\mathrm{p}} - \rho_{\mathrm{d}})(1-\phi)g}{18\mu\chi}\, d_{\mathrm{v}}^2 \tag{3.10}$$

According to Stoke's law, the sedimentation velocity (v_s) of suspended drug particles in a pMDI is a function of the square root of the drug volume equivalent diameter and the difference in propellant and particle densities. The respective densities of HFA-134a, HFA-227ea and HFO-1234ze were presented in Table 2.2. As explained in detail in Chapter 2, rugosity and porosity play a vital role in suspension stability. Despite the difference between the true density of rugose lipid particles (1.1 g/cm^3) and propellants (1.18-1.41 g/cm^3) the suspensions maintained an excellent colloidal stability throughout the one-year study, highlighting the effect of suspension stabilizers. Cocks et al. [143] conducted a study confirming the role of stabilizers. Their results showed that with an optimum concentration of the stabilizer, a stable suspension with PLGA porous particles can be achieved.

3.3.5. Effect of atmospheric conditions

In suspension pMDIs, the water uptake can potentially trigger particle growth or the degradation of active ingredients. Williams et al. [120] conducted a comprehensive study exploring the impact of water levels on both suspension and solution pMDIs. Their findings revealed an increase in the mean particle size in water-spiked suspension pMDIs. They argued that water penetration into the formulation occurs through diffusion, which depends on the relative humidity of the environment. Their results also indicated that pMDIs reach an equilibrium in water content after a specific period.

`

The influence of relative humidity extends beyond water uptake in pMDIs. High relative humidity can also affect the size of aerosols generated by pMDIs [144]. The condensation of water on dry particles that occurs in high RH environments results in an increase in the $MMAD_r$. Shemirani et al. investigated the effect of temperature and relative humidity on the throat deposition and lung dose of two commercial suspension and solution pMDIs. Their results demonstrated that in suspension pMDIs, an increase in RH would increase throat deposition and decrease lung dose. They found that an increase in temperature did not significantly affect lung and throat deposition, while in the solution pMDI, a decrease was observed in throat deposition when the temperature was elevated from 20 °C to 40 °C. In another study, Morin et al. [73] explored the effect of ambient and device temperature on lung dose. Four different pMDIs were tested at various ambient temperatures (-10°C, 0°C, 10°C, 20°C, 40°C) and device temperatures (-10°C, 20°C). Results showed a decrease in lung dose at lower ambient temperatures. At -10 °C device temperature, a decrease in lung dose was also observed due to the decrease in vapor pressure of the propellant, leading to a coarser droplet size distribution. The authors argued that both ambient and device temperature may influence the APSD of the aerosol. This effect was demonstrated to be more significant in suspension pMDIs than in solution pMDIs. The results from these studies underscore the impact of environmental conditions on APSD, an aspect beyond the scope of the simulation presented in this study. This limitation indicates the need for further advancements in simulation methods to enhance the understanding and optimization of pMDI performance.

`

3.4. Conclusion

In conclusion, although *in vitro* experiments are essential for evaluating various metered dose inhaler formulations, well-structured simulations offer the advantage of expediting the aerosol performance of pMDIs. Employing a robust approach to estimating the initial droplet diameter enhances the realism of the simulated results for mass mean diameter of residual particles emitted by pMDIs. Additionally, achieving an optimal micronized drug concentration and size is important for ensuring effective drug delivery to the lungs.

While simulation methods prove valuable in predicting the aerosol performance of pMDIs, it is crucial to acknowledge their limitations, as they may not account for certain factors such as environmental conditions and physicochemical properties of the formulation, for instance suspension stability. Therefore, a comprehensive research approach should involve factors like the compatibility of pMDI components and relative humidity, ensuring an overall understanding of the system's behavior.

`

Chapter 4 Conclusion

pMDIs continue to be a leading choice for drug delivery due to their cost-effectiveness and ease of use. However, precise drug delivery to the targeted region necessitates meticulous formulation and design. Chapter 1 provided an in-depth review of aerosol drug delivery, with a focus on pMDI devices and their characteristics.

Chapter 2 investigated the impact of physical stability factors, such as suspension stability, particle morphology, and size, on pMDI performance. The potential of novel rugose lipid particles in pMDIs with both new and established propellants was also assessed. These particles exhibited excellent colloidal stability in various propellants, making them promising candidates for suspension stabilizers and dispersing agents. Furthermore, because of their chemical composition they are endogenous to lungs and thus safe for patient use. The compatibility of HFO-1234ze, an environmentally friendly propellant, with rugose lipid particles was also confirmed, indicating progress towards sustainable propellant options.

Chapter 3 emphasized the importance of appropriate modeling approaches for predicting pMDI performance. A Monte Carlo approach, adapted from previous studies and further developed, was used to investigate the influence of various factors on the aerodynamic particle size distribution of residual particles emitted from pMDIs. The significance of the size of initial droplets in the sprayed aerosol on the final particle size was highlighted, along with the challenges associated with the experimental measurement of this parameter. The need for proper drug micronization methodology was highlighted, as poorly micronized drugs were found to negatively affect the final particle size. While the simulation methods outlined here provided valuable insights for pMDI development, the potential impact of unaccounted-for parameters, such as atmospheric conditions, on the models should not be underestimated.

In summary, this thesis highlights the importance of careful formulation, design, and modeling in optimizing pMDI performance and contributes to the development of more effective and sustainable inhaler technologies.

Bibliography

1. Ferkol T, Schraufnagel D. The global burden of respiratory disease. Ann Am Thorac Soc. 2014;11(4):405-416. doi:10.1513/AnnalsATS.201311-405PS
2. Levine SM, Marciniuk DD. Global Impact of Respiratory Disease: What Can We Do, Together, to Make a Difference? Chest. 2022;161(1):7-11. doi:10.1016/j.chest.2022.01.014
3. Mishra B, Singh J. Novel drug delivery systems and significance in respiratory diseases. In: Targeting Chronic Inflammatory Lung Diseases Using Advanced Drug Delivery Systems. Elsevier; 2020:57-95. doi:10.1016/B978-0-12-820658-4.00004-2
4. Xie M, Liu X, Cao X, et al. Trends in prevalence and incidence of chronic respiratory diseases from 1990 to 2017. Respir Res. 2020;21(1):34. Published 2020 Feb 11. doi:10.1186/s12931-020-1291-8
5. Natarajan A, Beena PM, Devnikar AV, Mali S. A systemic review on tuberculosis. Indian J Tuberc. 2020;67(3):295-311. doi:10.1016/J.IJTB.2020.02.005
6. Stein SW, Thiel CG. The History of Therapeutic Aerosols: A Chronological Review. J Aerosol Med Pulm Drug Deliv. 2017;30(1):1-24. doi:10.1089/jamp.2016.1297
7. Rathbone M. Advances in Delivery Science and Technology. Springer; 2011. Accessed July 18, 2023. https://www.springer.com/series/8875/books
8. Anderson S, Atkins P, et al. Inhaled Medicines: Past, Present, and Future. Pharmacol Rev. 2022;74(1):50-118. doi:10.1124/PHARMREV.120.000108
9. Newman SP. Delivering drugs to the lungs: The history of repurposing in the treatment of respiratory diseases. Adv Drug Deliv Rev. 2018;133:5-18. doi:10.1016/j.addr.2018.04.010
10. Keller LA, Merkel O, Popp A. Intranasal drug delivery: opportunities and toxicologic challenges during drug development. Drug Deliv Transl Res. 2022;12(3):735-757. doi:10.1007/s13346-020-00891-5
11. Menon M, Dalby RN, Naik I, Savla H, Kalola K. Pulmonary, Nasal, and Topical Aerosol Drug Delivery Systems. In: Remington: The Science and Practice of Pharmacy. Academic Press; 2021:605-622. doi:10.1016/B978-0-12-820007-0.00030-1
12. Masjedi M, Montahaei T, Sharafi Z, Jalali A. Pulmonary vaccine delivery: An emerging strategy for vaccination and immunotherapy. J Drug Deliv Sci Technol. 2022;76:103184. doi:10.1016/j.jddst.2022.103184

`

13. Ari A, Fink JB. Recent advances in aerosol devices for the delivery of inhaled medications. Expert Opin Drug Deliv. 2020;17(1):1-16. doi:10.1080/17425247.2020.1712356
14. Martin AR, Finlay WH. Nebulizers for drug delivery to the lungs. Expert Opin Drug Deliv. 2015;12(1):89-101. doi:10.1517/17425247.2015.995087
15. Longest PW, Spence BM, Hindle M. Devices for Improved Delivery of Nebulized Pharmaceutical Aerosols to the Lungs. J Aerosol Med Pulm Drug Deliv. 2019;32(5):317-339. doi:10.1089/jamp.2018.1508
16. Howe C, Momin MAM, Farkas DR, et al. Advancement of the Infant Air-Jet Dry Powder Inhaler (DPI): Evaluation of Different Positive-Pressure Air Sources and Flow Rates. Pharm Res. 2021;38(4):1615-1632. doi:10.1007/s11095-021-03094-w
17. Shetty N, Cipolla D, Park H, Zhou QT. Physical stability of dry powder inhaler formulations. Expert Opin Drug Deliv. 2020;17(1):77-96. doi:10.1080/17425247.2020.1702643
18. Emeryk A, Sosnowski TR, Kupczyk M, et al. Impact of inhalers used in the treatment of respiratory diseases on global warming. Adv Respir Med. 2021;89(5):427-438. doi:10.5603/ARM.a2021.0092
19. Stein SW, Sheth P, Hodson PD, Myrdal PB. Advances in metered dose inhaler technology: Hardware development. AAPS PharmSciTech. 2014;15(2):510-522. doi:10.1208/s12249-013-0062-y
20. Cripps A, Riebe M, Schulze M, Woodhouse R. Pharmaceutical transition to non-CFC pressurized metered dose inhalers. Respir Med. 2000;94 Suppl B:S3-S9. doi:10.1016/s0954-6111(00)80143-2
21. Smyth HDC. The influence of formulation variables on the performance of alternative propellant-driven metered dose inhalers. Adv Drug Deliv Rev. 2003;55(7):807-828. doi:10.1016/S0169-409X(03)00079-6
22. Jones S. Suspension versus solution metered dose inhalers: different products, different particles? J Drug Deliv Sci Technol. 2011;21(4):319-322. https://doi.org/10.1016/S1773-2247(11)50049-8
23. Myrdal PB, Sheth P, Stein SW. Advances in metered dose inhaler technology: Formulation development. AAPS PharmSciTech. 2014;15(2):473-487. doi:10.1208/s12249-013-0063-x

`

24. Ooi J, Traini D, Boyd BJ, Gaisford S, Young PM. Determination of physical and chemical stability in pressurised metered dose inhalers: Potential new techniques. Expert Opin Drug Deliv. 2015;12(10):1517-1530. doi:10.1517/17425247.2015.1046834
25. Verma S, Kumar S, Gokhale R, Burgess DJ. Physical stability of nanosuspensions: Investigation of the role of stabilizers on Ostwald ripening. Int J Pharm. 2011;406(1-2):145-152. doi:10.1016/j.ijpharm.2010.12.027
26. Vehring R, Lechuga-Ballesteros D, Joshi V, et al. Cosuspensions of microcrystals and engineered microparticles for uniform and efficient delivery of respiratory therapeutics from pressurized metered dose inhalers. Langmuir. 2012;28(20):15015-15023. doi:10.1021/la302281n
27. Yang L, Da Rocha SRP. Understanding solvation in the low global warming hydrofluoroolefin HFO-1234ze propellant. J Phys Chem B. 2014;118(31):10675-10687. doi:10.1021/jp5059319
28. Sellers WFS. Asthma pressurised metered dose inhaler performance: Propellant effect studies in delivery systems. Allergy Asthma Clin Immunol. 2017;13:202. doi:10.1186/s13223-017-0202-0
29. Wilkinson A, Woodcock A. The environmental impact of inhalers for asthma: A green challenge and a golden opportunity. Br J Clin Pharmacol. 2021. doi:10.1111/bcp.15135
30. Panigone S, et al. Environmental impact of inhalers for respiratory diseases: Decreasing the carbon footprint while preserving patient-tailored treatment. BMJ Open Respir Res. 2020;7(1):e000571. doi:10.1136/bmjresp-2020-000571
31. Environmental Investigation Agency. High Stakes: Implementing and strengthening climate and ozone commitments under the Montreal Protocol. 2019. https://us.eia.org/report/high-stakes-implementing-and-strengthening-climate-and-ozone-commitments-under-the-montreal-protocol/. Accessed 18 May 2023.
32. Corr S, Noakes TD. Pressurized Metered Dose Inhaler Propellants: Going Forward. In: Respiratory drug delivery. 2017.
33. Buttini F, et al. Metered dose inhalers in the transition to low GWP propellants: what we know and what is missing to make it happen. Expert Opin Drug Deliv. 2023:1-16. doi:10.1080/17425247.2023.2264184

`

34. Lindley AA, Noakes TJ. Consideration of Hydrofluoroolefins (HFOs) as potential candidate medical propellants.
35. Pritchard JN. The climate is changing for metered-dose inhalers and action is needed. Drug Des Devel Ther. 2020;14:3043-3055. doi:10.2147/DDDT.S262141
36. Baron C, Shur J. Investigating the Propellant Pathways Leading to a Sustainable Future for MDIs. ONdrugDelivery. 2022;(131):49-52.
37. Rossi I, et al. Fundamental properties of propellant aerosols can guide transition to low global warming potential pMDIs: size, velocity and surface charge.
38. Lechuga-Ballesteros D, et al. Particle Engineering Technology for Inhaled Therapies. In: Pharmaceutical Inhalation Aerosol Technology.
39. Ordoubadi M, et al. On the Physical Stability of Leucine-Containing Spray-Dried Powders for Respiratory Drug Delivery. Pharmaceutics. 2023;15(2):435. doi:10.3390/pharmaceutics15020435
40. Mah PT, et al. The use of hydrophobic amino acids in protecting spray dried trehalose formulations against moisture-induced changes. Eur J Pharm Biopharm. 2019;144:139-153. doi:10.1016/j.ejpb.2019.09.014
41. Wang Z, et al. Leucine enhances the dispersibility of trehalose-containing spray-dried powders on exposure to a high-humidity environment. Int J Pharm. 2021;601:120561. doi:10.1016/j.ijpharm.2021.120561
42. Wauthoz N, Amighi K. Phospholipids in pulmonary drug delivery. Eur J Lipid Sci Technol. 2014;116(6):748-762. doi:10.1002/ejlt.201300368
43. Wang H, et al. Inhalable microparticle platform based on a novel shell-forming lipid excipient and its feasibility for respirable delivery of biologics. Eur J Pharm Biopharm. 2022;177:308-322. doi:10.1016/j.ejpb.2022.07.013
44. Weers J, Tarara TE. The PulmoSphereTM platform for pulmonary drug delivery. Ther Deliv. 2014;5(9):947-950. doi:10.4155/tde.14.63
45. Duddu SP, et al. Improved Lung Delivery from a Passive Dry Powder Inhaler Using an Engineered PulmoSphere Powder. 2002.
46. Weers JG, et al. Spray-Dried PulmoSphereTM Formulations for Inhalation Comprising Crystalline Drug Particles. AAPS PharmSciTech. 2019;20(1):10. doi:10.1208/s12249-018-1280-0

`

47. Lechuga-Ballesteros D, et al. Novel cosuspension metered-dose inhalers for the combination therapy of chronic obstructive pulmonary disease and asthma. Future Med Chem. 2011;3(14):1807-1822. doi:10.4155/fmc.11.133
48. Lechuga-Ballesteros D, et al. Dose Proportionality in a Triple Therapy Cosuspension pMDI with Multiple Strengths of an Inhaled Corticosteroid. Am J Respir Crit Care Med. 2013;187:A2173.
49. Wang H, et al. Spray Dried Rugose Lipid Particle Platform for Respiratory Drug Delivery. Pharm Res. 2022;39(3):805-823. doi:10.1007/s11095-022-03242-w
50. Vehring R. Pharmaceutical particle engineering via spray drying. Pharm Res. 2008;25(5):999-1022. doi:10.1007/s11095-007-9475-1
51. Carrigy NB, Vehring R. Engineering Stable Spray-Dried Biologic Powder for Inhalation. In: Pharmaceutical Inhalation Aerosol Technology.
52. Vehring R, Foss WR, Lechuga-Ballesteros D. Particle formation in spray drying. J Aerosol Sci. 2007;38(7):728-746. doi:10.1016/j.jaerosci.2007.04.005
53. Ordoubadi M, et al. Multi-Solvent Microdroplet Evaporation: Modeling and Measurement of Spray-Drying Kinetics with Inhalable Pharmaceutics. Pharm Res. 2019;36(8):123. doi:10.1007/s11095-019-2630-7
54. Dellamary LA, Tarara TE, Smith DJ, et al. Hollow Porous Particles in Metered Dose Inhalers. Pharm Res. 2000;17(2):168-174. doi:10.1023/A:1007513213292
55. Son YJ, Miller DP, Weers JG. Optimizing Spray-Dried Porous Particles for High Dose Deliv-ery with a Portable Dry Powder Inhaler. Published online July 14, 2021. doi:10.20944/preprints202107.0641.v1
56. Wang H, Tan P, Barona D, et al. Characterization of the suspension stability of pharmaceuticals using a shadowgraphic imaging method. Int J Pharm. 2018;548:128-138. doi:10.1016/j.ijpharm.2018.06.053
57. Finlay WH. Introduction to the respiratory tract. In: The Mechanics of Inhaled Pharmaceutical Aerosols. Elsevier; 2019:103-116. doi:10.1016/b978-0-08-102749-3.00005-1
58. Weibel ER. The Pathway for Oxygen: Structure and Function in the Mammalian Respiratory System. Harvard University Press; 1984.

`

59. Finlay WH. Particle deposition in the respiratory tract. In: The Mechanics of Inhaled Pharmaceutical Aerosols. Elsevier; 2019:133-182. doi:10.1016/B978-0-08-102749-3.00007-5
60. Hofmann W. Modelling inhaled particle deposition in the human lung-A review. J Aerosol Sci. 2011;42(10):693-724. doi:10.1016/j.jaerosci.2011.05.007
61. Ivey JW, Vehring R, Finlay WH. Understanding pressurized metered dose inhaler performance. Expert Opin Drug Deliv. 2015;12(6):901-916. doi:10.1517/17425247.2015.984683
62. Shemirani FM, Church TK, Lewis DA, Finlay WH, Vehring R. Onset of Flash Atomization in a Propellant Microjet. J Fluids Eng. 2015;137(3). doi:10.1115/1.4030089
63. de Charras YL, Ramírez-Rigo MV, Bertin DE. Prediction of the particle size distribution of the aerosol generated by a pressurized metered-dose inhaler. Powder Technol. 2022;399:117151. doi:10.1016/j.powtec.2022.117151
64. Johal B, Murphy S, Tuohy J, Marshall J. Plume characteristics of two HFA-driven inhaled corticosteroid/long-acting beta2-agonist combination pressurized metered-dose inhalers. Adv Ther. 2015;32(6):567-579. doi:10.1007/s12325-015-0219-z
65. Talaat M, Si X, Xi J. Effect of MDI actuation timing on inhalation dosimetry in a human respiratory tract model. Pharmaceuticals (Basel). 2022;15(1):61. doi:10.3390/ph15010061
66. Stein SW, Myatt BJ, Cocks P, et al. Experimental and theoretical investigations of pMDI atomization and plume characteristics using alternative propellants. 2021.
67. Lavorini F, Fontana GA, Usmani OS. New inhaler devices - the good, the bad and the ugly. Respiration. 2014;88(1):3-15. doi:10.1159/000363390
68. Ju D, Shrimpton J, Bowdrey M, Hearn A. Effect of expansion chamber geometry on atomization and spray dispersion characters of a flashing mixture containing inerts. Part II: high speed imaging measurements. Int J Pharm. 2012;432(1-2):32-41. doi:10.1016/j.ijpharm.2012.04.064
69. Hochrainer D, Hölz H, Kreher C, et al. Comparison of the aerosol velocity and spray duration of Respimat Soft Mist inhaler and pressurized metered dose inhalers. J Aerosol Med. 2005;18(3):273-282. doi:10.1089/jam.2005.18.273

`

70. Duke DJ, Nguyen DT, dos Reis LG, et al. Increasing the fine particle fraction of pressurised metered dose inhaler solutions with novel actuator shapes. Int J Pharm. 2021;597:120341. doi:10.1016/j.ijpharm.2021.120341
71. Dhand R. Aerosol plumes: slow and steady wins the race. J Aerosol Med. 2005;18(3):261-263. doi:10.1089/jam.2005.18.261
72. Ivey JW, Bhambri P, Church TK, et al. Humidity affects the morphology of particles emitted from beclomethasone dipropionate pressurized metered dose inhalers. Int J Pharm. 2017;520(1-2):207-215. doi:10.1016/j.ijpharm.2017.01.062
73. Morin CM, Ivey JW, Titosky JT, et al. Performance of pressurized metered-dose inhalers at extreme temperature conditions. J Pharm Sci. 2014;103(11):3553-3559. doi:10.1002/jps.24145
74. Shemirani FM, Hoe S, Lewis D, et al. *In vitro* investigation of the effect of ambient humidity on regional delivered dose with solution and suspension MDIs. J Aerosol Med Pulm Drug Deliv. 2013;26(4):215-222. doi:10.1089/jamp.2012.0991
75. Tavernini S, Farina DJ, Martin AR, Finlay WH. Using Filters to Estimate Regional Lung Deposition with Pressurized Metered Dose Inhalers. Pharm Res. 2022;39(8):3371-3380. doi:10.1007/s11095-022-03421-9
76. Mitchell JP, Suggett JA. Developing ways to evaluate in the laboratory how inhalation devices will be used by patients and care-givers: the need for clinically appropriate testing. AAPS PharmSciTech. 2014;15(5):1217-1223. doi:10.1208/s12249-014-0145-4
77. Myers TR. The science guiding selection of an aerosol delivery device. Respir Care. 2013;58(11):1963-1973. doi:10.4187/respcare.02812
78. Marple VA, Hochrainer D, Roberts DL, et al. Next generation pharmaceutical impactor (a new impactor for pharmaceutical inhaler testing). Part I: Design. J Aerosol Med. 2003;16(3):283-299. doi:10.1089/089426803769017659
79. Golshahi L, Finlay WH. An idealized child throat that mimics average pediatric oropharyngeal deposition. Aerosol Sci Technol. 2012;46(9):974-983. doi:10.1080/02786826.2012.667170
80. Zhou Y, Sun J, Cheng YS. Comparison of deposition in the USP and physical mouth-throat models with solid and liquid particles. J Aerosol Med Pulm Drug Deliv. 2011;24(5):277-284. doi:10.1089/jamp.2011.0882

`

81. Ruzycki CA, Finlay WH, Martin AR. Estimating clinically relevant measures of inhaled pharmaceutical aerosol performance with advanced in vitro and in silico methods. In: Organ Specific Drug Delivery and Targeting to the Lungs. Boca Raton, FL: CRC Press/Taylor & Francis; 2022:3-46.
82. Yeaton A. Metered dose inhaler (MDI) and dry powder inhaler (DPI) products-quality considerations guidance for industry draft guidance. Food and Drug Administration, Center for Drug Evaluation and Research (CDER); 2018.
83. Baron PA. Calibration and use of the aerodynamic particle sizer (APS 3300). Aerosol Sci Technol. 1986;5(1):55-67. doi:10.1080/02786828608959076
84. Sridhar K, Chari S, Kleinstreuer C. A computational study of droplet-spray formation from pressurized metered dose inhalers with applications to drug deposition in a human lung-airway model. Aerosol Sci Technol. 2023;57(5):434-449. doi:10.1080/02786826.2023.2189927
85. Clark AR. Metered atomisation for respiratory drug delivery. [doctoral thesis]. Loughborough University; 1991. http://hdl.handle.net/2134/7313. Accessed July 18, 2023.
86. Gavtash B, Versteeg HK, Hargrave G, et al. A model of transient internal flow and atomization of propellant/ethanol mixtures in pressurized metered dose inhalers (pMDI). Aerosol Sci Technol. 2018;52(5):494-504. doi:10.1080/02786826.2018.1433814
87. Gavtash B, Versteeg HK, Hargrave G, et al. Transient aerodynamic atomization model to predict aerosol droplet size of pressurized metered dose inhalers (pMDI). Aerosol Sci Technol. 2017;51(9):998-1008. doi:10.1080/02786826.2017.1327121
88. Ivey JW, Lewis D, Church T, Finlay WH, Vehring R. A correlation equation for the mass median aerodynamic diameter of the aerosol emitted by solution metered dose inhalers. Int J Pharm. 2014;465(1-2):207-214. doi:10.1016/j.ijpharm.2014.01.006
89. Chan HK, Gonda I. Development of a systematic theory of suspension inhalation aerosols. II. Aggregates of monodisperse particles nebulized in polydisperse droplets. Int J Pharm. 1988;41(1-2):93-104. doi:10.1016/0378-5173(88)90198-0
90. Stein SW, Sheth P, Myrdal PB. A model for predicting size distributions delivered from pMDIs with suspended drug. Int J Pharm. 2012;422(1-2):101-115. doi:10.1016/j.ijpharm.2011.10.035

`

91. Martin AR, Finlay WH. The effect of humidity on the size of particles delivered from metered-dose inhalers. Aerosol Sci Technol. 2005;39(4):283-289. doi:10.1080/027868290929314
92. Li HY, Xu EY. Innovative pMDI formulations of spray-dried nanoparticles for efficient pulmonary drug delivery. Int J Pharm. 2017;530:12-20. doi:10.1016/j.ijpharm.2017.07.040
93. Traini D, Young PM, Rogueda P, Price R. In vitro investigation of drug particulates interactions and aerosol performance of pressurised metered dose inhalers. Pharm Res. 2007;24(1):125-135. doi:10.1007/s11095-006-9130-2
94. Chunhachaichana C, Sawatdee S, Rugmai S, Srichana T. Development and characterization of nanodispersion-based sildenafil pressurized metered-dose inhaler using combined small-angle X-ray scattering, dynamic light scattering, and impactors. J Drug Deliv Sci Technol. 2022;76. doi:10.1016/j.jddst.2022.103749
95. Heyder J. Deposition of inhaled particles in the human respiratory tract and consequences for regional targeting in respiratory drug delivery. Proc Am Thorac Soc. 2004. doi:10.1513/pats.200409-046TA
96. Cocks E, Somavarapu S, Alpar O, Greenleaf D. Influence of suspension stabilisers on the delivery of protein-loaded porous poly (DL-lactide-co-glycolide) (PLGA) microparticles via pressurised metered dose inhaler (pMDI). Pharm Res. 2014;31(8):2000-2009. doi:10.1007/s11095-014-1302-x
97. Saleem IY, Smyth HDC. Tuning aerosol particle size distribution of metered dose inhalers using cosolvents and surfactants. Biomed Res Int. 2013. doi:10.1155/2013/574310
98. Williams RL, Adams WP, Poochikian G, Hauck WW. Content Uniformity and Dose Uniformity: Current Approaches, Statistical Analyses, and Presentation of an Alternative Approach, with Special Reference to Oral Inhalation and Nasal Drug Products.
99. Corzo C, et al. Lipid-microparticles for pulmonary delivery of active pharmaceutical ingredients: Impact of lipid crystallization on spray-drying processability. Int J Pharm. 2021;610. doi:10.1016/j.ijpharm.2021.121259
100. Hoe S, et al. Use of a fundamental approach to spray-drying formulation design to facilitate the development of multi-component dry powder aerosols for respiratory drug delivery. Pharm Res. 2014;31(2):449-465. doi:10.1007/s11095-013-1174-5

`

101. Ivey J. Particle Formation from Evaporating Microdroplets for Inhaled Drug Delivery. Published online 2018. doi:10.7939/R3RB6WJ3S

102. Decaire B, Conviser S. Materials compatibility testing of Honeywell's new low global warming potential propellants. Aptar Pharma, France;2011. https://sustainability.honeywell.com/content/dam/sustainability/en/documents/document-lists/technical/poster-honeywell-propellants.pdf. Accessed July 18, 2023.

103. SolkaneTM 227 and 134a pharma. Daikin Industries Ltd website. https://www.daikinchem.de/products-and-performance/pharma-propellants. Accessed July 18, 2023.

104. HFO-1234ze(E) Safety Data Sheet. Honeywell website. https://www.honeywellsds.com. Published 2021. Accessed July 18, 2023.

105. Smith C, et al. The Earth's Energy Budget, Climate Feedbacks and Climate Sensitivity Supplementary Material Lead Authors: Contributing Authors.

106. Ivey JW, et al. Humidity affects the morphology of particles emitted from beclomethasone dipropionate pressurized metered dose inhalers. Int J Pharm. 2017;520:207-215. doi:10.1016/j.ijpharm.2017.01.062

107. Wang H, Barona D. A new shadowgraphic imaging method for the suspension stability analysis of pressurized metered dose inhalers Spray drying a tuberculosis vaccine candidate View project Create new project "Sprayable Superhydrophobic Surfaces" View project.

108. Wang H, et al. Design and pharmaceutical applications of a low-flow-rate single-nozzle impactor. Int J Pharm. 2017;533:14-25. doi:10.1016/j.ijpharm.2017.09.047

109. Wang H, Nobes DS, Vehring R. Particle Surface Roughness Improves Colloidal Stability of Pressurized Pharmaceutical Suspensions. Pharm Res. 2019;36. doi:10.1007/s11095-019-2572-0

110. Flament MP, Leterme P, Gayot A. The influence of carrier roughness on adhesion, content uniformity and the in vitro deposition of terbutaline sulphate from dry powder inhalers. Int J Pharm. 2004;275(1-2):201-209. doi:10.1016/j.ijpharm.2004.02.002

111. Carrigy NB, et al. Amorphous pullulan trehalose microparticle platform for respiratory delivery. Int J Pharm. 2019;563:156-168. doi:10.1016/j.ijpharm.2019.04.004

112. Gomez M, et al. Development of a formulation platform for a spray-dried, inhalable tuberculosis vaccine candidate. Int J Pharm. 2021;593. doi:10.1016/j.ijpharm.2020.120121

`

113. Ordoubadi M, et al. On the particle formation of leucine in spray drying of inhalable microparticles. Int J Pharm. 2021;592. doi:10.1016/j.ijpharm.2020.120102

114. Wang H, Nobes DS, Vehring R. Agitation Method Affects Colloidal Stability of Pharmaceutical Suspensions.

115. Usmani OS, et al. Consistent pulmonary drug delivery with whole lung deposition using the aerosphere inhaler: A review of the evidence. Int J Chron Obstruct Pulmon Dis. 2021;16:113-124. doi:10.2147/COPD.S274846

116. Lechuga-Ballesteros D, Vehring R, Dwivedi SK. A New Co-Suspension MDI Platform: Scientific Foundations of Mono, Dual and Triple Combination Products.

117. Weers JG, Miller DP, Tarara TE. Spray-Dried PulmoSphereTM Formulations for Inhalation Comprising Crystalline Drug Particles. AAPS PharmSciTech. 2019. doi:10.1208/s12249-018-1280-0

118. Wolska E. Fine powder of lipid microparticles – spray drying process development and optimization. J Drug Deliv Sci Technol. 2021;64. doi:10.1016/j.jddst.2021.102640

119. Weers JG, Tarara TE, Dellamary LA, et al. US7442388. 2008

120. Williams RO, Hu C. Moisture uptake and its influence on pressurized metered-dose inhalers. Pharm Dev Technol. 2000;5(2):153-162. doi:10.1081/PDT-100100530

121. Amaro MI, et al. Co-Spray dried carbohydrate microparticles: Crystallisation delay/inhibition and improved aerosolization characteristics through the incorporation of hydroxypropyl-β-cyclodextrin with amorphous raffinose or trehalose. Pharm Res. 2015;32(1):180-195. doi:10.1007/s11095-014-1454-8

122. Murata S, Izumi T, Ito H. Effect of the moisture content in aerosol on the spray performance of Stmerin ® hydrofluoroalkane preparations (2). Chem Pharm Bull. 2012;60.

123. Roche N, Dekhuijzen PNR. The evolution of pressurized metered-dose inhalers from early to modern devices. J Aerosol Med Pulm Drug Deliv. 2016. https://doi.org/10.1089/jamp.2015.1232.

124. Principles of metered-dose inhaler design. Respir Care. 2005;50(9):1177-1190.

125. Sheth P, Stein SW, Myrdal PB. Factors influencing aerodynamic particle size distribution of suspension pressurized metered dose inhalers. AAPS PharmSciTech. 2014;16:192-201. https://doi.org/10.1208/s12249-014-0210-z.

`

126. Kim CS, Trujillo D, Sackner MA. Size aspects of metered-dose inhaler aerosols 1-3. 1985.

127. Stein SW, Myrdal PB. The relative influence of atomization and evaporation on metered dose inhaler drug delivery efficiency. Aerosol Sci Technol. 2006;40:335-347. https://doi.org/10.1080/02786820600612268

128. Stein SW. Estimating the number of droplets and drug particles emitted from MDIs. AAPS PharmSciTech. 2008;9:112-115. https://doi.org/10.1208/s12249-007-9006-8

129. Sheth P, Stein SW, Myrdal PB. The influence of initial atomized droplet size on residual particle size from pressurized metered dose inhalers. Int J Pharm. 2013;455:57-65. https://doi.org/10.1016/j.ijpharm.2013.07.061

130. Stein SW, Sheth P, Younis US, Mogalian E, Myrdal PB. Modeling and understanding combination pMDI formulations with both dissolved and suspended drugs. Mol Pharm. 2015;12:3455-3467. https://doi.org/10.1021/acs.molpharmaceut.5b00467

131. Chow MYT, Kwok PCL, Yang R, Chan HK. Predicting the composition and size distribution of dry particles for aerosols and sprays of suspension: a Monte Carlo approach. Int J Pharm. 2020;582. https://doi.org/10.1016/j.ijpharm.2020.119311

132. Wang H, Leal J, Ordoubadi M, et al. Understanding the performance of pressurized metered dose inhalers formulated with low global warming potential propellants. Aerosol Sci Technol. 2023.

133. Ivey J, Vehring R. An in-silico investigation of formulation and device effects on the aerodynamic particle size distributions of suspension pressurized metered dose inhalers. Respir Drug Deliv. 2018.

134. Stein SW, Myrdal PB. A theoretical and experimental analysis of formulation and device parameters affecting solution MDI size distributions. J Pharm Sci. 2004;93:2158-2175. https://doi.org/10.1002/jps.20116

135. Wang H. Droplet characteristics of low global warming potential propellants at different ambient humidities. Respir Drug Deliv. 2023.

136. Berry J, Kline LC, Sherwood JK, et al. Influence of the size of micronized active pharmaceutical ingredient on the aerodynamic particle size and stability of a metered dose inhaler. Drug Dev Ind Pharm. 2004;30:705-714. https://doi.org/10.1081/DDC-120039213

`

137. Sheth P, Stein SW, Myrdal PB. Theoretical and experimental behavior of suspension pressurized metered dose inhalers. 2014.

138. Polli GP, Grim WM, Bacher FA, Yunker MH. Influence of formulation on aerosol particle size.

139. Wang H, Nobes DS, Finlay WH, Vehring R. Agitation method affects colloidal stability of pharmaceutical suspensions. 2019.

140. D'Angelo D, Chierici V, Quarta E, et al. No-shaking and shake-fire delays affect respirable dose for suspension but not solution pMDIs. Int J Pharm. 2023;631. https://doi.org/10.1016/j.ijpharm.2022.122478

141. Chierici V, Cavalieri L, Piraino A, et al. Consequences of not-shaking and shake-fire delays on the emitted dose of some commercial solution and suspension pressurized metered dose inhalers. Expert Opin Drug Deliv. 2020;17(9):1025-1039. doi:10.1080/17425247.2020.1767066

142. Tarara TE, Hartman MS, Gill H, Kennedy AA, Weers JG. Characterization of suspension-based metered dose inhaler formulations composed of spray-dried budesonide microcrystals dispersed in HFA-134a. 2004.

143. Cocks E, Somavarapu S, Alpar O, Greenleaf D. Influence of suspension stabilisers on the delivery of protein-loaded porous poly (DL-lactide-co-glycolide) (PLGA) microparticles via pressurised metered dose inhaler (pMDI). Pharm Res. 2014;31(8):2000-2009. doi:10.1007/s11095-014-1302-x

144. Martin AR, Finlay WH. The effect of humidity on the size of particles delivered from metered-dose inhalers. Aerosol Sci Technol. 2005;39(4):283-289. doi:10.1080/027868290929314

`

Appendices

Appendix A

ISAM congress abstract

Zahra Minootan[1], Hui Wang[1], Nicholas Carrigy[2], Kellisa Lachacz[2], David Lechuga-Ballesteros[2], Andrew R. Martin[1], Reinhard Vehring[1]

[1]Department of Mechanical Engineering, University of Alberta, Edmonton, AB, Canada

[2]Inhalation Product Development, Pharmaceutical Technology & Development, Operations, AstraZeneca, Durham, NC, USA

Part of the effort to reduce the carbon footprint is associated with propellants used in medical devices such as pressurized metered dose inhalers (pMDIs). For example, HFO-1234ze is a low global warming potential (GWP) propellant currently in research and development to investigate its suitability as a replacement for established pMDI propellants. As most drugs are not soluble in propellants and do not suspend well, engineered porous microparticles have been used to form uniform suspensions in pMDIs [1]. For this purpose, novel DSPC (distearoyl phosphatidylcholine) rugose lipid particles (RLPs) have recently been introduced and their simple manufacturing process eliminates the need for pore-forming agents [2].

In this study, pMDI canisters containing spray-dried RLPs were filled with either established HFA propellants (HFA-227ea and HFA-134a) or the new propellant HFO-1234ze. Canisters were stored at 40°C for up to three months. Colloidal stability of RLPs, evaluated by shadowgraphic imaging method, was excellent in all three propellants. Also, particles were physically stable in the propellants, retaining their highly rugose morphology. This study suggests the co-suspension formulation approach is a promising option for developing green pMDI products.

1. Vehring, R., Lechuga-Ballesteros, D., Joshi, V et al. (2012), Langmuir 28, 15015-23. doi:10.1021/la302281n

2. Wang, H., Ordoubadi, M., Connaughton, P et al. (2022), Pharm Res 39, 805–823. doi:10.1007/s11095-022-03242-w

`

Appendix B

Python coding for the simulation in section 3.2

```
import numpy as np
import matplotlib.pyplot as plt
import pandas as pd
from scipy.stats import lognorm, poisson
# Inputs
num_droplets = 10000
concentration_drug = 0.1
density_formulation = 1226
density_drug = 1100
propellant_density=1220
pmc=5.72*10**5 #HFA-134a Pa
#pmc=3.90*10**5 #HFA-227ea Pa
#pmc=4.27*10**5 #HFO-1234ze Pa
T=20+273
#mmd_droplet= (6.90 + (0.0441*50))*10**-6
KL=0.08335 #(W/mK)
M=0.102 #(kg/mol)
CpL=1402
alfa=KL/(propellant_density*CpL)
#propellant_surface_tension=8.786e-3 #HFA-134a N/m
#propellant_surface_tension=6.96e-3 #HFA-227ea N/m
#propellant_surface_tension=8.55e-3 #HFO-1234ze N/m
#z=((alfa**2)*propellant_density/propellant_surface_tension)
#mmd_droplet=(1274*(propellant_surface_tension/pmc))-(139000*z)
#mmd_droplet = 416*(propellant_surface_tension/pmc)
#mmd_droplet= 10.5*10**-6 #wang HFA-134a
#mmd_droplet= 10.8*10**-6 #wang HFA-227ea
mmd_droplet= 11.5*10**-6 #wang HFO-1234ze
print(mmd_droplet)
#print(mmd_droplet1)
gsd_drug = 1.6
mmad_drug = 2*10**-6
mmd_drug=mmad_drug*(1000/density_drug)**(1/2)
gsd_droplet_initial = 1.8
cmd_drug = mmd_drug*np.exp(-3*(np.log(gsd_drug))**2)
cmd_droplet_initial = mmd_droplet*np.exp(-3*(np.log(gsd_droplet_initial))**2)
print(cmd_droplet_initial)
#num_droplets = int(input("Enter the number of droplets to generate: "))
#concentration_drug = float(input("Enter the concentration of the drug (g/g): "))
#density_formulation = float(input("Enter the density of the formulation (kg/m³): "))
#density_drug = float(input("Enter the density of the drug (kg/m³): "))
#gsd_drug = float(input("Enter the GSD of drug: "))
#cmd_drug = float(input("Enter the CMD of drug (meters): "))
#mmd_drug = float(input("Enter the MMD of drug (meters): "))
#pmc= float(input("Enter the propellant vapour pressure at 20C (in Pa): "))
#propellant_surface_tension= float(input("Enter the propellant surface tension at 20C (in N/m): "))
#gsd_droplet_initial = float(input("Enter the GSD of initial droplet: "))
# Arrays to store results
particle_diameters = []
```

`

```
particle_masses = []
particle_volumes=[]
n=[]
dd=[]
droplets=[]
multiplets=[]
n0=[]
n1=[]
n2=[]
n3=[]
n4=[]
n5=[]
n6=[]
# Initialize variables
v0t = 0.0  # Sum volume of droplets
mt = 0.0  # Sum mass of drug particles
for _ in range(num_droplets):
    initial_droplet_diameter = np.random.lognormal(np.log(cmd_droplet_initial), np.log(gsd_droplet_initial))
    # Generate a droplet and append it to the array
    v_droplet = (4/3) * np.pi * (initial_droplet_diameter / 2)**3
    droplets.append(v_droplet)
    V0t=np.sum(droplets)
    s=v_droplet*concentration_drug * density_formulation/density_drug
    d0 = (6*s/np.pi)**(1/3)*10**6
    dd.append(d0)
print(np.mean(dd))
sat=concentration_drug * density_formulation * V0t
print(sat)
 # 3. Calculate PPUV
ppuv = (np.exp(4.5 * (np.log(gsd_drug)) ** 2)) / (
        np.pi / 6 * (mmd_drug ** 3)) * concentration_drug * (
            density_formulation / density_drug)
while mt <= sat:

    # 4. Calculate expected number of particles
    for v_droplet in droplets:
     if mt<=sat:
        expected_number=ppuv*v_droplet
        num_particles = np.random.poisson(expected_number)

    # 5. Generate random drug particles for the droplet
        drug_diameters = np.random.lognormal(np.log(cmd_drug), np.log(gsd_drug), num_particles)

    # 6. Calculate the sum volume of drug particles in the droplet
        vt = np.sum((4/3) * np.pi * (drug_diameters / 2)**3)
    #v0t += v_droplet
        #if vt > v_droplet:
         #   v_droplet=vt

        if vt <= v_droplet:
    # 7. Convert vt to mass using drug density
         xt = vt * density_drug
         D = (6*vt/np.pi)**(1/3)*10**6
    # 8. Append mass and diameter to arrays
         n.extend([num_particles])
         if num_particles < 1:
```

`

```
            n0.append(num_particles)
        if num_particles == 1:
            n1.append(num_particles)
        if num_particles == 2:
            n2.append(num_particles)
        if num_particles>=2:
            multiplets.append(num_particles)
        if num_particles == 3:
            n3.append(num_particles)
        if num_particles == 4:
            n4.append(num_particles)
        if num_particles == 5:
            n5.append(num_particles)
        if num_particles >= 6:
            n6.append(num_particles)
        if num_particles >= 1:
         if num_particles == 1:
            result = 1
         elif num_particles == 2:
            result = 1.02
         elif num_particles == 3:
            result = 1.08
         elif num_particles == 4:
            result = 1.12
         elif num_particles == 5:
            result = 1.07
         elif num_particles == 6:
            result = 1.05
         elif num_particles == 7:
            result = 1.08
         elif num_particles == 8:
            result = 1.1
         else:
            result = 1.1  # Default value if num_particles>8
         Dt=D*((density_drug/1000)/result)**0.5
         particle_diameters.extend([Dt])
         particle_masses.extend([xt])
         particle_volumes.extend([vt])
    # 9. Update v0t and mt
         mt += xt
average=np.mean(particle_diameters)
print(mt)
print(average)

#print(len(n0))
num_droplets_0 = len(n0)
num_droplets_1 = len(n1)
num_droplets_2 = len(n2)
num_droplets_3 = len(n3)
num_droplets_4 = len(n4)
num_droplets_5 = len(n5)
num_droplets_6_or_more = len(n6)
num_multiplets=len(multiplets)
print(num_droplets_0)
print(num_droplets_1)
print(num_multiplets)
```

`

```
# Create a bar plot
labels = ['0', '1', '2', '3', '4', '5', '6+']
counts = [num_droplets_0, num_droplets_1, num_droplets_2, num_droplets_3, num_droplets_4, num_droplets_5,
num_droplets_6_or_more]
plt.bar(labels, counts)
plt.xlabel('Number of Particles in Droplet')
plt.ylabel('Number of Droplets')
plt.title('Distribution of Particle Counts in Droplets')
plt.grid(axis='y')
plt.show()
#print(n)
#print(particle_masses)
#print(particle_diameters)
particle_diameters = np.array(particle_diameters)
particle_masses = np.array(particle_masses)

combined_data = list(zip(particle_diameters, particle_masses))
combined_data.sort(key=lambda x: x[0])  # Sort by diameter
particle_diameters, particle_masses = zip(*combined_data)

# Normalize the masses
normalized_masses = np.array(particle_masses) / np.sum(particle_masses)

# Calculate the cumulative distribution
cumulative_distribution = np.cumsum(normalized_masses)

# Plot the cumulative size distribution
plt.plot(particle_diameters, cumulative_distribution, color='blue')
plt.xlabel('Aerodynamic Diameter (μm)')
plt.ylabel('Normalized Cumulative Mass Distribution')
plt.title('Cumulative Size Distribution Based on Normalized Mass')
plt.grid(True)


plt.show()
```

`

Appendix C

Sample Simulation results

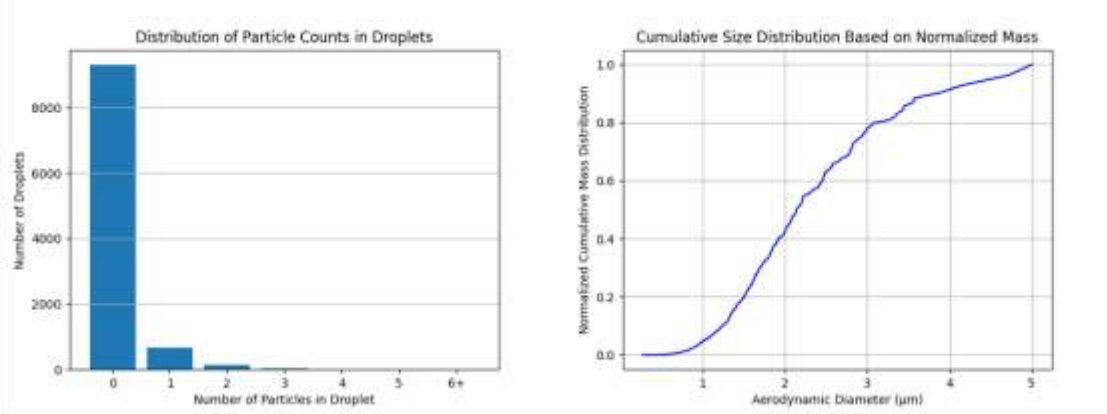

Figure C1. Simulation output using Ivey correlation for calculating initial droplet diameter of HFA-134a

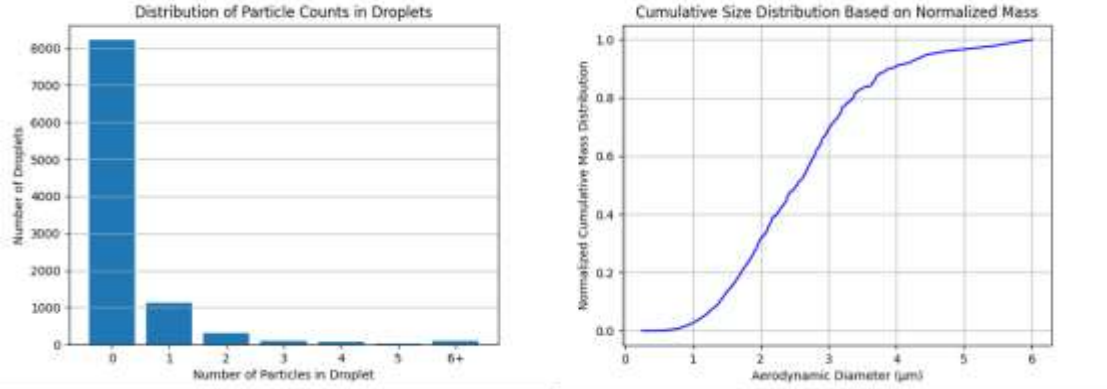

Figure C2. Simulation output using Stein correlation for calculating initial droplet diameter of HFA-134a

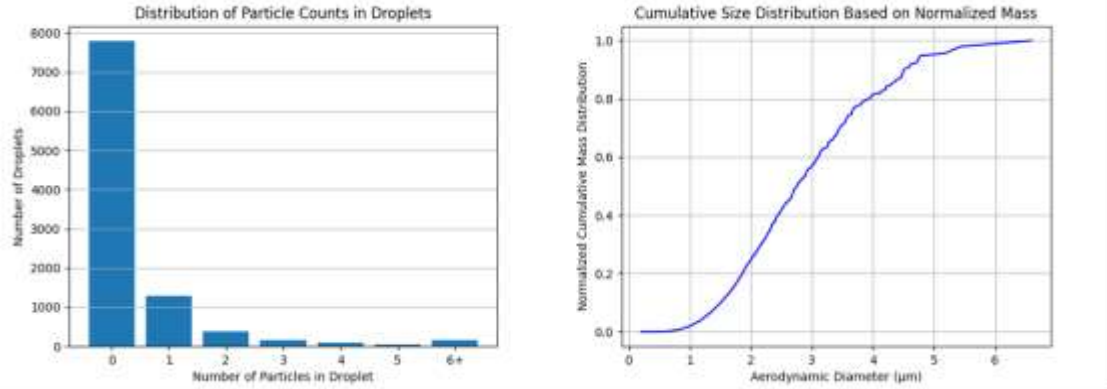

Figure C3. Simulation output using Wang estimated initial droplets for HFA-134a.

`

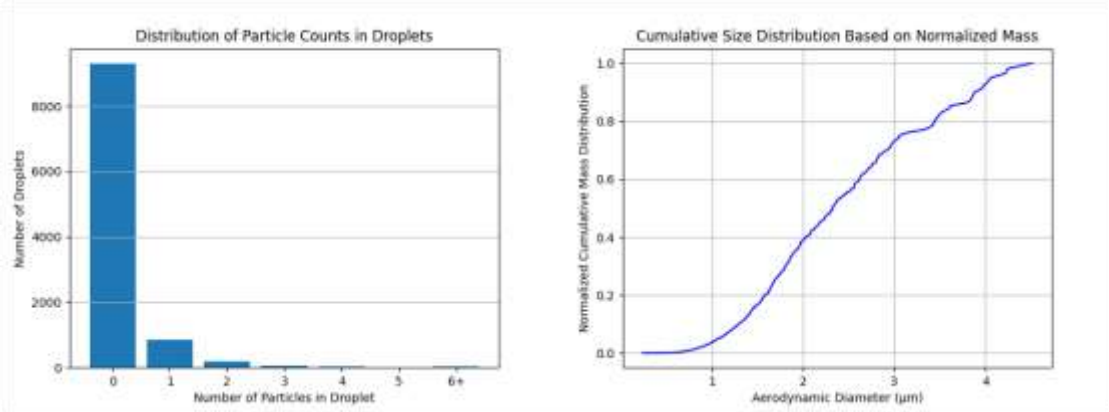

Figure C4. Simulation output using Ivey correlation for calculating initial droplet diameter of HFA-227ea

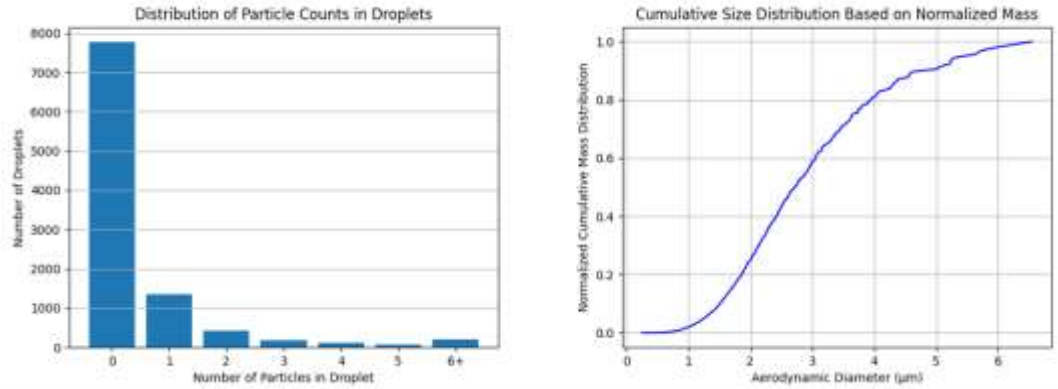

Figure C5. Simulation output using Wang estimated initial droplets diameter of HFA-227ea

`

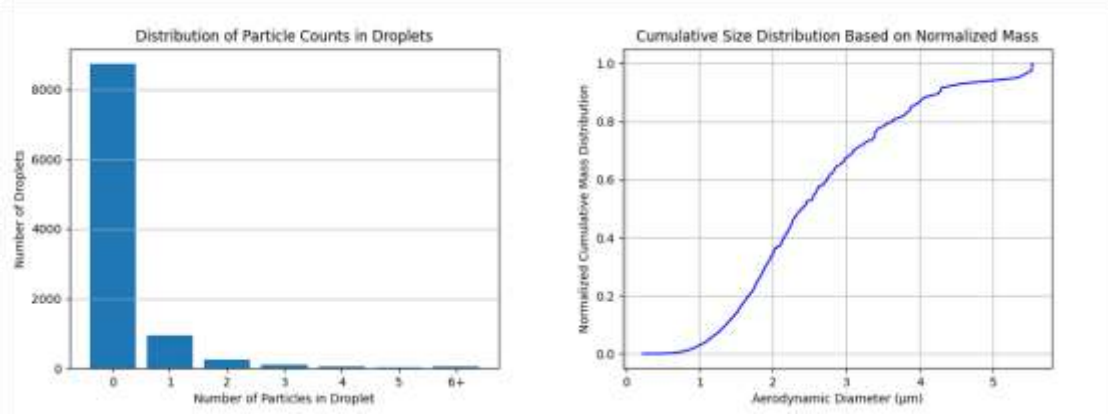

Figure C6. Simulation output using Ivey correlation for calculating initial droplet diameter of HFO-1234ze.

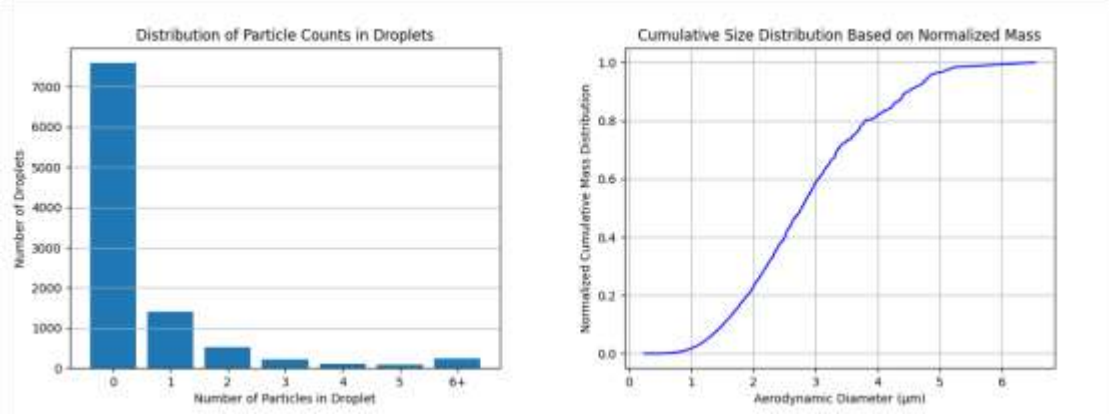

Figure C7. Simulation output using Wang estimated initial droplets diameter of HFO-1234ze.

`

Appendix D

SEM images taken at different time points: RLP 55 in HFA-134a

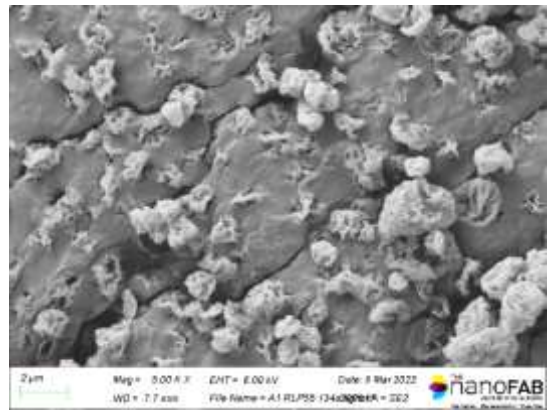

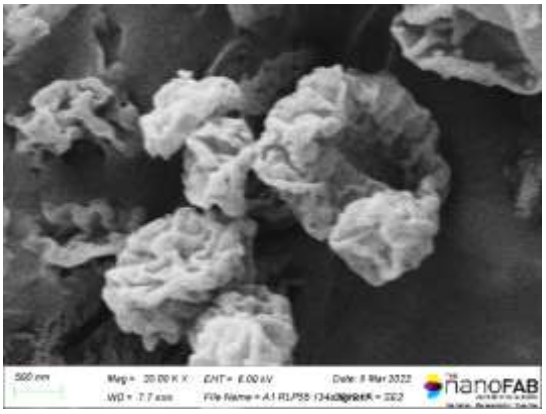

Day zero

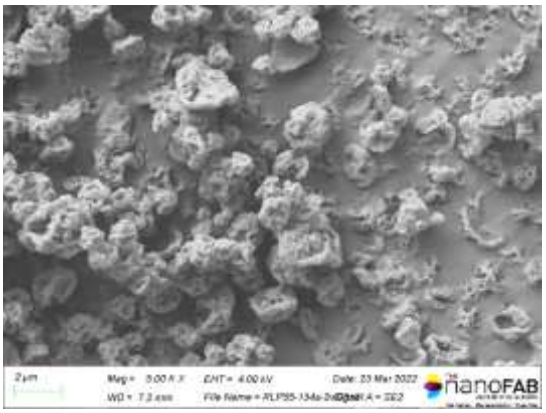

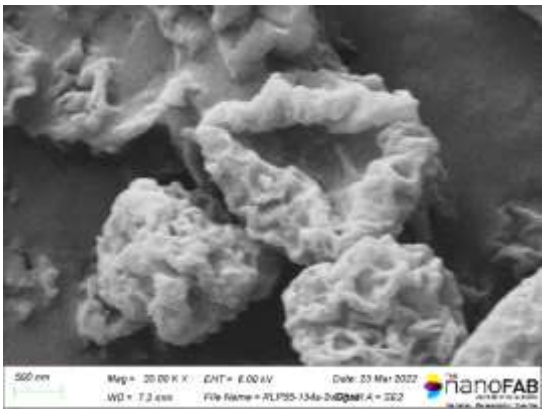

two weeks

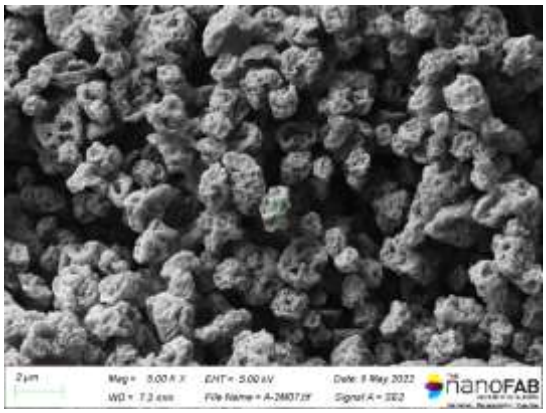

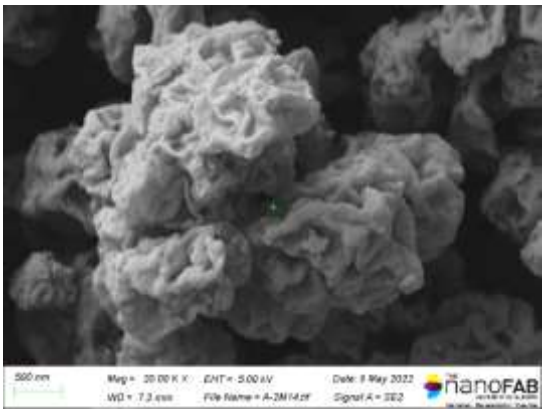

two months

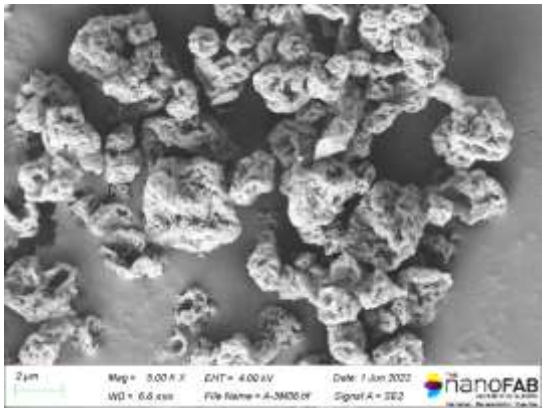

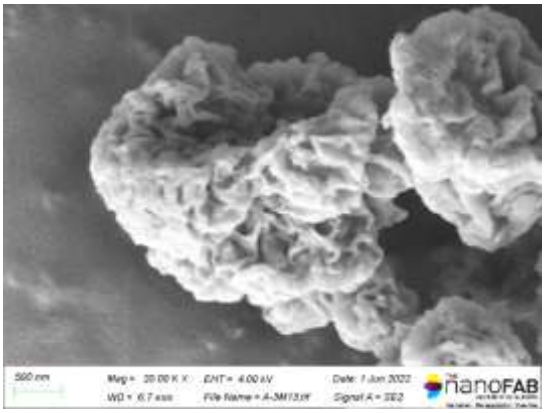

three months

`

`RLP55 in HFA-227ea

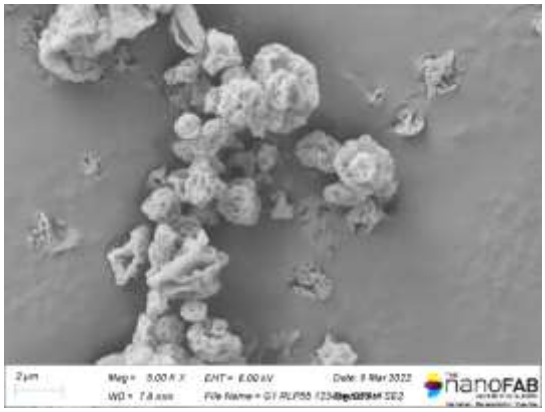

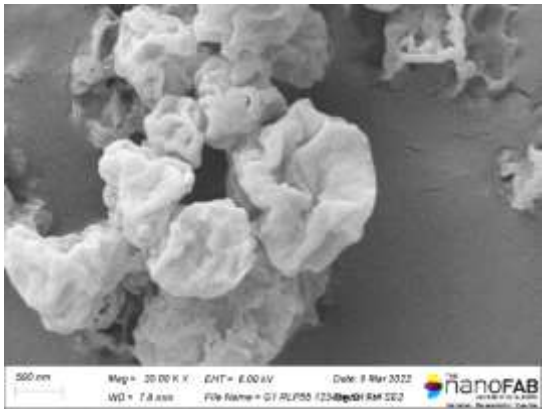

Day zero

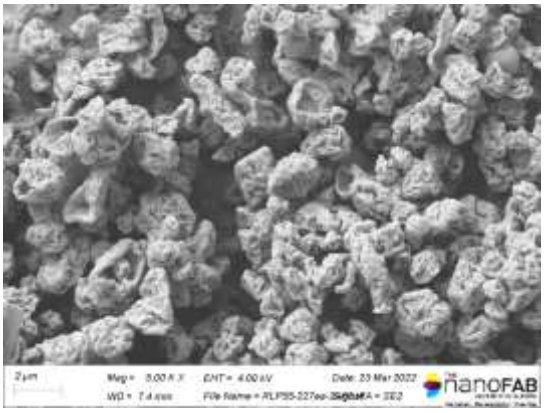

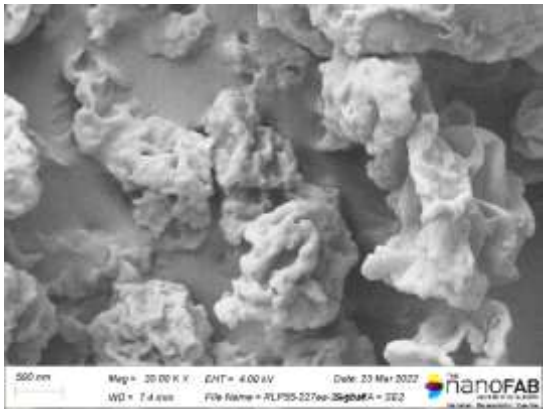

two weeks

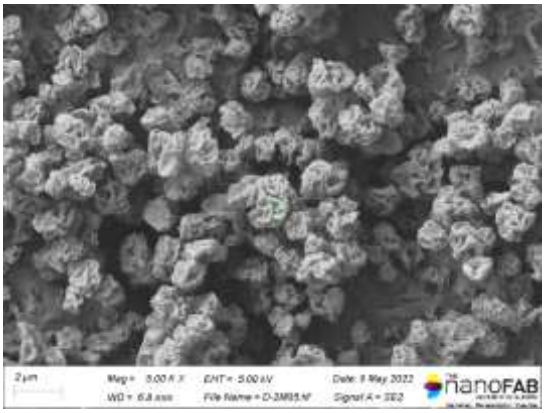

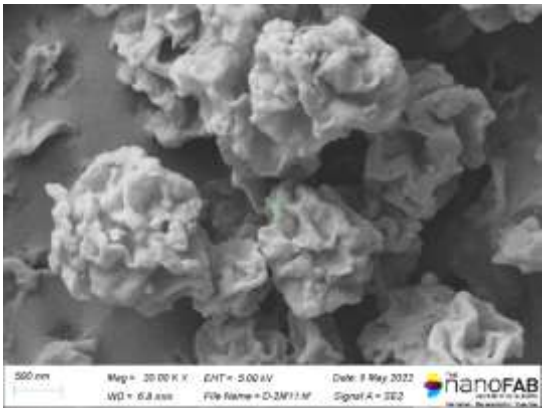

two months

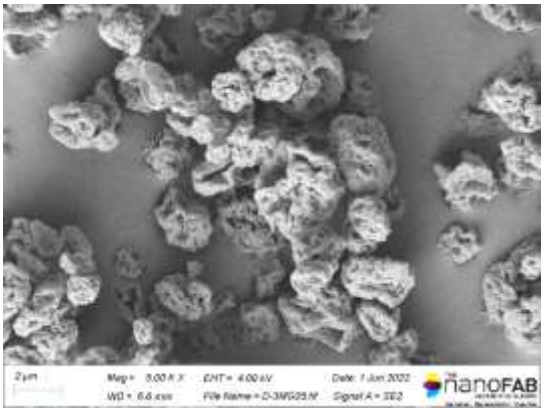

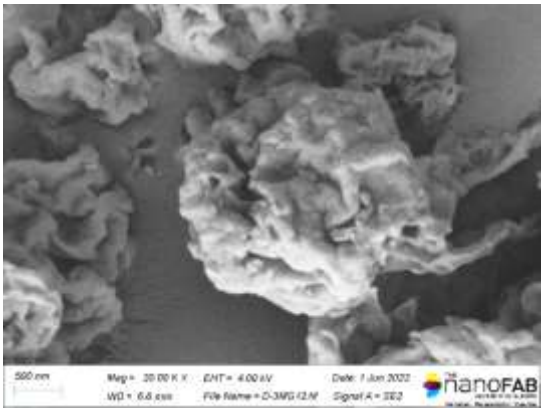

three months

`

RLP55 in HFO-1234ze

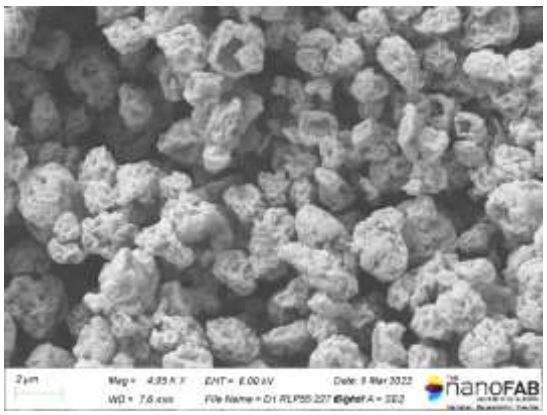

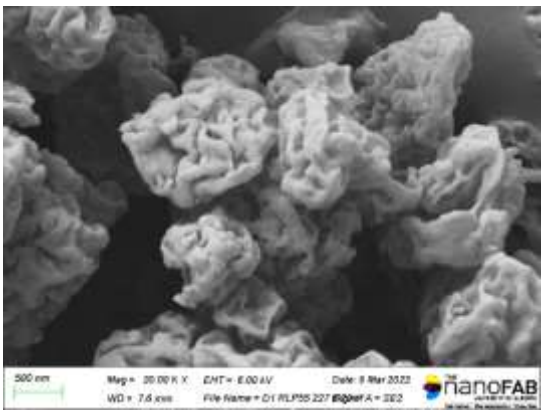

Day zero

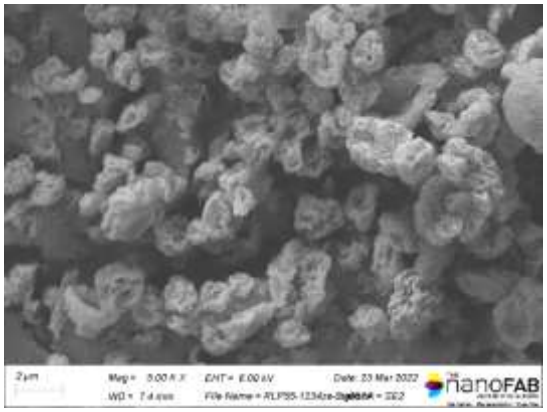

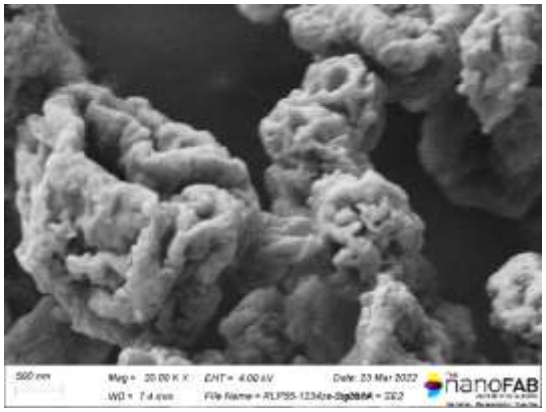

two weeks

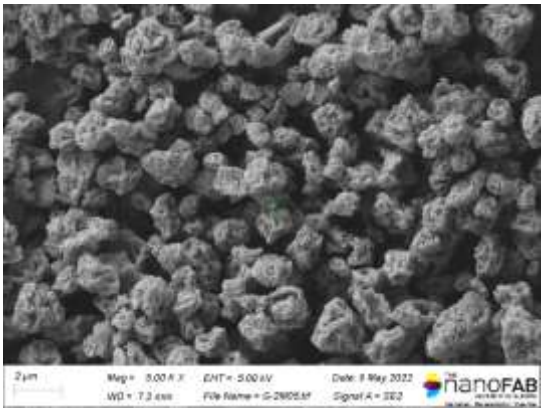

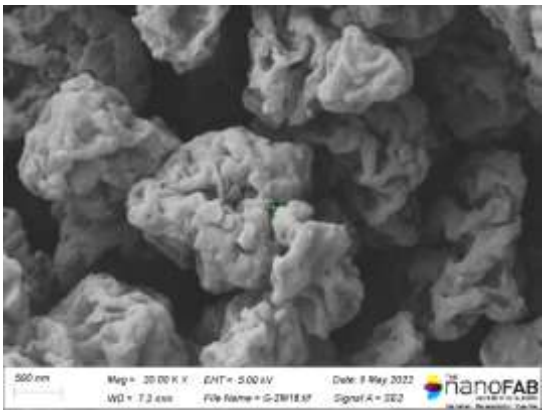

two months

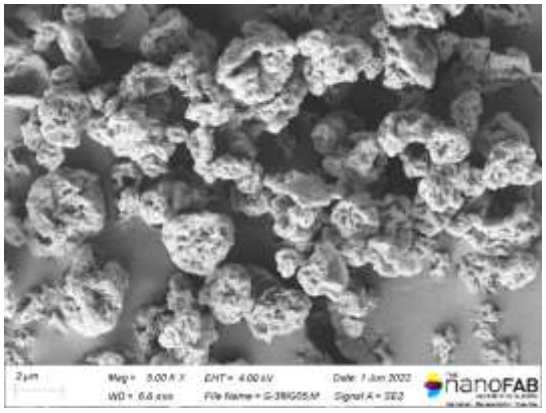

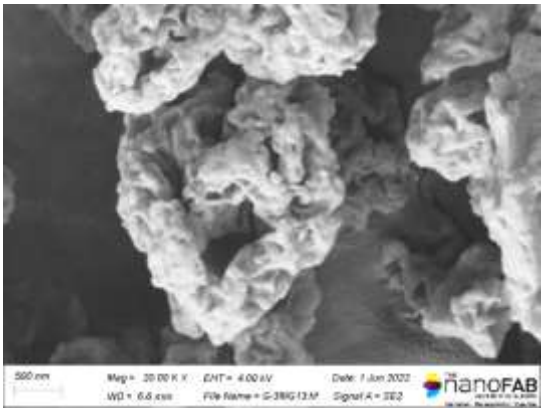

three months

`

RLP75 in HFA-134a

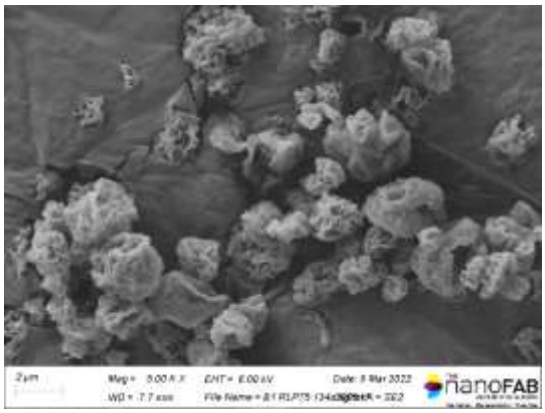

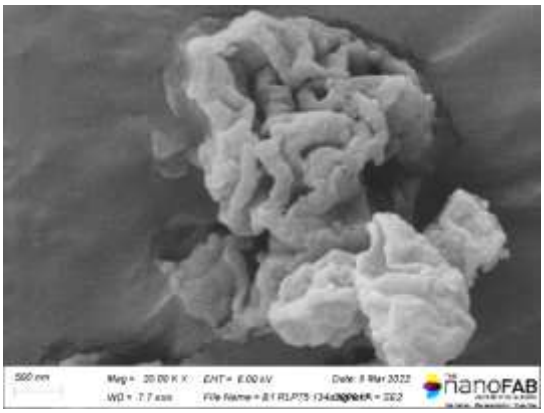

Day zero

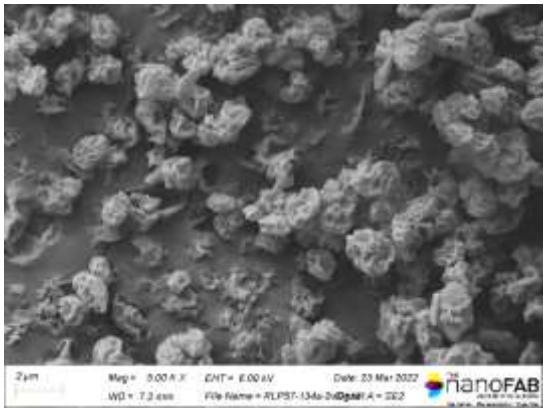

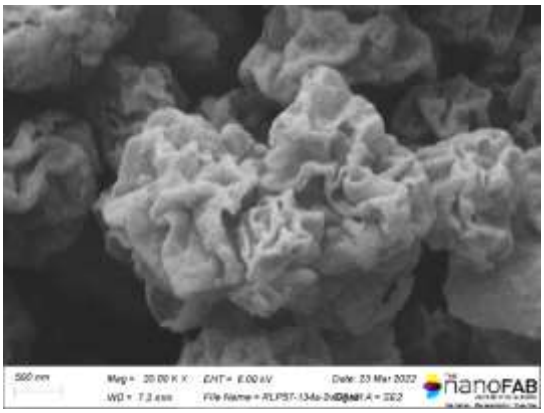

two weeks

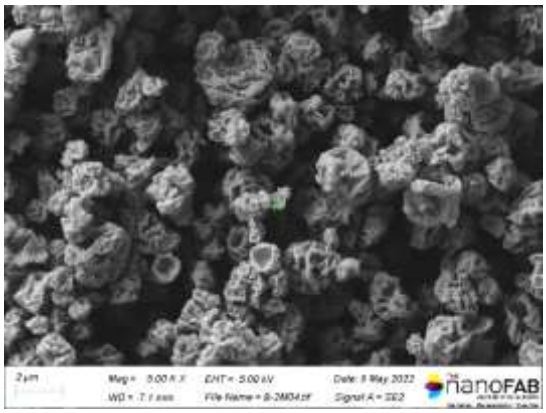

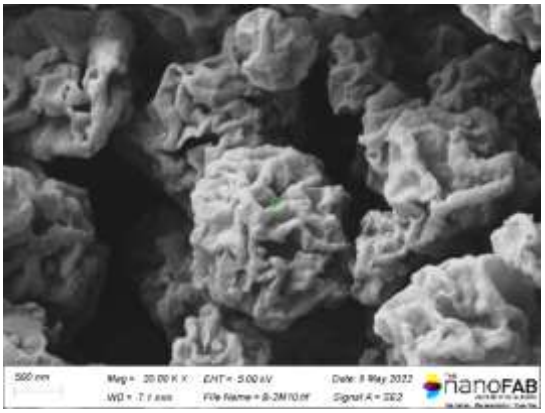

two months

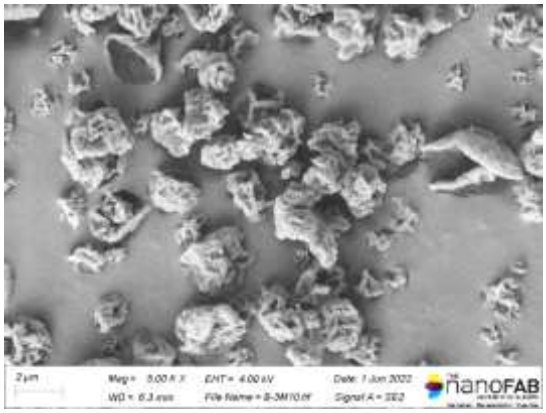

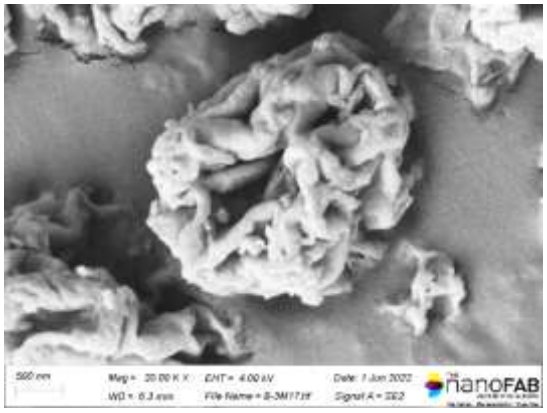

three months

`

RLP75 in HFA-227ea

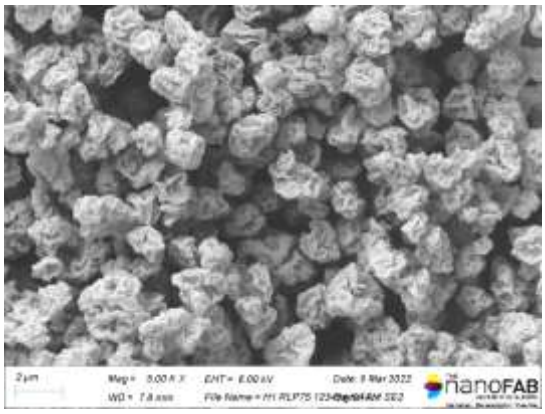

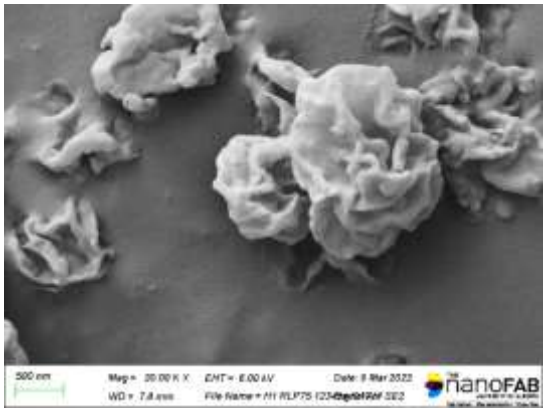

Day zero

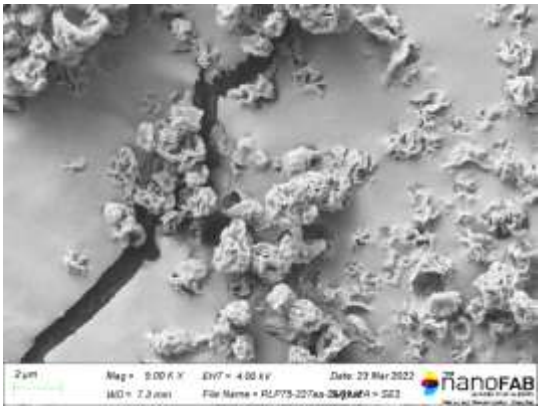

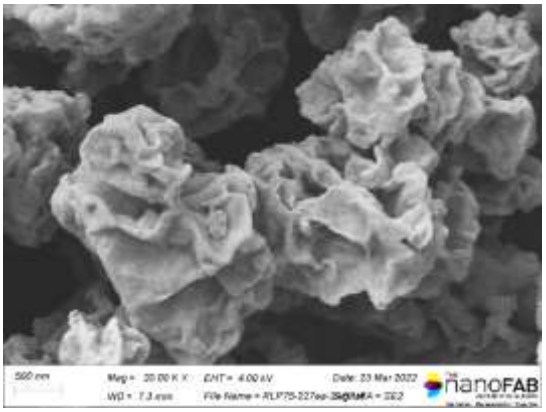

two weeks

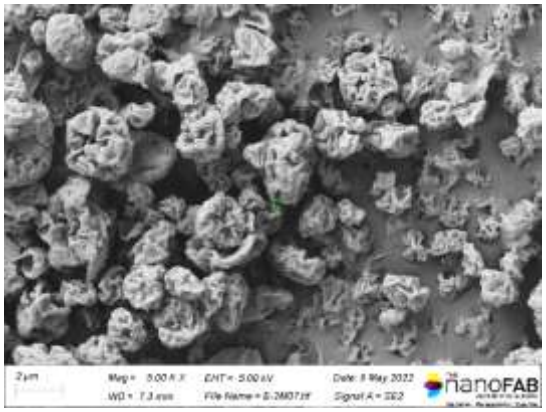

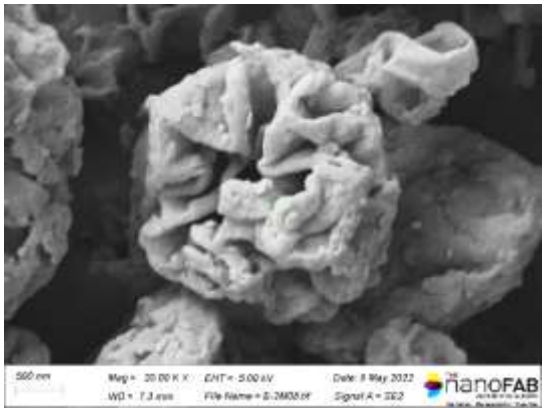

two months

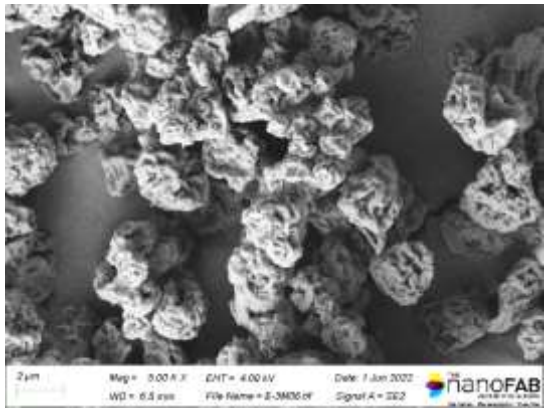

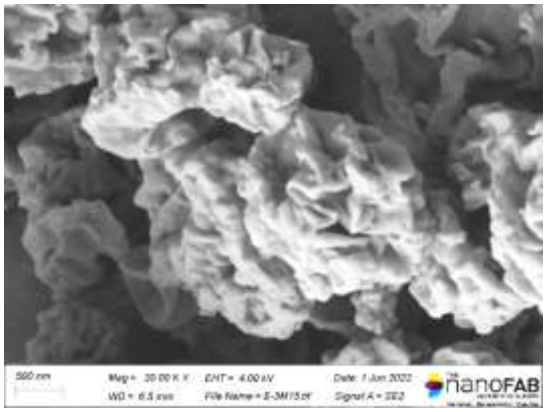

three months

`

RLP75 in HFO-1234ze

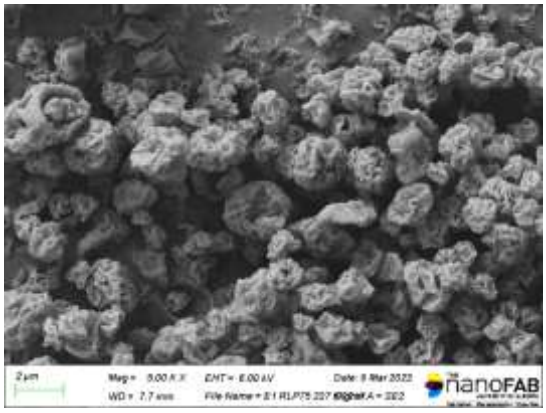

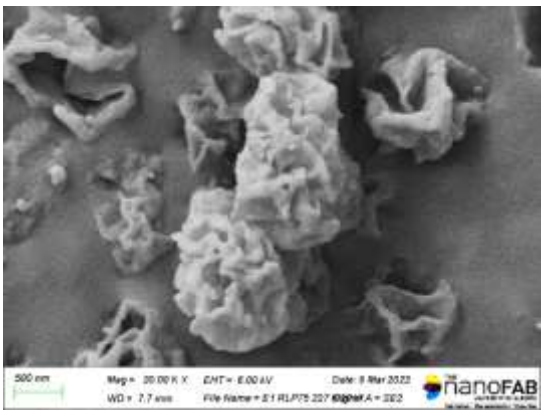

Day zero

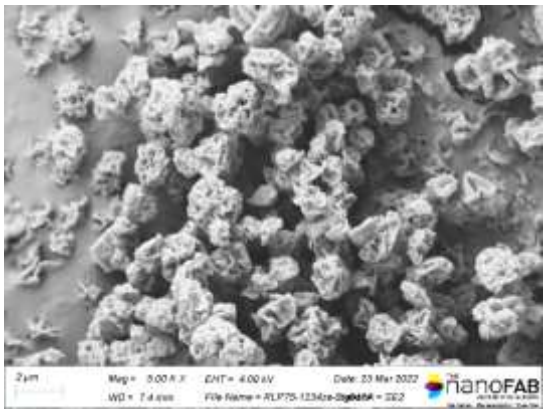

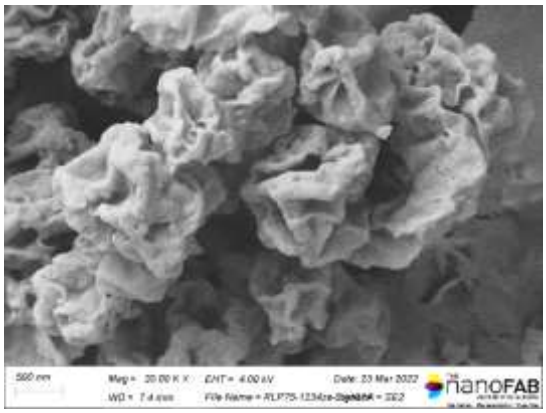

two weeks

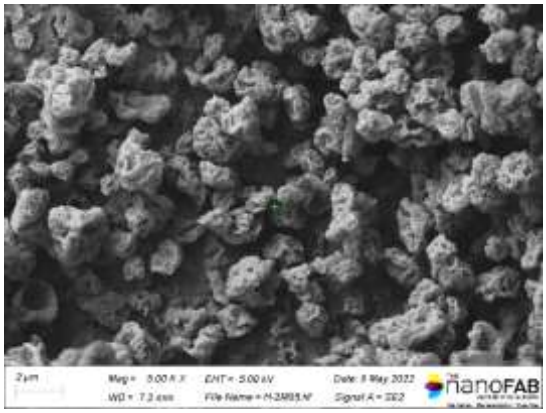

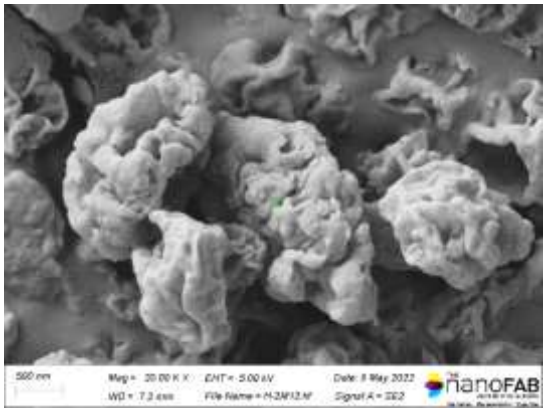

two months

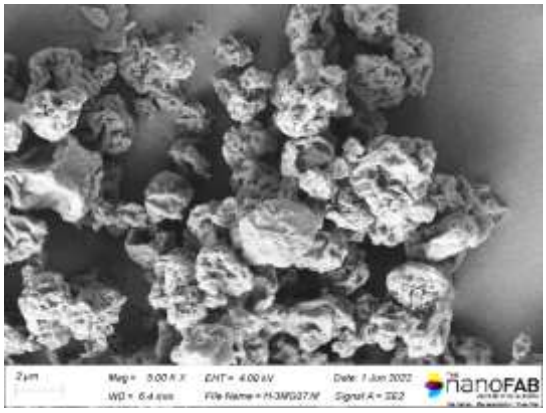

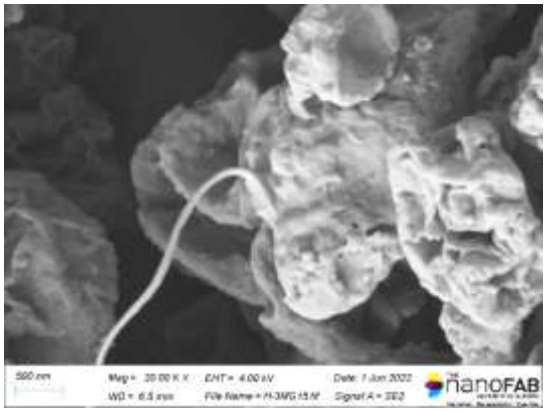

three months

`

80T20L in HFA-134a

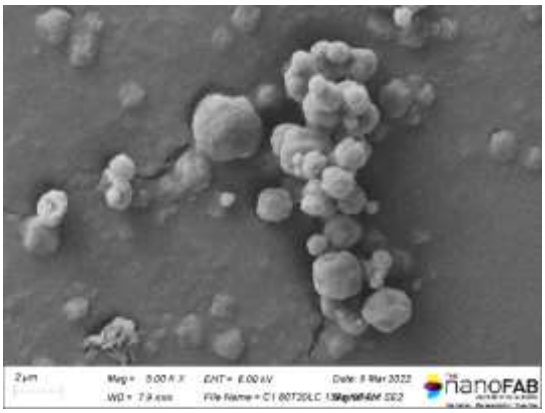

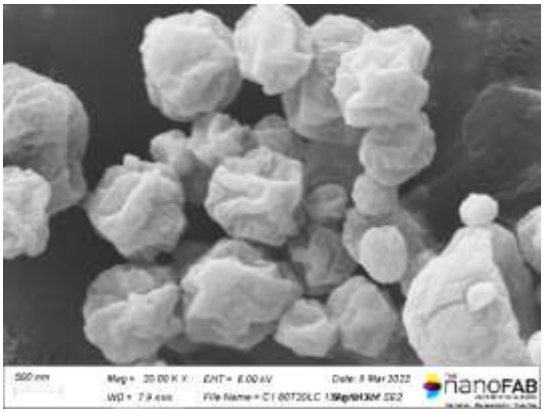

Day zero

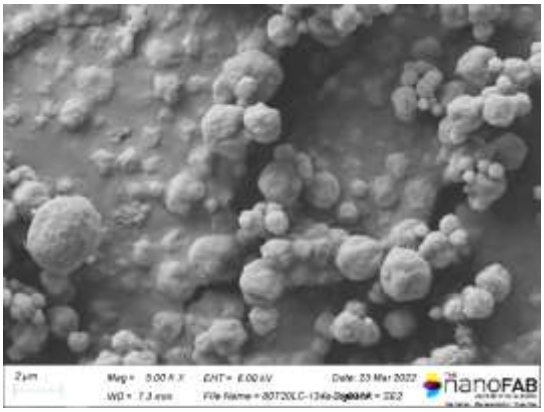

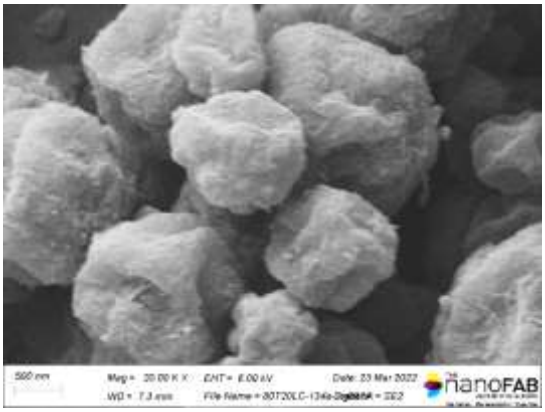

two weeks

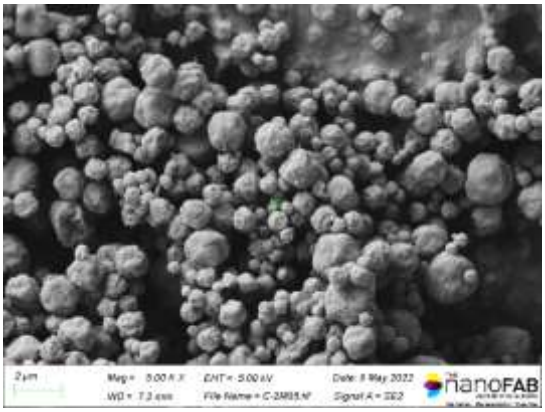

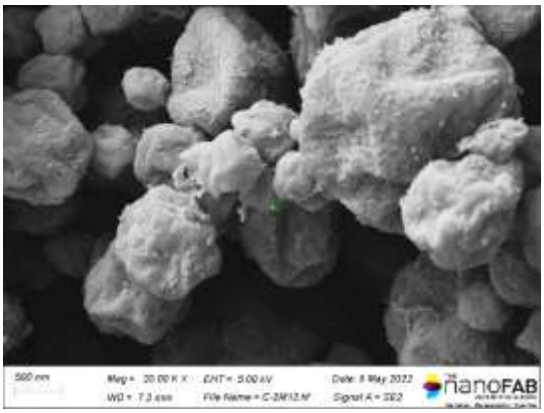

two months

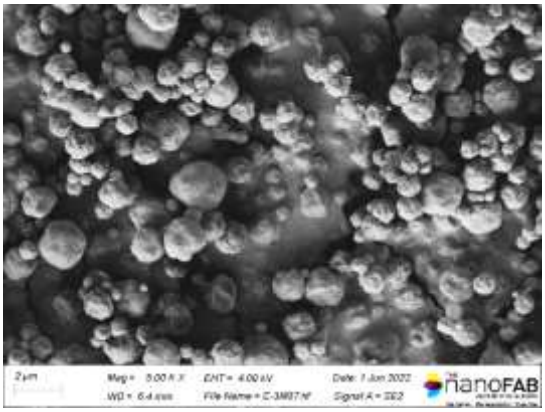

three months

`

80T20L in HFA-227ea

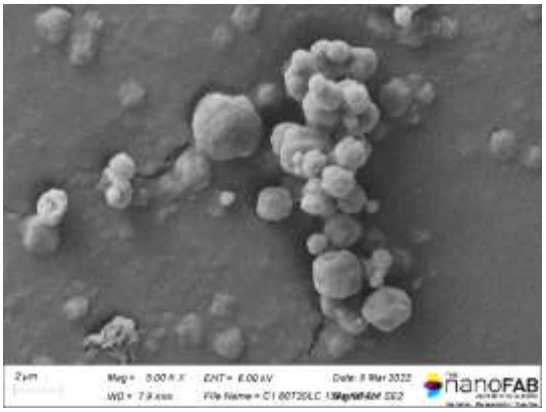

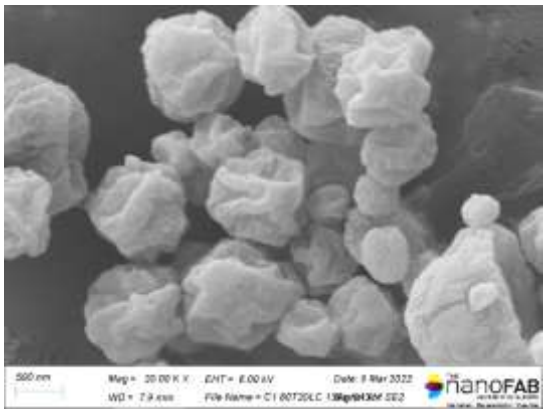

Day zero

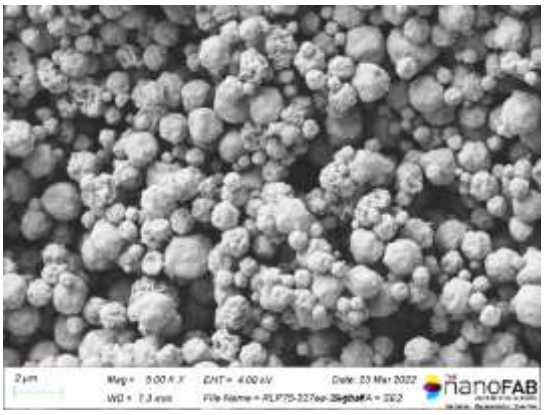

two weeks

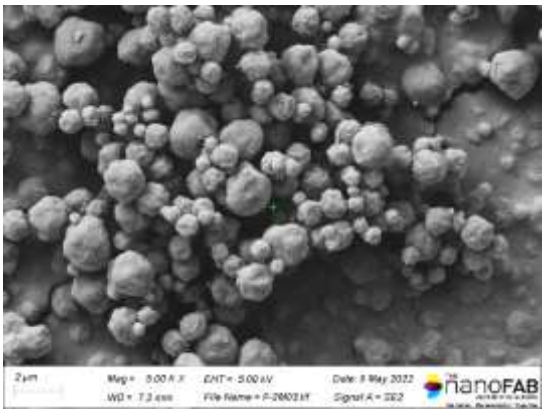

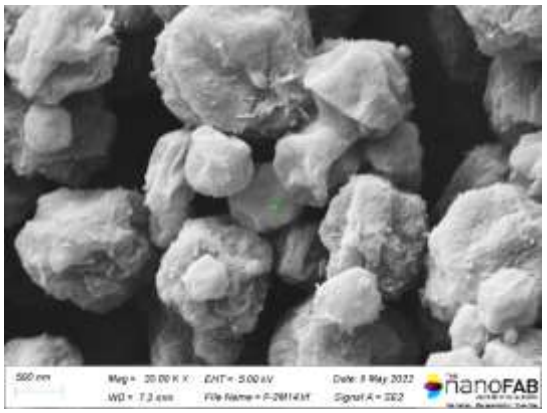

two months

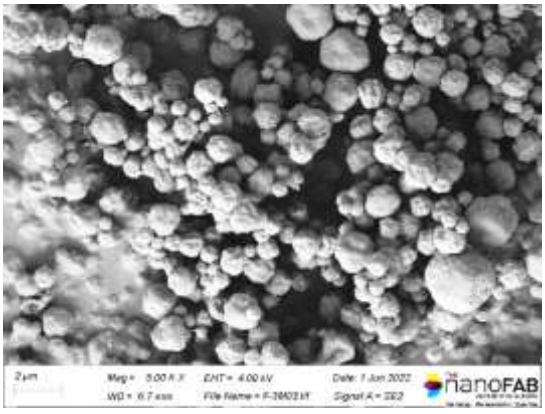

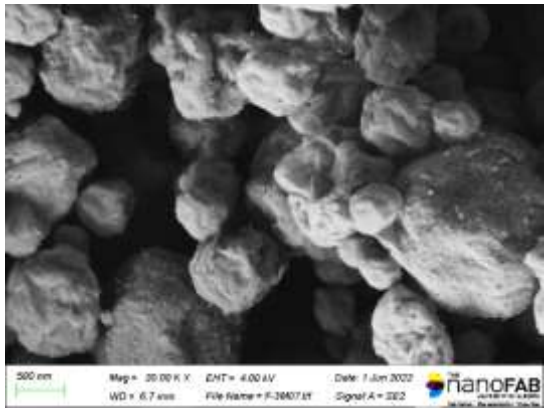

three months

`

80T20L in HFO-1234ze

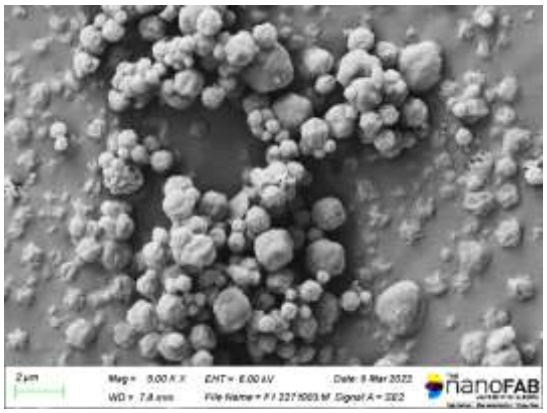

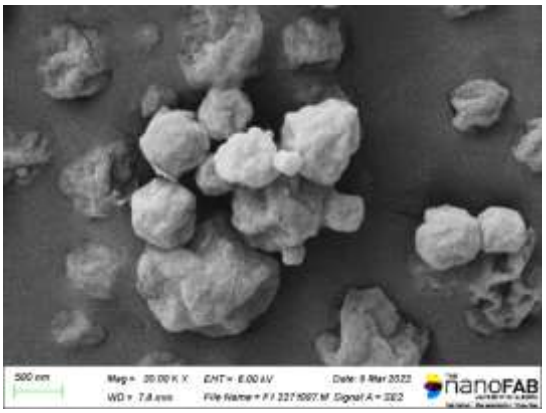

Day zero

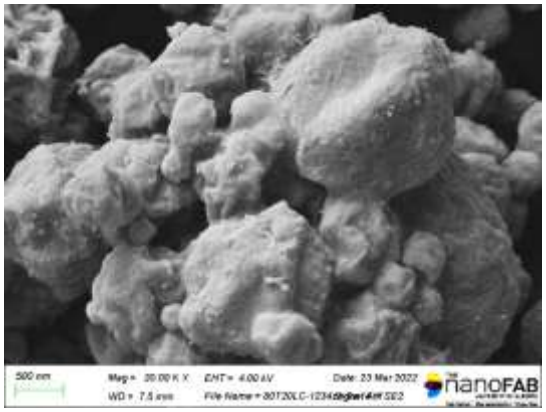

two weeks

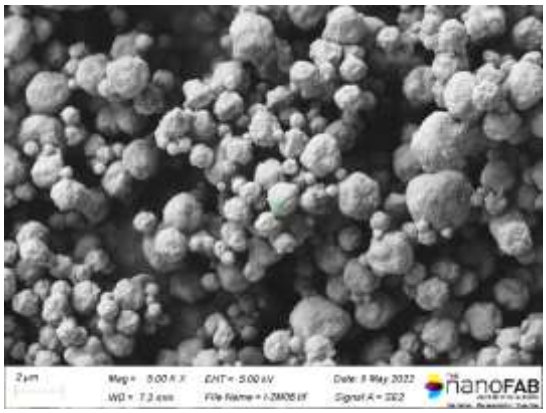

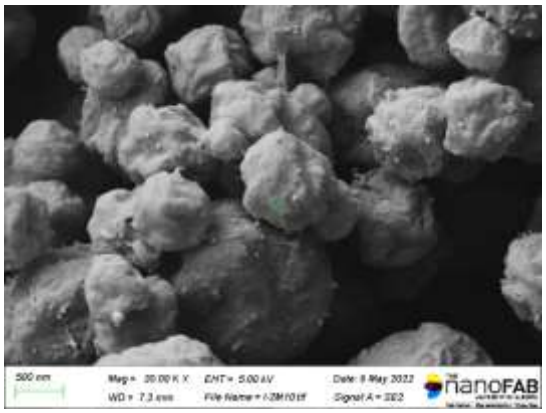

two months

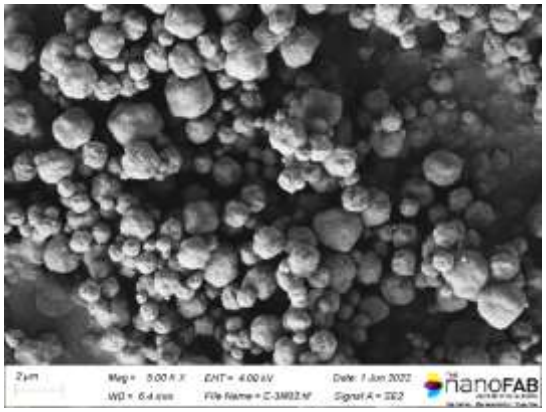

three months

`

Appendix E

Permission for reusing Figure 1.2:

This Agreement between Zahra Minootan ("You") and Elsevier ("Elsevier") consists of your license details and the terms and conditions provided by Elsevier and Copyright Clearance Center.

License Number	5692660338465
License date	Dec 19, 2023
Licensed Content Publisher	Elsevier
Licensed Content Publication	Journal of Aerosol Science
Licensed Content Title	Modelling inhaled particle deposition in the human lung—A review
Licensed Content Author	Werner Hofmann
Licensed Content Date	Oct 1, 2011
Licensed Content Volume	42
Licensed Content Issue	10
Licensed Content Pages	32
Start Page	693
End Page	724
Type of Use	reuse in a thesis/dissertation
Portion	figures/tables/illustrations
Number of figures/tables/illustrations	1
Format	both print and electronic
Are you the author of this Elsevier article?	No
Will you be translating?	No

`

Title of new work	Advancements in Metered-Dose Inhalers Technology: Feasibility of Excipients and Particle Size Prediction
Institution name	University of Alberta
Expected presentation date	Jan 2024
Portions	Fig. 1
Requestor Location	Zahra Minootan 11307 99 Ave Edmonton, AB T5K0H2 Canada Attn: Zahra Minootan
Publisher Tax ID	GB 494 6272 12
Total	0.00 CAD

`

Permission for reusing Figure 1.3:

License Number	5692660641862
License date	Dec 19, 2023
Licensed Content Publisher	Elsevier
Licensed Content Publication	Powder Technology
Licensed Content Title	Prediction of the particle size distribution of the aerosol generated by a pressurized metered-dose inhaler
Licensed Content Author	Yamila L. de Charras,M. Verónica Ramírez-Rigo,Diego E. Bertin
Licensed Content Date	Feb 1, 2022
Licensed Content Volume	399
Licensed Content Issue	n/a
Licensed Content Pages	1
Start Page	117151
End Page	0
Type of Use	reuse in a thesis/dissertation
Portion	figures/tables/illustrations
Number of figures/tables/illustrations	1
Format	both print and electronic
Are you the author of this Elsevier article?	No
Will you be translating?	No
Title of new work	Advancements in Metered-Dose Inhalers Technology: Feasibility of Excipients and Particle Size Prediction
Institution name	University of Alberta

`

Expected presentation date	Jan 2024
Portions	fig. 1
	Zahra Minootan 11307 99 Ave
Requestor Location	
	Edmonton, AB T5K0H2 Canada Attn: Zahra Minootan
Publisher Tax ID	GB 494 6272 12
Total	0.00 CAD